RECEIVED
LAWRENCE
RADIATION LABORATORY

LIBRARY AND
DOCUMENTS SECTION

UCRL-20142
c.2

RADIATIVE LIFETIME OF THE 2^1S_0 METASTABLE STATE OF HELIUM

Robert Spaulding Van Dyck, Jr.
(Ph. D. Thesis)

November 20, 1970

AEC Contract No. W-7405-eng-48

TWO-WEEK LOAN COPY

This is a Library Circulating Copy
which may be borrowed for two weeks.
For a personal retention copy, call
Tech. Info. Division, Ext. 5545

LAWRENCE RADIATION LABORATORY
UNIVERSITY of CALIFORNIA BERKELEY

UCRL-20142 c.2

DISCLAIMER

This document was prepared as an account of work sponsored by the United States Government. While this document is believed to contain correct information, neither the United States Government nor any agency thereof, nor the Regents of the University of California, nor any of their employees, makes any warranty, express or implied, or assumes any legal responsibility for the accuracy, completeness, or usefulness of any information, apparatus, product, or process disclosed, or represents that its use would not infringe privately owned rights. Reference herein to any specific commercial product, process, or service by its trade name, trademark, manufacturer, or otherwise, does not necessarily constitute or imply its endorsement, recommendation, or favoring by the United States Government or any agency thereof, or the Regents of the University of California. The views and opinions of authors expressed herein do not necessarily state or reflect those of the United States Government or any agency thereof or the Regents of the University of California.

RADIATIVE LIFETIME OF THE 2^1S_0 METASTABLE STATE OF HELIUM

Contents

Abstract vi

List of Illustrations viii

I. Introduction 1

II. Theory 5

A. History 5

B. Terminology 7

C. Selection Rules 8

D. Lifetimes and Decay Mechanisms 11

E. Helium Metastable States 12

F. 2^1S_0 Helium Lifetime 15

G. Principle of the Experiment 21

1. General Formalism 21

2. Helium 25

III. Experiment 30

A. General Description 30

B. Vacuum System 34

C. Gas Handling System 39

D. Source Assembly 45

E. Metastabilizer 47

F. Discharge Lamp 57

G. Collimation 62

H. Deflection Plates 67

I. Magnet 67

J. Detection System 70
1. Targets 70
2. Electron Multiplier 74
3. Amplifiers and Discriminators 77
4. Computer Network 78
K. Experimental Procedures 82
IV. Analysis and Conclusions 86
A. Analysis Program ANALZ 86
B. Data 96
1. Helium 96
2. Helium Lifetimes 108
3. Neon 111
C. Error Analysis 114
1. Statistical Error 115
2. Experimental Uncertainty 116
3. Systematic Error 117
4. Total Error 119
D. Conclusions 119
1. Improvements 119
2. Measurable Lifetimes 120
3. Summary 122
Appendices 124
A. Transition Probability 124
B. Inelastic Collisions 131
1. Final Speed 131

2. Cross Electron Beam 134

3. Antiparallel Electron Beam 135

C. Pressure in Source Tube 136

D. Fraction of 2^1S_0 Metastable Atoms in Beam 138

E. Ion Deflection in Electric and Magnetic Fields 140

1. Magnetic Field 140

2. Electric Field 141

F. Convolution Studies 143

1. Limit on the Size of δt 143

2. Detailed Convolution 147

G. Analysis Program 153

H. LINFIT Theory 161

Acknowledgments 164

References 165

RADIATIVE LIFETIME OF THE 2^1S_0 METASTABLE STATE OF HELIUM

Robert Spaulding Van Dyck, Jr.

Department of Physics
and
Lawrence Radiation Laboratory
University of California
Berkeley, California

November 20, 1970

ABSTRACT

A time-of-flight technique has been used to measure the radiative lifetime of the 2^1S_0 state of helium. After passing from a cooled source, helium atoms are excited to the 2^1S_0 state by a pulsed electron gun. The atomic beam then contains primarily ground state helium atoms and metastable atoms in both the 2^3S_1 and the 2^1S_0 excited states. The time-of-flight spectrum for the metastable 2^1S_0 state can be separated from the 2^3S_1 state by using an rf-discharge helium lamp: The 2^1S_0 state is quenched by absorption of a 20,581 Å photon, raising the atom to the 2^1P_1 state, which then decays preferentially to the $^1S_0$ ground state; the 2^3S_1 state remains unaffected because it is the ground state for the triplet system. The time-of-flight spectrum for the 2^1S_0 atoms is therefore obtained from the difference between the full beam and the quenched beam.

The metastable atoms are then detected at two positions –

d_1 = 1.9 meters and d_2 = 6.7 meters from the electron gun — by Auger ejection of an electron from a copper target, the first of which is a 60% transmitting mesh. Neutral helium atoms cannot cause an electron to be ejected and are not detected. A comparison of the number of metastables within a given velocity interval at the two detectors determines the number which decay in flight and yields a value for the two-photon radiative lifetime τ.

The final value for the singlet lifetime,

$$20.2 \pm 1.0 \text{ msec},$$

is consistent with a previous lower limit (STE 69) and agrees with the calculated value of 19.5 msec (DRA 69), but disagrees with the value $\tau = 38 \pm 8$ msec reported by Pearl using a movable detector (PEA 70). The 1.0 msec error is one standard deviation determined primarily from the uncertainty arising from the sensitivity of the analysis program to small errors in d_1 and d_2, and includes an estimate of the remaining systematic error in the experiment.

List of Illustrations

Figure		Page
1.	Lowest-lying states of helium	13
2.	Schematic of time-of-flight apparatus	22
3a.	Schematic of the upper section of the metastable beam machine	31
3b.	Schematic of the lower section of the metastable beam machine	32
4.	Photograph of the actual metastable beam machine	33
5.	Schematic of the central foreline manifold	36
6.	Schematic of the gas handling system	41
7.	Photograph of the present gas handling system	42
8.	Precision metering flow rate graph	44
9.	Schematic of source assembly	46
10.	Exploded view of sheath electrode gun	48
11.	Photograph of present electron gun	51
12.	Schematic of gun support systems	52
13.	Filament heater circuit	53
14.	Emission current pulsing circuit	55
15.	Electron impact excitation functions for metastable helium	56
16.	Solenoid pulsing circuit	58
17.	Illustration of the quenching mechanism	60
18.	Photograph of the helium discharge lamp	61
19.	Discharge lamp circuit	63
20.	Collimator - separation plate	65
21.	Collimation scheme	66

Figure		Page
22.	Magnet cross section	68
23.	Auger electron ejection mechanism	73
24.	Detection system	75
25.	Photograph of lower detector	76
26.	Block diagram of the total collection network	79
27.	Time base circuit	80
28.	Timing scheme	81
29.	Oscilloscope photograph of data collected	87
30.	Metastable singlet time-of-flight spectrum for detector 2	89
31.	Logarithmic plot of R(t) versus time-of-flight	91
32.	Two-photon decay process	126
33.	Inelastic collision process	132

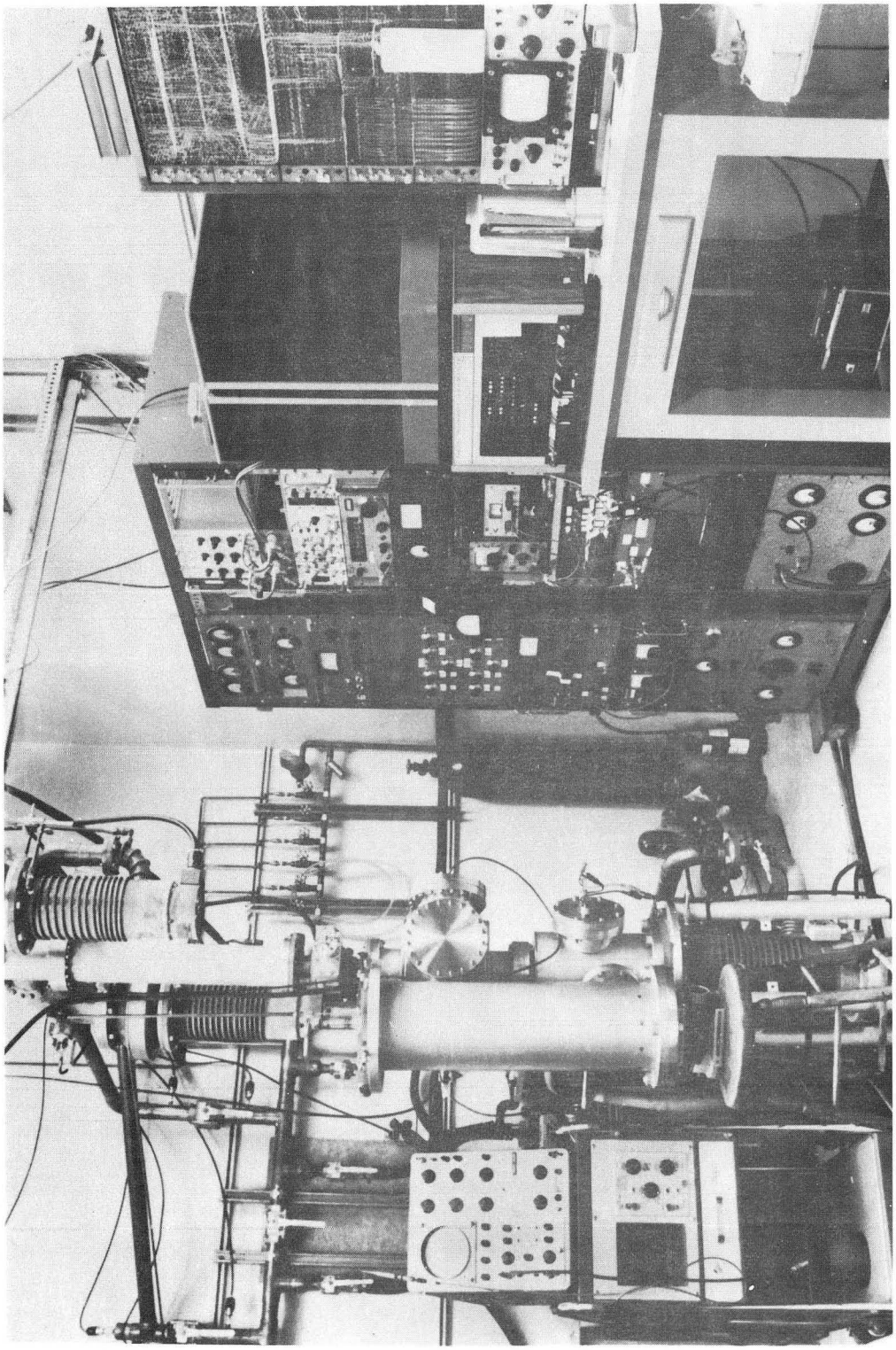

XBB 7010-4707

hole 0.25 inch in diameter, used for vacuum separation and beam collimation. This first buffer chamber contains the lamp re-entrant port and also the electric field deflection plates which can be used to learn if the beam contains fast ions. Above this chamber is the separation valve which allows one vacuum system to remain pumping while the other is opened to atmospheric pressure. Next there is a tube 23 inches long and 4 inches in diameter which can be replaced by a similar 2-inch diameter tube containing Stern-Gerlach magnet pole tips. The last chamber, containing separation plates above and below, is the second buffer chamber, providing the final vacuum isolation for the drift region.

This lower section of the machine is 77.5 inches long from the source chamber to the third collimator, and is also made entirely of stainless steel except for the brass adapting flanges on the separation valve. All ports and flanges above the source chamber are of Varian-type with copper O-rings to allow for mild baking, except at the valve and at throats of all pumps, which have viton O-rings. Each chamber has its own oil diffusion pump, and the magnet chamber and second buffer chamber each have a liquid nitrogen cryo-trap.

A Varian ionization gauge for measuring pressure is included with each diffusion pump of both sections.

B. Vacuum System

The vacuum system is divided into two separate parts by the separation valve. The lower vacuum system contains the source chamber and the first buffer chamber. The upper vacuum system contains the magnet

I. INTRODUCTION

This thesis describes an experiment designed to measure the lifetime τ of the long-lived 2^1S_0 metastable state of helium. Originally it was hoped that this experiment would become a test of the theoretical prediction of 19.5 msec (DRA 69). But, because of the difficulty with systematic errors, it is only possible to determine τ consistent with the calculated value. The experimental apparatus used is presently the most accurate available for measuring atomic lifetimes of the order of tens of milliseconds.

The primary reason for measuring lifetimes of metastable states is to increase our fundamental understanding of the properties of matter in these various electronic states. In particular the lifetime of the metastable state in question is very sensitive to the exact wavefunctions describing states that can be reached from the metastable state by means of electric dipole radiation. Such will be true of any metastable state which decays predominantly by two photons.

Metastable helium is also of interest to astrophysicists (SPI 51). In particular, metastable helium is quite abundant in the atmospheres of certain Be stars and can be used for studying various properties of these stars (ALL 54, pp. 144-148). In general, metastable states of atoms provide for much of the light emitted from planetary nebulae, where the density of matter is very tenuous ($\approx$1000 atoms/cm^3). Atoms can travel a long time before making collisions and, provided the radiation density is not too large, will live long enough to decay spon-

taneously, giving off forbidden radiation. Measuring the intensity of these forbidden lines yields information concerning the density, temperature, chemical composition, and other important properties of these non-terrestrial bodies. For instance, the two-photon decay of the $2^2S_{1/2}$ metastable state of hydrogen is used to explain the continuous emission spectra of the planetary nebulae (SPI 51).

In the past, experimenters have tried to measure metastable lifetimes using a bulb with a few microns of gas, just enough to sustain a pulsed discharge. By looking at either the electron density or the resonant absorption of light by the metastable state as a function of time after the discharge is turned off, it was hoped that one could deduce the lifetime after taking account of all possible means of losing metastable atoms in the gaseous atmosphere. This usually consists of fitting a formula of the form (GIB 63)

$$\frac{1}{T} = \frac{D}{Nd^2} + f_3N^2 + aAN - AN\frac{R}{M} + \frac{1}{T_{SE}}, \qquad (1)$$

where T is the time it takes for the metastables to decay. The first term represents the diffusion of metastables to the walls; the second term is the three-body collision rate for losing metastables; the third term is the normal two-body collision rate for the loss of metastables; and the fourth term is the two-body collision rate for producing metastables. The last term represents the natural radiative lifetime.

The more that people learned about bulb experiments, the less they tried to measure metastable lifetimes. In particular, Blevis found

that in an experiment on $Ne(^3P_2)$ he could fit his data to yield a natural lifetime of 8 msec (BLE 57), but Phelps found that he could fit similar data with the inclusion of a three-body collision rate, without considering any radiative lifetime (PHE 59). In conclusion, bulb experiments are not capable of measuring the radiative lifetime of a long-lived metastable atom.

The first beam experiment on metastable helium was performed by Pearl in 1968, in which he found that $\tau(2^1S_0) > 1.3$ msec (PEA 68). But as early as 1965, Steinberg had begun building an atomic beam machine which had two fixed, spatially separated detectors and utilized the time-of-flight method for determining lifetimes (STE 68). When completed, this metastable beam machine was found to be severely pressure-limited and was only capable of measuring a lower limit to the helium lifetime $\tau(2^1S_0) > 9$ msec. In early 1970, Pearl had completed building his second metastable beam machine in which a single traveling detector was used (PEA 70). His experiment was done in two parts: First, he measured the total attenuation of a dc beam over a distance of 1 meter using a cooled source; then he measured the average time of flight for a pulsed beam. With these two separate experiments, he calculated that

$$\tau(2^1S_0) = 38 \pm 8 \text{ msec} \tag{2}$$

with a lower limit of 30 msec. The experiment discussed in this thesis used a beam machine very similar to that built by Steinberg, and it also utilized the time-of-flight technique. The final lifetime obtained is

$$\tau(2^1S_0) = 20.2 \pm 1.0 \text{ msec}, \tag{3}$$

in satisfactory agreement with theory.

The thesis is organized with the theory for the experiment immediately following this section. Within the theory section is a brief history of calculations made on two-photon decay modes, especially emphasizing those for helium. Also contained in the theory section are the basic principles of the experiment and the analysis theory. Section III contains a complete description of the experimental apparatus, including the experimental technique of data-taking. Section IV discusses the results of checks on systematic errors and parameter dependences. The final error is calculated and conclusions given.

II. THEORY

A. History

A metastable state of an excited atom was once thought capable of existing for a very long time, only being able to change state by means of collisions of the first and second kind, absorption of radiation, or perturbation by external fields. The appearance of forbidden lines, once thought to belong to unidentified elements, initiated a large amount of research and theory on the many secondary mechanisms by which an excited state could decay. The early pioneering work was done on the unidentified lines from planetary nebulae, the sun's corona, and the polar aurora. For instance, Bowen found that some unidentified lines from nebulae were the forbidden lines of the atomic O I, N II, and O III, while the lines in the aurora were forbidden lines of O I (BOW 28). Today most of the "forbidden" lines have been examined and found to be the difference between two term values of known atoms or their multiply-ionized states. These observations provided scientists with solid evidence for the existence of second-order multipole radiation (electric quadrupole and magnetic dipole), where before, they had devoted all their attention to electric dipole radiation.

With this new attention on secondary decay mechanisms, Maria Goeppert-Mayer developed her theory of multiple quanta radiation (MAY 31). In 1940, Breit and Teller predicted the lifetime of the metastable $(2s)^2S_{1/2}$ state of hydrogen, based on a two-photon decay process, to be 143 msec (BRE 40). Because of the similarity with the $(1s2s)^1S_0$ metastable state of helium, they also predicted the lifetime of this state

to be of the order of magnitude of 143 msec, being much shorter than the other, $(1s2s)^3S_1$ metastable state of helium.

Next it was the astrophysicists who took interest in the two-photon decay mode. In 1951, Spitzer and Greenstein seized upon the theoretical prediction of two-photon decay for the hydrogen metastable to explain the continuous emission spectra observed in planetary nebulae (SPI 51, SEA 55). They also calculated the two-photon transition probability which was later found to agree with the rate $(8.226 \pm 001)Z^6$ sec^{-1} calculated by Shapiro and Breit in 1959 (SHA 59). The first laboratory evidence to support the two-photon emission process was provided by Novick in 1965 with his celebrated He^+ experiment (LIP 65). Using a coincidence counting technique, he showed that coincidence counts collected by two independent counters were correlated with the angular dependence of the counters according to $1 + \cos^2\theta$, where θ = angle between counters. This is the exact dependence expected for this two-photon decay (HAM 40).

Until the last five years, most interest in the two-photon decay process for metastable atoms centered around hydrogen. Then, in 1966, Dalgarno made his first prediction of the lifetime of the 2^1S_0 metastable state of helium, utilizing sum rules of oscillator strengths experimentally and theoretically determined (DAL 66). The lifetime obtained for $\tau(2^1S_0)$ was 22 msec. Later the same year, Dalgarno and Victor calculated the lifetime to be 12 msec, using a special sum rule with initial and final state wavefunctions obtained from the time-dependent, uncoupled Hartree Fock approximation (terms in the pertur-

bation expansion are approximated as uncoupled) which is a simpler but less accurate method of calculation (DAL 66a). In 1967, Victor calculated that $\tau(2^1S_0)$ = 20 msec using wavefunctions obtained from the time-dependent, coupled Hartree Fock approximation, which is tedious but accurate (VIC 67). The most recent and most accurate calculation, made by Drake, Victor, and Dalgarno, gives $\tau(2^1S_0)$ = 19.5 msec (DRA 69). In this calculation, correlation-type wavefunctions are used, in which the positions of the two electrons are correlated by including a dependence on the distance between electrons.

These authors also predict that the two-photon decay mode for the 2^3S_1 helium metastable state should have a lifetime of $2.5 \cdot 10^8$ sec (DRA 69). But much skepticism has developed concerning two-photon emission as the most probable mode of decay for this state. Schwartz claims that this state can also decay by relativistically allowed magnetic dipole radiation with an expected lifetime of 10^5 sec (SCH 69).

B. Terminology

The metastable state of a given atomic electron configuration is defined as one which is very long-lived and can only be connected by a transition to a lower energy state by emitting forbidden radiation (or highly improbable electric dipole radiation). There have been many definitions of forbidden radiation since its discovery.

(a) All spectral lines are divided into two groups: those which satisfy all selection rules are called permitted lines and all others are forbidden (BAT 62).

(b) Forbidden radiation has low transition probability, 10^2 sec^{-1} or less (BOW 36).

(c) Forbidden radiation has very small transition probability as compared with the probability of the strongest lines in levels with similar quantum numbers, their ratio being 10^{-3} to 10^{-4} (MRO 44).

(d) All transitions which violate rigorous electric dipole selection rules in free atoms are forbidden (BAT 62).

(e) All transitions which violate any electric dipole selection rule for free atoms are forbidden (HER 44).

Definition (a) does not include higher-order multipole radiation as forbidden. Definition (b) does not make allowance for change in transition probability with quantum numbers. Though definition (c) makes up for this shortcoming, it still leads to a classification system involving certain difficulties (lack of precision, for instance). Definition (d) is commonly used by spectroscopists who do not want to include intercombination lines as being forbidden. Definition (e) is another commonly used definition which does include intercombination lines; and this is the definition used in this thesis.

C. Selection Rules

Selection rules are derived from the evaluation of the matrix elements appearing in the expressions of transition probability A. Any condition which predicts that the transition probability for a given type of radiation shall vanish leads to a selection rule. The more common multipole radiations have the following transition probabilities:

$$A_d = \frac{64\pi^4\nu^3}{3hc^3} \sum_{a,b} |\langle a|\vec{P}|b\rangle|^2 \qquad \text{E1 Type}$$

$$A_m = \frac{64\pi^4\nu^3}{3hc^3} \sum_{a,b} |\langle a|\vec{M}|b\rangle|^2 \qquad \text{M1 Type}$$

$$A_q = \frac{32\pi^6\nu^5}{5hc^5} \sum_{a,b} |\langle a|\overleftrightarrow{Q}|b\rangle|^2 \qquad \text{E2 Type} \qquad (4)$$

where

$$\vec{P} = -e \sum_i \vec{r}_i$$

$$\vec{M} = \mu_B \sum_i (\vec{L}_i + 2\vec{S}_i)$$

$$Q_{\alpha\beta} = \frac{1}{3} \sum_i e_i (3x_{i\alpha}x_{i\beta} - r_i^2\, \delta_{\alpha\beta}) \ .$$

An energy level in the initial state is represented by the eigenvector $|a\rangle$, and an energy level in the final state is represented by the eigenvector $|b\rangle$. The frequency of the transition is ν.

These matrix elements were first computed by Rubinowicz et al. in 1932 (RUB 32), and since then by many authors. Table 1 gives a summary of the selection rules for the common types of radiation encountered in atomic spectroscopy as well as some rules for arbitrary multipoles. These rules are divided into three groups. The first group consists of rules (1), (2), and (3), which are called rigorous or general selection rules. They always hold in the absence of nuclear perturbations or the two-photon process. The second group consists of rules (4) and (5), which hold only for the LS coupling scheme. Hence, they hold only in degrees, since LS coupling is an approximation to all

Table 1. Selection rules.

	Electric Dipole (E1)	Magnetic Dipole (M1)	Electric Quadrupole (E2)	General 2^k-pole, Mk = magnetic, Ek = electric
(1)	$\Delta J = 0, \pm 1$ not $0 \leftrightarrow 0$	$\Delta J = 0, \pm 1$ not $0 \leftrightarrow 0$	$\Delta J = 0, \pm 1, \pm 2$ not $0 \leftrightarrow 0$, $\frac{1}{2} \leftrightarrow \frac{1}{2}$, $0 \leftrightarrow 1$	$\Delta J = 0, \pm 1, \pm 2, \cdots, \pm k$ $J_i + J_f \geq k$
(2)	$\Delta M = 0, \pm 1$	$\Delta M = 0, \pm 1$	$\Delta M = 0, \pm 1, \pm 2$	$\Delta M = 0, \pm 1, \pm 2, \cdots, \pm k$
(3)	Parity change	No parity change	No parity change	Parity for k: Mk: even — Change; odd — No change Ek: even — No change; odd — Change
(4)	$\Delta S = 0$	$\Delta S = 0$	$\Delta S = 0$	$\Delta S = 0$
(5)	$\Delta L = 0, \pm 1$ not $0 \leftrightarrow 0$	$\Delta L = 0$	$\Delta L = 0, \pm 1, \pm 2$ not $0 \leftrightarrow 0$, $0 \leftrightarrow 1$	Ek: $\Delta L = 0, \pm 1, \pm 2, \cdots, \pm k$ $L_i + L_f \geq k$ Mk: $\Delta L = 0, \pm 1, \pm 2, \cdots, \pm (k-1)$ $L_i + L_f \geq k-1$
(6)	One electron jump $\Delta \ell = \pm 1$	No electron jump $\Delta \ell = 0$ $\Delta n = 0$	One or no electron jump $\Delta \ell = 0, \pm 2$	

real cases of electron coupling. The third group consists on rule (6) and it holds only when configuration interaction can be neglected, which is again an approximation of degree.

D. Lifetimes and Decay Mechanisms

Consider an initial energy level i which may consist of w_i degenerate sublevels and similarly a final state f which may have w_f degenerate sublevels. If A_{nm} is the probability for spontaneous emission from the nth sublevel of level i to the mth sublevel of level f, then

$$\frac{1}{\tau_i} = \sum_{\substack{\text{final} \\ \text{states } f}} \sum_{n=1}^{w_i} \sum_{m=1}^{w_f} \frac{1}{w_i} A_{nm} \tag{5}$$

and, in the case that all $A_{nm} = A_{ij}$ for $n = 1, \cdots, w_i$ and $m = 1, \cdots, w_f$,

$$\frac{1}{\tau_i} = w_f \sum_{\substack{\text{final} \\ \text{states } f}} A_{ij} \ . \tag{6}$$

In general,

$$A_{nm} = \sum_k A_{nm}^k \ , \tag{7}$$

where k is a representative index running through all decay mechanisms available for spontaneous emission. Besides the allowed E1 radiation, there are (1) radiation of the pure E2 or pure M1 types, (2) radiation-violating LS coupling rules, (3) enforced dipole radiation due to

external fields, (4) radiation due to electron coupling with nuclear spin, and (5) two-photon decay radiation. A^k_{nm} for the types E1, M1, and E2 are listed in Eq. 4. A good discussion of each can be found in Atomic and Molecular Processes by Bates (BAT 62). It is primarily the last mechanism which concerns the remainder of this thesis.

E. Helium Metastable States

The lowest-lying energy levels of helium are shown in Fig. 1. In the orthohelium system (triplets) the $(1s2s)^3S_1$ state is the effective ground state. The only transition possible is the intercombination of $2^3S_1 \rightarrow 1^1S_0$. For many years after the discovery of forbidden lines, it was thought that this transition could occur only by two-photon emission with a transition probability between 10^{-8} and 10^{-9} sec^{-1}. Since parity does not change, the transition cannot occur by emitting electric dipole radiation. And since this is a $J = 1 \rightarrow J = 0$ transition it cannot be accomplished by emitting electric quadrupole radiation. The transition does satisfy all the rigorous selection rules for magnetic dipole radiation, but since LS coupling is an excellent approximation for helium, the selection rule $\Delta S = 0$ would be violated for pure M1 radiation. The selection rule requiring no electron jump would also be violated. The rule $\Delta S = 0$ can be bypassed by considering the 2^3S_1 multiplet of the (1s2s) configuration to be weakly mixed with the $^3P_1$ multiplet of the (2p3p) configuration by the very small spin orbit interaction (coefficients $\approx 10^{-5}$). Also, the $(1s^2)^1S_0$ has a weak admixture of $(2p3p)^3P_0$. Thus the ratio of this M1 transition probability to

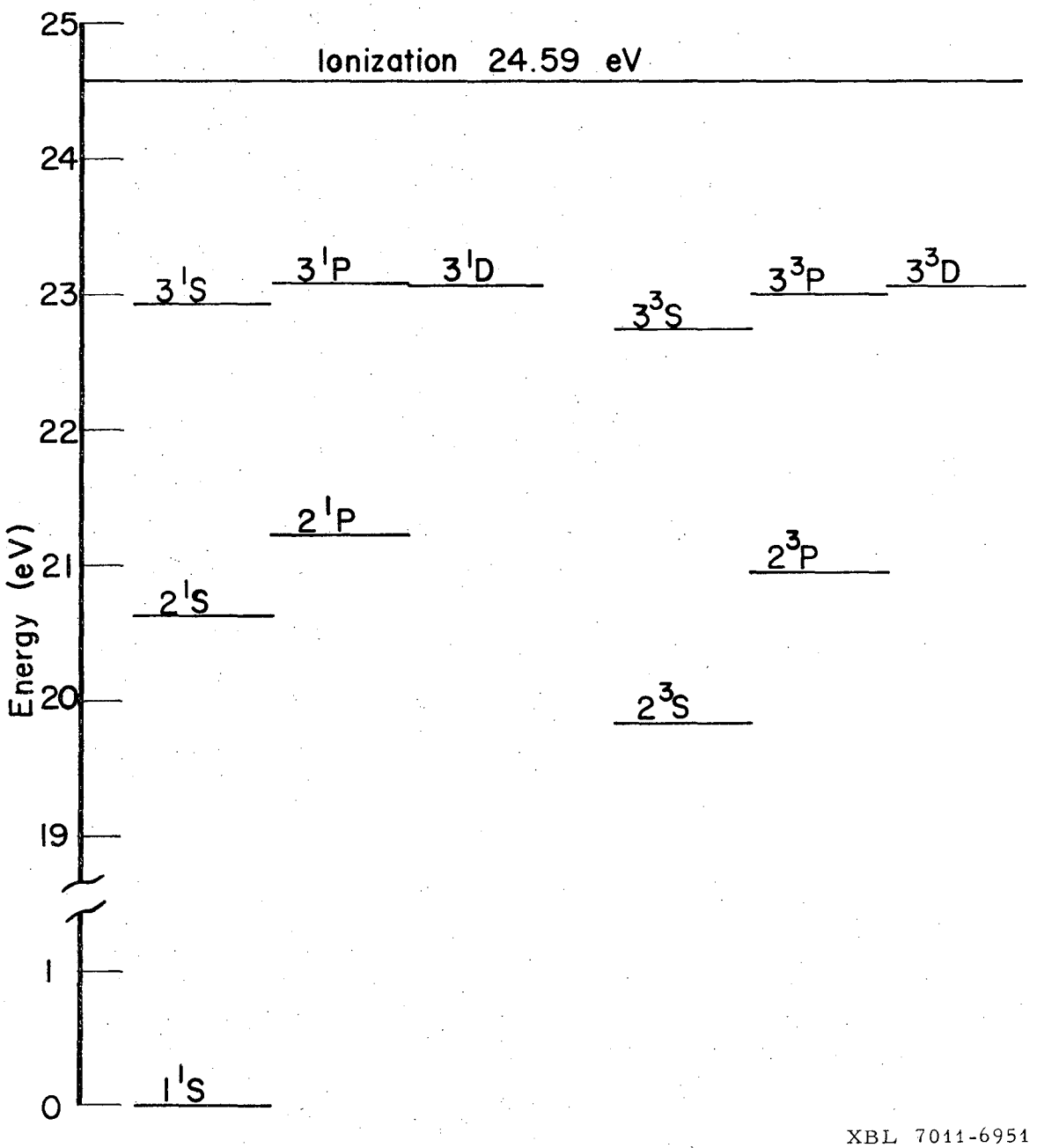

Fig. 1. Energy level diagram for helium showing the lowest-lying states of both the singlet system and the triplet system.

that for E1 radiation with a typical unit oscillator strength is about 10^{-24}; hence $\tau \approx 10^{16}$ sec if this were the only decay mode. The rule $\Delta n = 0$ is weakly violated by considering relativistic wavefunctions. The calculation using relativistic operators was made for the hydrogen metastable state $2^2S_{1/2}$ decaying to the ground state giving off relativistic M1 radiation and was found to have a transition probability $= 5 \cdot 10^{-6}$ sec^{-1} (BRE 40). Recently, Schwartz demonstrated that there are spin-dependent relativistic correction operators to the magnetic dipole operator which allows a non-zero relativistic magnetic dipole transition to exist directly between the 2^3S_1 state and the 1^1S_0 ground state of helium. He found that the corresponding transition probability $= 10^{-5}$ sec^{-1} (SCH 69). Hence the 2^3S_1 metastable state decays by relativistic M1 radiation with mean life approximately 10^5 sec.

The $(1s2s)^1S_0$ state lies above both $(1s2s)^3S_1$ and $(1s^2)^1S_0$ states. The same arguments given for $2^3S_1 \rightarrow 1^1S_0$ apply to $2^1S_0 \rightarrow 2^3S_1$ intercombination which is subsequently very improbable also (actually having probabilities 10^{-5} smaller due to smaller energy differences). The only other possibility is the $2^1S_0 \rightarrow 1^1S_0$ transition. Since this is a $J = 0 \rightarrow J = 0$ transition, it is rigorously forbidden for all orders of single-photon multipole radiation. The next most probable decay mechanism available is the emission of two E1 photons (hence, no total parity change). The best calculation for this transition is 19.5 msec, which is much shorter than the lifetime of the triplet metastable atom. Hence, relative to the singlet lifetime, the triplet lifetime is essentially infinite.

F. 2^1S_0 Helium Lifetime

As discussed in the previous section, the 2^1S_0 state of helium must decay by two photons. Thus the expression for the probability of emitting two photons spontaneously, with one photon having a frequency between ν_1 and $\nu_1 + d\nu_1$, is the following (see Appendix A):

$$A(\nu_1)d\nu_1 = \frac{2^{10}\pi^6 e^4}{h^2 c^6} \nu_1^3 (\frac{E}{h} - \nu_1)^3 \, |M_{fi}|^2_{av} \, d\nu_1 \tag{8}$$

where, by conservation of energy,

$$\begin{aligned} E &= h\nu_1 + h\nu_2 \\ &= E_i - E_f \, . \end{aligned} \tag{9}$$

The average must be taken over the directions of propagation and over the directions of polarization $\hat{\varepsilon}$, independently for both photons. The expression for the large matrix element M_{fi} is

$$M_{fi} = \sum_n \left[\frac{(\hat{\varepsilon}_1 \cdot \vec{r})_{fn} \, (\hat{\varepsilon}_2 \cdot \vec{r})_{ni}}{\nu_{ni} + \nu_2} + \frac{(\hat{\varepsilon}_2 \cdot \vec{r})_{fn} \, (\hat{\varepsilon}_1 \cdot \vec{r})_{ni}}{\nu_{ni} + \nu_1} \right] , \tag{10}$$

where subscript f refers to the final 1^1S_0 state and the subscript i refers to the initial 2^1S_0 state. Energy $h\nu_{ni}$ is the difference between intermediate and initial state energies (Appendix A). The summation over n is carried out over all possible real intermediate states of the atom, including states in the continuum. Since matrix elements representing allowed electric dipole transitions will usually be far greater in magnitude than those representing any other decay modes, the inter-

mediate states must be only those which can be reached from the 2^1S_0 state (and also the 1^1S_0) by absorption of a single photon with one unit of angular momentum. This criterion is well satisfied by the n^1P states in helium which are therefore the ones to enter into the summation over n. Thus, terms like $(\hat{\varepsilon}_1 \cdot \vec{r})_{fn}$ are the usual electric dipole matrix elements in which $\vec{r}$ is the vector sum of the position vectors representing each of the two electrons in the helium atom.

To arrive at the total emission probability, the expression in Eq. 8 must be integrated over frequency ν, since one does not measure this frequency in a lifetime experiment. Thus

$$A_T = \frac{1}{2} \int_0^{E/h} A(\nu_1) d\nu_1 \tag{11}$$

where the 1/2 faction comes from counting photon-1 twice in the frequency interval [0, E/h]. And, since two-photon emission is the most predominant decay mode for the 2^1S_0 state, all other factors in Eq. 7 can be ignored; thus, from Eq. 6:

$$\tau(2^1S_0) = \frac{1}{A_T} . \tag{12}$$

In applying Eq. 8 to the 2^1S_0 state, fine structure and hyperfine structure were ignored since nuclear and electronic spin both equal zero. But even if the experiment were carried out on He^3 (I = 1/2), hyperfine structure could still be ignored, since the operator $\vec{r}$ is diagonal with respect to nuclear spin (and also electronic spin). Thus, each n^1P_1 level is only triply degenerate and one usually represents

each of the three linearly independent states by eigenfunctions ξ, η, and ζ (normally called P-functions), which have the transformation properties of the x, y, and z cartesian coordinates respectively (FAL 67). Now, one carries out the summation in Eq. 10 in two parts. First, the summation over the three degenerate energy levels of a given n^1P state contributes terms like

$$\sum_{\xi,\eta,\zeta} (\hat{\varepsilon}_1\cdot\vec{r})_{fn}\,(\hat{\varepsilon}_2\cdot\vec{r})_{ni} = (\hat{\varepsilon}_1\cdot\vec{r})_{f\xi}\,(\hat{\varepsilon}_2\cdot\vec{r})_{\xi i} + (\hat{\varepsilon}_1\cdot\vec{r})_{f\eta}\,(\hat{\varepsilon}_2\cdot\vec{r})_{\eta i} + (\hat{\varepsilon}_1\cdot\vec{r})_{f\zeta}\,(\hat{\varepsilon}_2\cdot\vec{r})_{\zeta i}\ . \quad (13)$$

Now expand the dot products and multiply out all expressions, to give a total of 27 terms. Because of the choice of basis eigenfunctions and the fact that all directions are equivalent, it follows that

$$x_{f\xi}\,x_{\xi i} = y_{f\eta}\,y_{\eta i} = z_{f\zeta}\,z_{\zeta i}$$
$$x_{f\eta} = x_{f\zeta} = \cdots = 0. \quad (14)$$

Then Eq. 13 collapses to the following:

$$\sum_{\xi,\eta,\zeta} (\hat{\varepsilon}_1\cdot\vec{r})_{fn}\,(\hat{\varepsilon}_2\cdot\vec{r})_{ni} = z_{f\zeta}\,z_{\zeta i}(\varepsilon_{1x}\,\varepsilon_{2x} + \varepsilon_{1y}\,\varepsilon_{2y} + \varepsilon_{1z}\,\varepsilon_{2z})$$
$$= (\hat{\varepsilon}_1\cdot\hat{\varepsilon}_2)z_{f\zeta}\,z_{\zeta i}\ . \quad (15)$$

Now, Eq. 10 can be simplified to

$$M_{fi} = (\hat{\varepsilon}_1\cdot\hat{\varepsilon}_2)\sum_{n=2} z_{fn}\,z_{ni}\left(\frac{1}{\nu_{ni}+\nu_2} + \frac{1}{\nu_{ni}+\nu_1}\right) \quad (16)$$

where the index n refers only to the principle quantum number of the

intermediate ^1P state and z_{fn} refers to the matrix element

$$\langle f|z|n, \text{ type } \zeta\rangle$$

and similarly for z_{ni}.

The expression $\hat{\varepsilon}_1 \cdot \hat{\varepsilon}_2$ shows the statistical relationship between the directions of polarization of the two photons. Thus the emission probability is proportional to the square of the cosine of the angle between the polarization directions. The necessary average over polarization directions is given by the integral

$$\int_{\substack{\text{all}\\ \text{directions}}} \cos^2\theta \, \frac{d\Omega}{4\pi}$$

whose value is 1/3. Thus Eq. 8 becomes

$$A(\nu_1)d\nu_1 = \frac{2^{10}\pi^6 e^6}{3h^2c^6} \nu_1^3 (E-\nu_1)^3 \left| \sum_{n=2} z_{fn} z_{ni} \left(\frac{1}{\nu_{ni}+\nu_1} + \frac{1}{\nu_{ni}+\frac{E}{h}-\nu_1} \right) \right|^2_{av} d\nu_1 , \tag{17}$$

where the summation extending into the continuum is understood.

Equation 17 provides the starting point for most theoretical calculations of the 2^1S_0 lifetime. It is possible to follow the procedure of Breit and Teller (BRE 40) and evaluate each matrix element z_{ni} and z_{fn} with known or approximate wavefunctions, carrying out the summation into the continuum. Or one could follow the method of Dalgarno's first calculation (DAL 66) in which the matrix elements of z are obtained from electric dipole oscillator strengths f_{1n} and f_{2n} for transi-

tions from the ground state and metastable state, respectively:

$$\langle 2^1S|z|n^1P\rangle = \left[\frac{f_{2n}}{E_2 - E_n}\right]^{\frac{1}{2}}$$

$$\langle n^1P|z|1^1S\rangle = \left[\frac{f_{1n}}{E_1 - E_n}\right]^{\frac{1}{2}} . \tag{18}$$

Subscripts 1 and 2 now refer to the initial and final states respectively. In latter calculations, Dalgarno used sum rules to get around having to calculate the wavefunctions for the intermediate states. Define the sum $T(\omega)$, with E_n as the eigenvalue of the intermediate state and $\{\psi_n\}$ constituting a complete set of eigenfunctions for the two-electron Hamiltonian $\mathcal{H}$ as follows:

$$T(\omega) = \sum_n \frac{\langle\psi_2|z|\psi_n\rangle\langle\psi_n|z|\psi_1\rangle}{E_n + \omega} \tag{19}$$

where it is arranged that $\langle\psi_1|z|\psi_1\rangle = \langle\psi_2|z|\psi_2\rangle = 0$. Then Eq. 19 can be evaluated using an elementary sum rule (DAL 63) of the form

$$T(\omega) = -\langle\chi_2|z|\psi_1\rangle$$

where

$$(\mathcal{H} + \omega)\chi_2 + z\psi_2 = (E_2 + \omega)\langle\chi_2|\psi_2\rangle\psi_2 \; , \tag{20}$$

or a similar set of formulas with index 1 and 2 interchanged. Eq. 20 is solved by finding the stationary value of the functional

$$J = \langle\chi_2|\mathcal{H}+\omega|\chi_2\rangle - (E_2+\omega)\langle\chi_2|\psi_2\rangle^2 + 2\langle\chi_2|\, z\, |\psi_2\rangle \tag{21}$$

with respect to a trial form of χ_2.

The wavefunctions ψ_1 and ψ_2 are then determined using either the uncoupled Hartree-Fock Approximation (DAL 66a) or the coupled Hartree-Fock Approximation (VIC 67). With reference to Eq. 17, ω is replaced by $-E_1 + h\nu_1$ or $-E_2 - h\nu_1$. All equations are solved using variational methods and the integral in Eq. 11 is evaluated numerically.

The best calculation to date is that by Drake, Victor, and Dalgarno (DRA 69), in which the infinite summation over intermediate states in Eq. 17 is performed by replacing the true eigenfunctions by a discrete set of correlation-type variational functions, where each function of the set has the form:

$$\psi^{LSM_L}(n) = (2)^{-\frac{1}{2}} (1+P_{12}) \sum_{ijk}^{N} a_{ijk}^{LS}(n)\ \phi_{ijk}^{LS}(\vec{r}_1,\vec{r}_2)\ \mathcal{Y}_{L\ell_1\ell_2}^{M_L}(\hat{r}_1,\hat{r}_2) \qquad (22)$$

for $n = 1, \cdots, N$ where

$$\mathcal{Y}_{L\ell_1\ell_2}^{M_L}(\hat{r}_1,\hat{r}_2) = \sum_{m_1 m_2} \langle \ell_1 m_1 \ell_2 m_2 | LM_L \rangle\ Y_{\ell_1 m_1}(\hat{r}_1) Y_{\ell_2 m_2}(\hat{r}_2)$$

$$\phi_{ijk}^{LS}(\vec{r}_1,\vec{r}_2) = r_1^i\ r_2^j\ r_{12}^k \exp(-\alpha^{LS} r_1 - \beta^{LS} r_2)$$

and quantities $\langle \ell_1 m_1 \ell_2 m_2 | LM_L \rangle$ with subscripts 1 and 2 referring to individual electrons, are vector coupling coefficients. The operator P_{12} generates interchange of electrons 1 and 2 and the quantities $a_{ijk}^{LS}(n)$ are the expansion coefficients. The parameters α and β are chosen to minimize the energy of the second root of each symmetry. All necessary integrals are evaluated analytically in closed form.

G. Principle of the Experiment

The experiment designed to measure this 2^1S_0 lifetime of helium is illustrated schematically in Fig. 2. The detectors must be able to detect only metastable atoms, and discriminate against neutrals. Thus, it is assumed that only metastable atoms exist in the beam and that uv-light photons, which can also be detected, are absent. The first detector must be partially transmitting in such a way that a random sample of atoms in the beam is detected at each position. An electron gun is used to pulse the beam, subsequently giving both a singlet and a triplet speed distribution of metastable helium atoms. In order to separate the effects of the two components, a helium rf-discharge lamp is turned on and off for alternate collection cycles. When the lamp is on, the 2^1S_0 metastable atoms are quenched, leaving the triplets unaffected (FRY 69). By taking the difference between the two collections, only the singlets will be analyzed.

The formalism for the analysis theory is first outlined for the general case of a pulse containing many different types of metastable atoms created instantaneously by the electron gun at a single point at time $t = 0$. Then, the theory will be applied to the case of helium, showing how the lifetime τ of the 2^1S_0 state can be determined.

1. General Formalism

Define $t_i = d_i/v$ as the time at which an atom of speed v arrives at detector i, at a distance d_i from the source where $i = 1,2$ stands for the lower and upper detectors respectively. It will be necessary to examine only those atoms whose speed lies between v and $v + \delta v$ at each

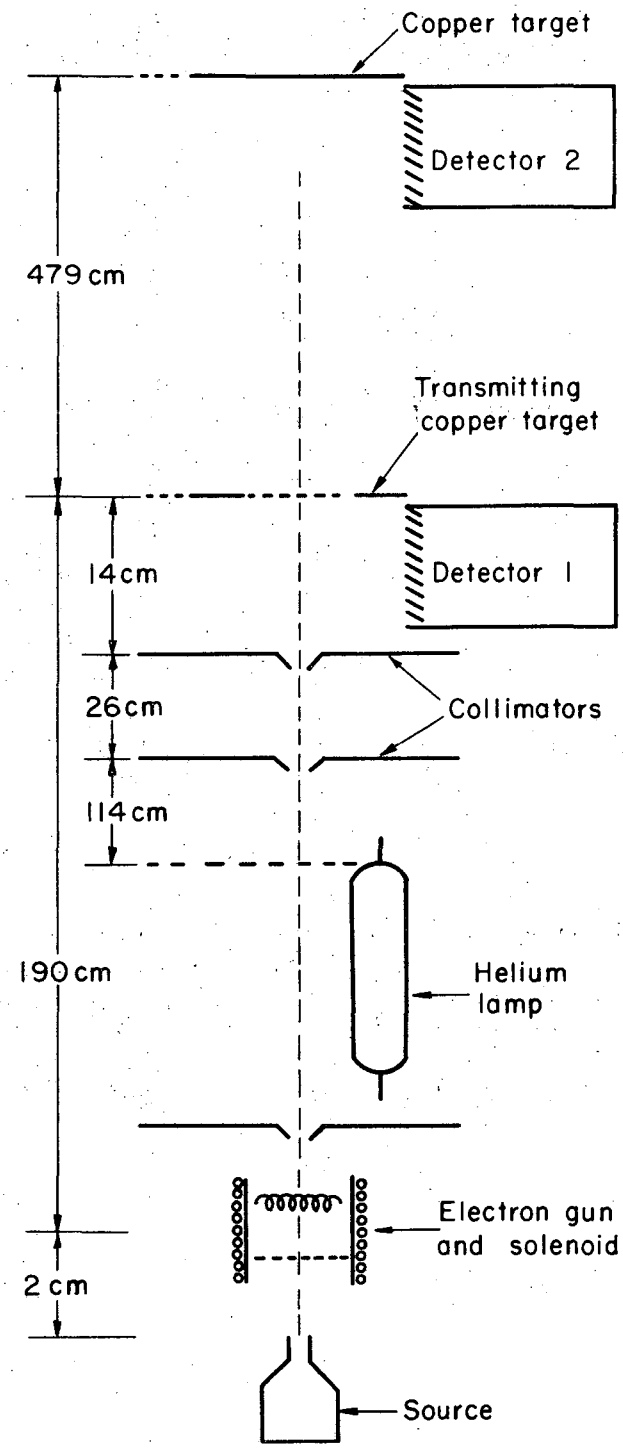

XBL708-3681

Fig. 2. Schematic diagram of the time-of-flight apparatus. Helium atoms effusing from a cooled source are metastabilized by an anti-parallel electron beam, collimated, and then detected at detectors 1 and 2; the discharge lamp allows the separation of the 2^1S_0 and the 2^3S_1 metastable states. A determination of the number of 2^1S_0 atoms decaying between the two detectors gives the radiative lifetime.

detector and the size of δv will be determined later. Thus only the counts which arrive between t_i and $t_i + \delta t_i$ are considered where $\delta t_i = (d_i/v^2)\delta v$. In order to include the possibility of scattering from the initial beam during flight to detector i, define the nonscattered fraction of the beam with speed v to be $\beta_i^k(v)$ for the kth type of metastable atom. Let $N_o^k(v)$ be the initial speed distribution of the kth type of metastable atoms at t = 0. Then the number of the kth type which have survived to reach detector 1 in the speed interval δv is

$$\beta_1^k(v)\ N_o^k(v)\ e^{-t_1/\tau_k}\ \delta v \tag{23}$$

where the simple decay formula

$$\frac{dn}{dt} = -\frac{n}{\tau} \tag{24}$$

provides for the experimental decay factor with mean life τ_k (a single factor being associated with each type of metastable). Also, it is assumed that the first detector intercepts a fraction r_1 of the beam randomly, leaving the fraction r_2 to be transmitted to the second detector, where

$$r_1 + r_2 = 1\ . \tag{25}$$

Then, multiplying the expression (23) by r_1 gives those metastable atoms of the kth type capable of being seen at detector 1, and a similar expression exists for detector 2.

In general, the efficiency per unit area for a metastable atom of type k with speed v to eject an electron from the point (x,y) of the

copper target i (Fig. 2), and subsequently have this electron collected by the detector i to become a single pulse, is defined to be $\varepsilon_i^k(x,y,v)$. The usual number of electrons per incident metastable atom of type k falling on an increment of area dxdy is $\varepsilon_i^k dxdy$. Thus the number of metastable atoms of the type k counted at detector i with speed between v and v + δv is

$$N_i^k(v)\delta v = \int_{S_i} r_i \beta_i^k(v)\ \varepsilon_i^k(x,y,v)\ N_o^k(x,y,v)\ e^{-t_i/\tau_k}\ dxdy\delta v \tag{26}$$

where N_o^k may also be explicitly a function of position on the detector if each point, for some reason, does not see the same speed distribution. S_i is the beam's entire cross-sectional area intersected by target i. Then, each detector registers a count rate n_i at detector i and at time t_i given by

$$n_i(t_i) = \sum_k N_i^k(t_i)\ \frac{d_i}{t_i^2} \tag{27}$$

where the size of δv, and thus δt_i, must be small enough that the various factors in Eq. 26 can be taken as constant for any speed v between v and v + δv. Then, by fitting the function

$$R(t_1,t_2) = \frac{n_2(t_2)}{n_1(t_1)}\ , \tag{28}$$

where $t_2/t_1 = d_2/d_1$, to experimental data collected at many sets of times (t_1,t_2), the lifetime can be obtained for the metastable atoms of

type k.

2. Helium

Let f(v) be the probability of quenching a 2^1S_0 metastable atom (k = 1) with speed v. Then, with the quench lamp on, the number of 2^1S_0 atoms arriving at detector i in δv becomes

$$r_i \beta_i^1(v)[1-f(v)]\, N_0^1(x,y,v) e^{-t_i/\tau_1}\, \delta v \ . \tag{29}$$

Thus, from Eq. 26,

$$[N_i^1(v)]_{on} \delta v = r_i \beta_i^1(v)[1-f(v)] e^{-t_i/\tau_1}\, \delta v \int_{S_i} N_0^1(x,y,v)\ \varepsilon_i^1(x,y,v)\, dxdy \ . \tag{30}$$

Since it is desirable for as many functions of v to cancel in Eq. 28, some assumptions must be made about the various factors in Eq. 30. The most important assumption is that the speed distribution N_o^k be uniform across the metastable beam; that is,

$$N_o^k(x,y,v) = N_o^k(0,0,v) \equiv N_o^k(v) \ . \tag{31}$$

There is experimental evidence, though, that this assumption is not entirely valid, as will be discussed in Section IV. This position dependence arises because of the excitation process occurring in the electron gun. A review of this excitation mechanism can be found in Appendix B. Essentially, the speed v of atoms excited along a given observation angle depends directly upon the angle of incidence of the neutral atom, before collision with an energetic electron. And, since a different area of the gun can have a

different set of angles of incidence, a different speed distribution arises. Then, because different positions on the target surface can see different portions of the gun (an extended source), each position will see a slightly different speed distribution.

When the assumption leading to Eq. 31 is valid, it is very reasonable that ε_i^k will be independent of speed. Indeed, ε_i^k would depend implicitly on v if each position on the detector has a different set of beam speeds associated with it. It need, however, only be assumed that the exact mechanism for electron ejection from the target be independent of the speed of the metastable atom approaching the surface, which does appear to be the case for the range of thermal speeds detected. Now, defining $\bar{\varepsilon}_i^k$ as the integral of $\varepsilon_i^k(x,y)$ over the beam cross section, it follows that

$$[N_i^1(v)]_{on}\delta v = r_i\beta_i^1(v)[1-f(v)]e^{-t_i/\tau_1}\ \bar{\varepsilon}_i^1\ N_0^1(v)\ \delta v\ ; \tag{32}$$

$$[N_i^1(v)]_{off}$$

has a similar expression with f = 0. Using Eq. 27,

$$[n_i(v)]_{on} = \frac{d_i}{t_i^2}\,[N_i^1(v)]_{on} + \frac{d_i}{t_i^2}\,N_i^3(v) \tag{33}$$

where, as originally assumed, the triplets (k = 3) are unaffected by the quench lamp. Upon taking the difference between the lamp-off count rate and the lamp-on count rate, the resulting effective rate $n_i(t_i)$ at

detector i and at time t_i is

$$n_i(t_i) = \frac{d_i}{t_i^2} r_i \beta_i^1(v) N_o^1(v) f(v) \bar{\varepsilon}_i^1 e^{-t_i/\tau_1} , \tag{34}$$

where, as usual, $v = d_i/t_i$.

Now applying Eq. 28:

$$R(t_1,t_2) \equiv R(t) = \frac{d_1 r_2 \bar{\varepsilon}_2^1}{d_2 r_1 \bar{\varepsilon}_1^1} \frac{\beta_2^1(v)}{\beta_1^1(v)} e^{-t/\tau} \tag{35}$$

where $\tau = \tau_1$ and $t = t_2 - t_1$, usually referred to as the time of flight between detectors for atoms of speed v. The important result here is that the ratio is independent of the modified speed distribution $f(v)N_o^1(v)$, which therefore can have any form.

The factor $\beta_i^k(v)$ is equal to the expression

$$\exp[-\int_{L_i} \eta(x) \sigma^k(v,x) dx]$$

where $\eta(x)$ is a continuously defined density of scattering centers along the beam path L_i to the detector i and, similarly, $\sigma^k(v,x)$ is the scattering cross section as a function of x along the path L_i for a metastable atom of type k with speed v. Thus,

$$\beta_2^k(v) = \exp(-\int_0^{L_1} \eta\sigma dx) \exp(-\int_{L_1}^{L_2} \eta\sigma dx) \tag{36}$$

$$= \beta_1^k(v) \beta^k(v)$$

where the second factor represents the nonscattered fraction surviving the flight between detectors.

Thus Eq. 35 simplifies to

$$R(t) = C\ \beta^1(v)\ e^{-t/\tau} \tag{37}$$

where

$$C = \frac{d_1 r_2 \bar{\varepsilon}_2^1}{d_2 r_1 \bar{\varepsilon}_1^1} = \text{constant} .$$

To force $\beta^1(v) \to 1$, one must reduce the density of scattering centers to zero. This can be effectively accomplished by lowering the pressure to a value such that

$$\eta\sigma \leq 2\cdot 10^{-6}\ \text{cm}^{-1}$$

for

$$1.0 \geq \beta^1 \geq 0.999 .$$

If one takes $\sigma \approx 100$ Å^2 (which may be realistic since $\sigma(^3S_1) = 145$ Å^2 [MUS 66]), then η must be $\leq 2\cdot 10^8$ atoms/cc or the pressure $\leq 5\cdot 10^{-9}$ torr, a condition which is basic to the time-of-flight principle which assumes that only radiative decay can occur for an atom of speed v drifting between the two fixed detectors. The problem of a pressure effect on the lifetime τ will also be analyzed in Section IV.

In summary, by counting all atoms with speed between **v** and $v + \delta v$ arriving at each detector and taking their ratio, Eq. 37 for $\beta^1 = 1$ then provides a curve of points where the speed v is incremented by a small amount from point to point. The slope of the log of the

above-defined curve is then $-1/\tau$.

III. EXPERIMENT

A. General Description

Displaying all essential components, Fig. 3a and 3b give an overall view of the entire beam machine. Fig. 4 is a photograph of the actual equipment. Basically, the machine is divided into two functionally different sections by the third collimator. The vacuum system is separated into two independent systems by the 2-inch gate valve, shown in Fig. 3b. The machine is also oriented vertically such that the atomic beam experiences negligible deflection due to gravity over the entire flight path.

The upper section of the machine shown in Fig. 3a constitutes the free drift region above the third collimator and is entirely bakeable. A detector chamber is located at each end of the flight tube, which is totally 197 inches in length and 4 inches in diameter, is made of stainless steel and has Varian-type flanges with copper O-rings for making vacuum seals. The drift tube is evacuated by three oil diffusion pumps, each with a liquid nitrogen cryo-trap.

The lower section of the machine shown in Fig. 3b contains the source, the metastabilizer, the lamp, the separation gate valve, and the buffering chambers. A support stand is attached to the lowest chamber which effectively holds the entire machine. Cross-supports assure that the machine remains vertical. Contained within the lowest chamber are both the electron gun assembly and the source assembly. Separating the source chamber from the buffer chamber above is a plate with a center

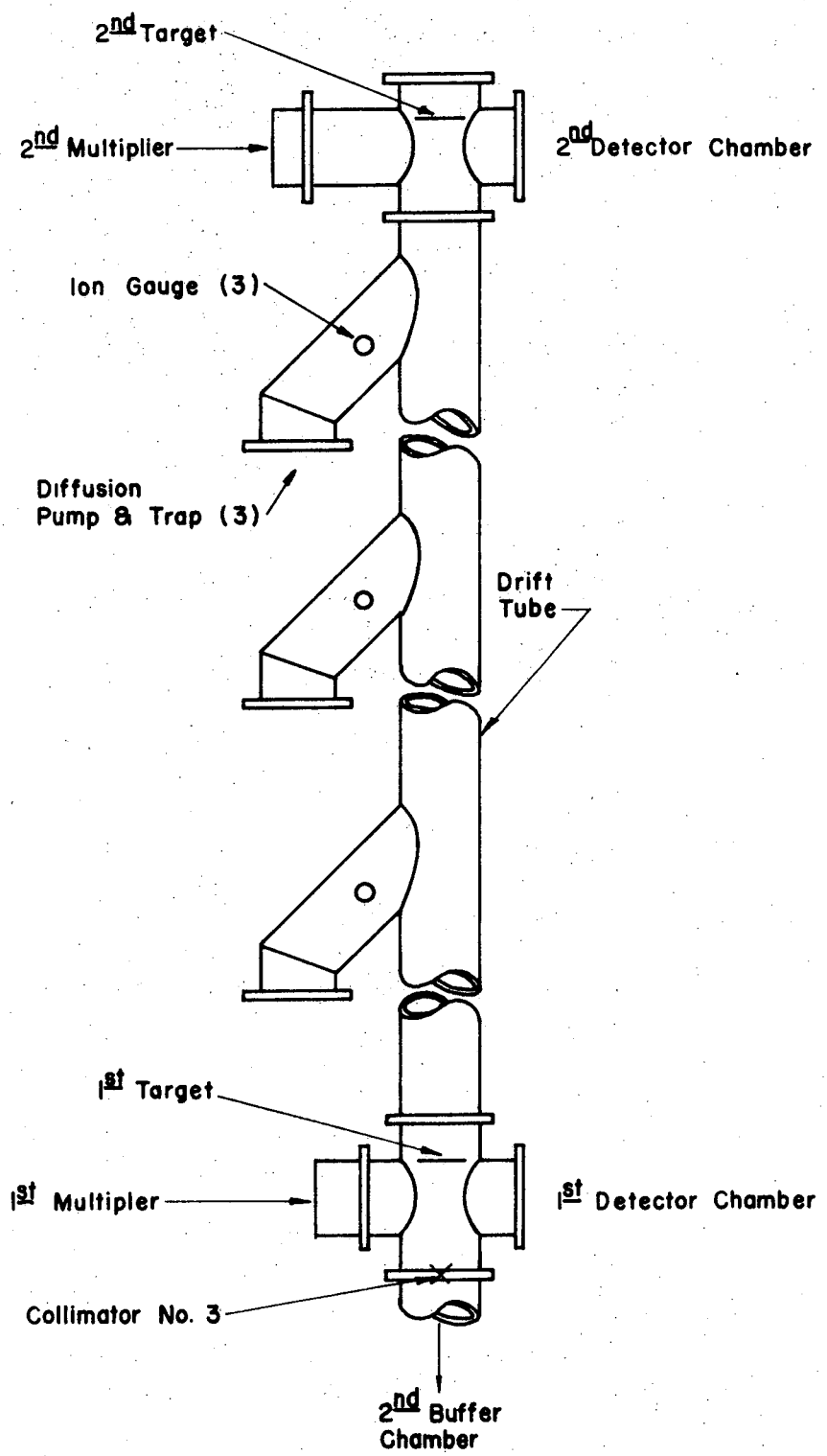

XBL 7011-6943

Fig. 3a. Schematic of the upper section of the metastable beam machine, consisting of drift tube and detector chambers.

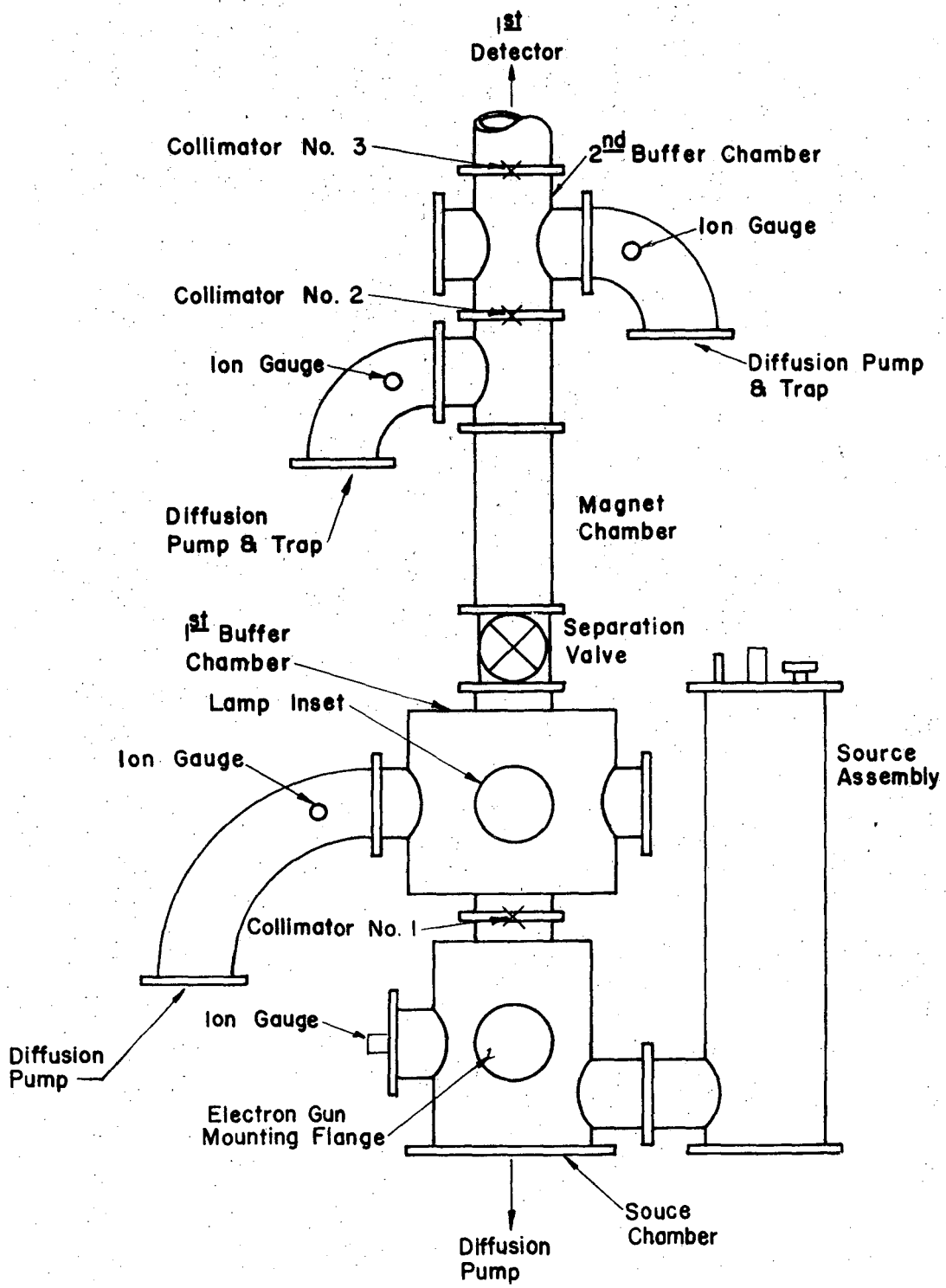

XBL 7011-6942

Fig. 3b. Schematic of the lower section of the metastable beam machine, consisting of buffer chambers, magnet chamber, source chamber, and source assembly.

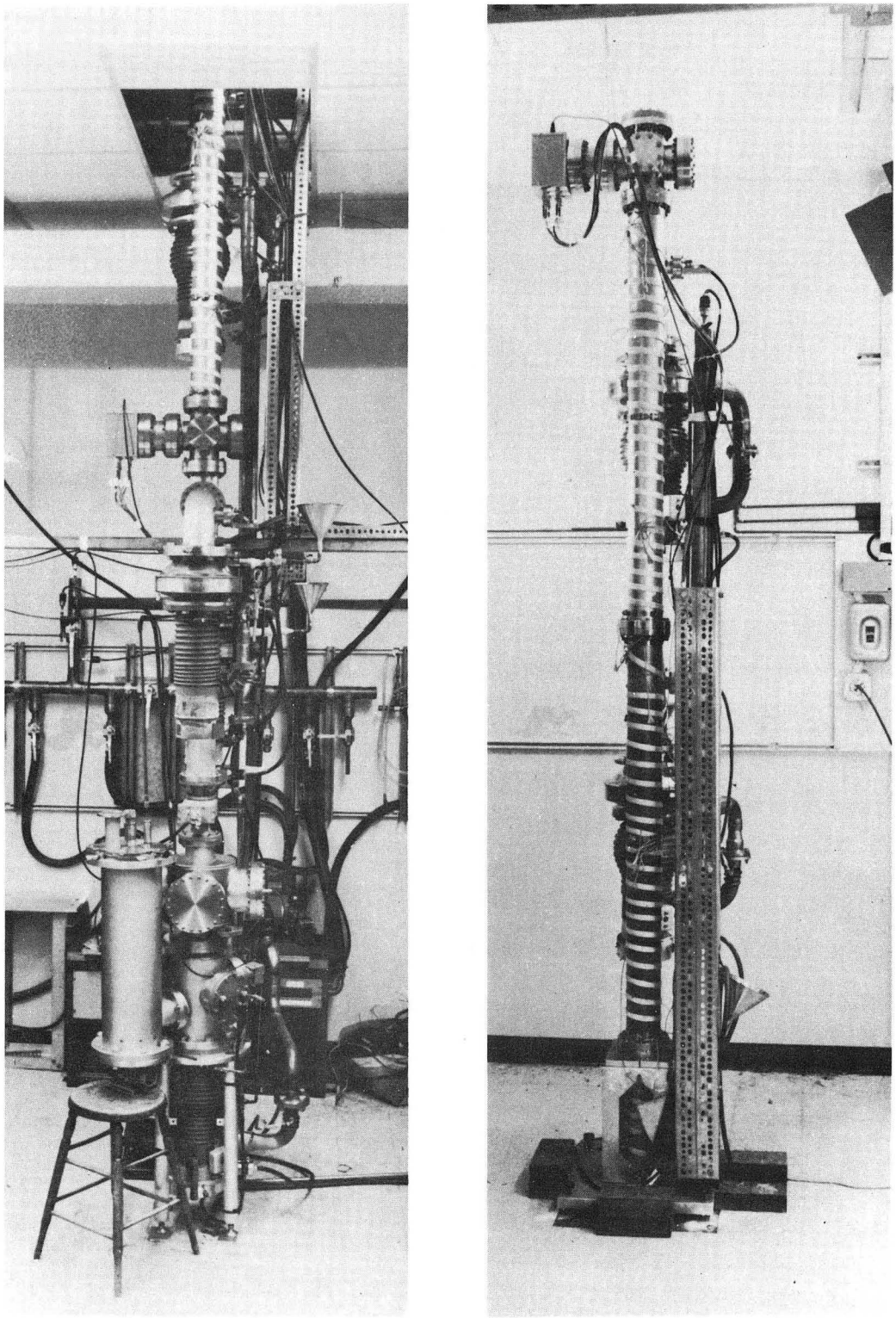

XBB 7010-4704

Fig. 4. Photograph of the actual metastable beam machine.

hole 0.25 inch in diameter, used for vacuum separation and beam collimation. This first buffer chamber contains the lamp re-entrant port and also the electric field deflection plates which can be used to learn if the beam contains fast ions. Above this chamber is the separation valve which allows one vacuum system to remain pumping while the other is opened to atmospheric pressure. Next there is a tube 23 inches long and 4 inches in diameter which can be replaced by a similar 2-inch diameter tube containing Stern-Gerlach magnet pole tips. The last chamber, containing separation plates above and below, is the second buffer chamber, providing the final vacuum isolation for the drift region.

This lower section of the machine is 77.5 inches long from the source chamber to the third collimator, and is also made entirely of stainless steel except for the brass adapting flanges on the separation valve. All ports and flanges above the source chamber are of Varian-type with copper O-rings to allow for mild baking, except at the valve and at throats of all pumps, which have viton O-rings. Each chamber has its own oil diffusion pump, and the magnet chamber and second buffer chamber each have a liquid nitrogen cryo-trap.

A Varian ionization gauge for measuring pressure is included with each diffusion pump of both sections.

B. Vacuum System

The vacuum system is divided into two separate parts by the separation valve. The lower vacuum system contains the source chamber and the first buffer chamber. The upper vacuum system contains the magnet

chamber, the second buffer chamber, and the drift tube. Each vacuum system consists of forepumps, manifold and foreline, diffusion pumps, TC and ionization gauges, and vacuum chambers.

The central foreline manifold is shown in Fig. 5. The two vacuum systems usually are totally isolated if the separation gate valve is closed, but may be joined together at the foreline manifold via the central ball valve if more pumping speed is needed for one system or the other. A venting ball valve may be selectively opened to allow one of the vacuum systems to attain atmospheric pressure, but, in the early stages of construction, the vent was also used to connect a helium leak detector into the system.

The manifold consists basically of 2-inch diameter copper tubing connecting the many ball valves in the system. The lower TC gauges are used to monitor the pressure below the system ball valves and the TC gauges above are used with the interlock system. Generally only two Model 1402 Welch DuoSeal mechanical pumps are connected to each system.

The forelines from the manifolds to the diffusion pumps also consist of 2-inch diameter copper tubing, but the upper foreline system contains flexible bellows sections at points of greatest stress (which exist when this system is baking). Before these bellows were added, the foreline would break when the drift tube expanded during a bake. Both forelines have a bellows to isolate the manifold vibrations from the beam machine itself. Also, all diffusion pumps on a given system have a common foreline.

Since it is well known that mechanical pumps can reduce pressure

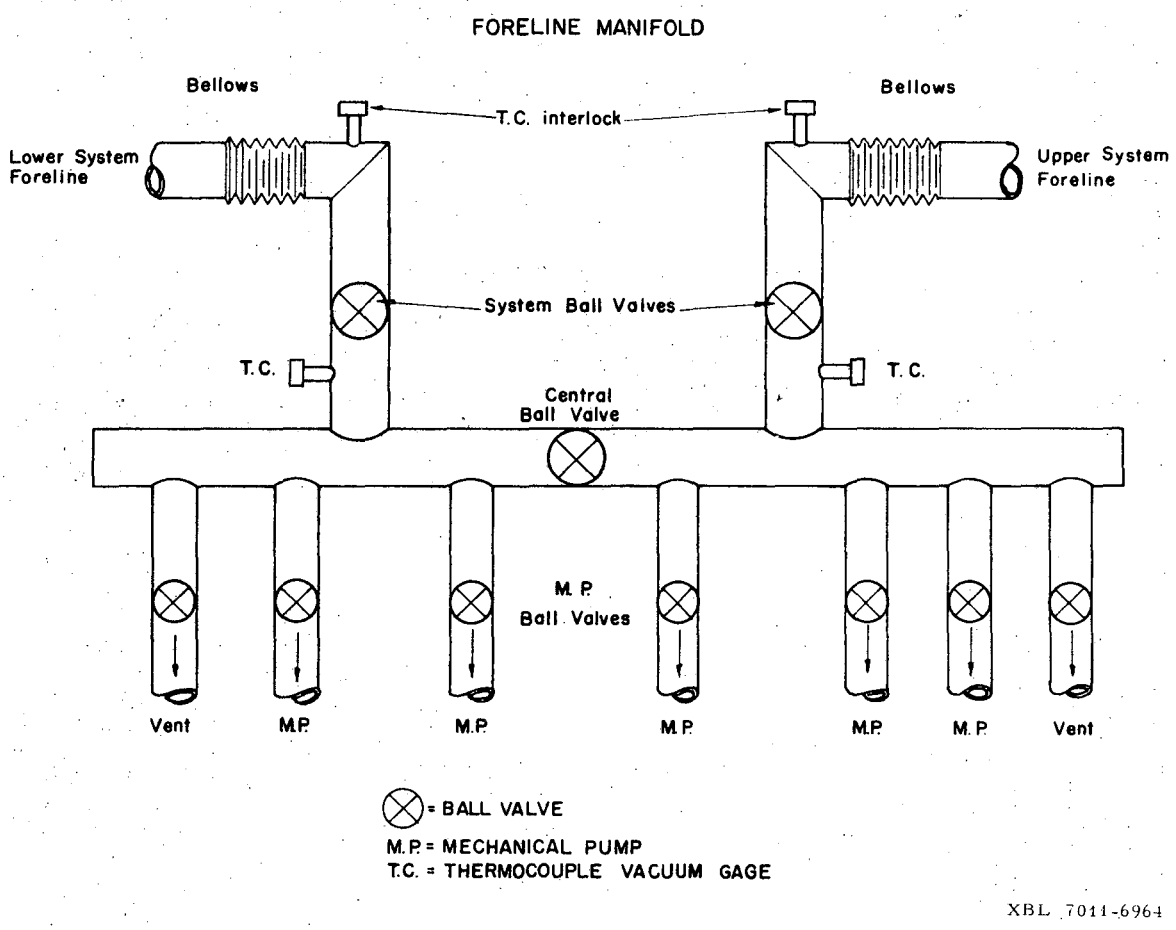

Fig. 5. Schematic illustration of the central foreline manifold. Separate vacuum systems exist when the central ball valve is closed.

only to $\approx 10^{-3}$ torr, oil diffusion pumps are used to further reduce pressures to 10^{-8} torr. The drift tube has three NRC Model VHS-4 high-speed diffusion pumps, each attached to an NRC Series 0316 4-inch cryo-trap, thus giving 600 liters/sec of helium pumping speed. A copper crush ring is used for sealing the trap to the main tube. This precaution allows much higher baking temperatures than those possible with common viton O-rings over the entire drift region. The other two chambers on the upper vacuum system have CVC Model PMC-720 diffusion pumps, each also with an NRC 4-inch cryo-trap. The lower system has two NRC Model VHS-6 oil diffusion pumps connected to the vacuum system without traps. Trapping does occur in the source chamber, though, when liquid nitrogen is placed in the source assembly. Thus, without traps, the full benefit of the pump's 3000 liters/sec pumping speed for helium can be realized. All the VHS diffusion pumps were specially ordered with 208-volt heaters, and the older PMC-720 diffusion pumps were rewired for 208-volt operation. Thus all diffusion pumps are able to run on a single 25-amp, three-phase circuit. Likewise, all mechanical pumps are connected to a separate 25-amp three-phase circuit to insure that they would continue to operate, even if power failed on the diffusion pump circuit.

The interlock system consists of a Hastings Dual Vacuum Interlock controller which normally sends current into a large relay. When pressure becomes high (>100 microns) in the foreline system, the controller deactivates the large relay, which then cuts the power to the diffusion pumps. An interlock system is connected to each separate vacuum system.

Pressures greater than 10^{-3} microns are measured by Hastings Thermocouple gauges. For pressures between 10^{-3} and 10^{-11} torr, Varian Model UHV-24 ion gauges must be used. These gauges are also bakeable, and project directly into the vacuum system. They always read lower values after first baking the walls nearest to the gauges, even after the system is opened to atmospheric pressure and then pumped down again. The problem is that these gauges must be kept as far from the surrounding walls as possible since they tend to read the local pressure of gas coming from the walls, being heated by the gauge filament itself, and not the equilibrium pressure far from the walls.

In order to obtain pressures less than 10^{-8} torr, the system is baked by means of many 300-watt heating tapes, all connected electrically in parallel and wrapped around the outside of the entire drift tube. Typical baking temperatures are 150 to 200°C and the duration of the bake is typically 48 hours. Pressures start at $1 \cdot 10^{-6}$ torr, but decrease finally to about 2 or $3 \cdot 10^{-7}$ torr. Often a factor of 10 can be gained in lower pressures after turning the bake off. Even lower pressures can be realized with longer, hotter bakes. Varian conflat flanges with copper O-rings are used at all joints in order to stand temperatures greater than 100°C. Preliminary to assembly, the various vacuum parts are electropolished and assembled with clean plastic gloves, after cleaning parts in ethyl alcohol.

The buffer chambers are very important in isolating the high pressure of the source from the very low pressure of the drift region. The evidence for the high quality of this isolation is that no detect-

able rise in pressure in the drift region occurs when the separation valve is opened, even with very high source chamber pressure ($\approx 10^{-3}$ torr) or while running an intense collimated beam. For a list of typical vacuum pressures for the various chambers in the two systems, see Table 2.

C. Gas Handling System

This system produces a variable flow rate into the source assembly with a high degree of stability over long periods of time (hours to days, depending on magnitude of flow rate). Originally three 5-liter storage bulbs were used to produce the constant atmosphere backpressure at the metering valve, as shown schematically in Fig. 6. But when one bulb became broken it was found that 10 liters of storage was quite sufficient. A photograph of the present system is shown in Fig. 7. An open-end mercury manometer monitors the quantity of stored gas, since density is proportional to pressure when volume and temperature are constant. Normally the operating pressure is 10-20% above atmospheric pressure, but when this pressure decreases 10-20% below 1 atmosphere, the bulbs are flushed out and refilled to their original pressure by manipulating stopcocks Nos. 1, 2, and 3. When very pure gas samples are needed, the final fill is done with liquid nitrogen surrounding the cold trap.

The open-end manometer acts as a safety valve when pressure gets too high in the storage bulbs, as may happen if the pressure regulator accidentally gives a burst of gas into the system. This feature was once found to be very useful when it was necessary to run gas contin-

Table 2. Typical pressures (in torr).

	Untrapped	Trapped
Drift tube unbaked	$1 \cdot 10^{-7}$	$2\text{-}4 \cdot 10^{-8}$
Drift tube baked	$1 \cdot 10^{-8}$	$2 \cdot 10^{-9}$
2nd buffer chamber	$1 \cdot 10^{-7}$	$1 \cdot 10^{-8}$
Magnet chamber	$1 \cdot 10^{-7}$	$1 \cdot 10^{-8}$
	No Beam	**With Beam**
1st buffer chamber	$2 \cdot 10^{-7}$	$4 \cdot 10^{-7}$
Source chamber (no LN and uncorrected for helium)	$7 \cdot 10^{-7}$	$1 \cdot 10^{-6}$

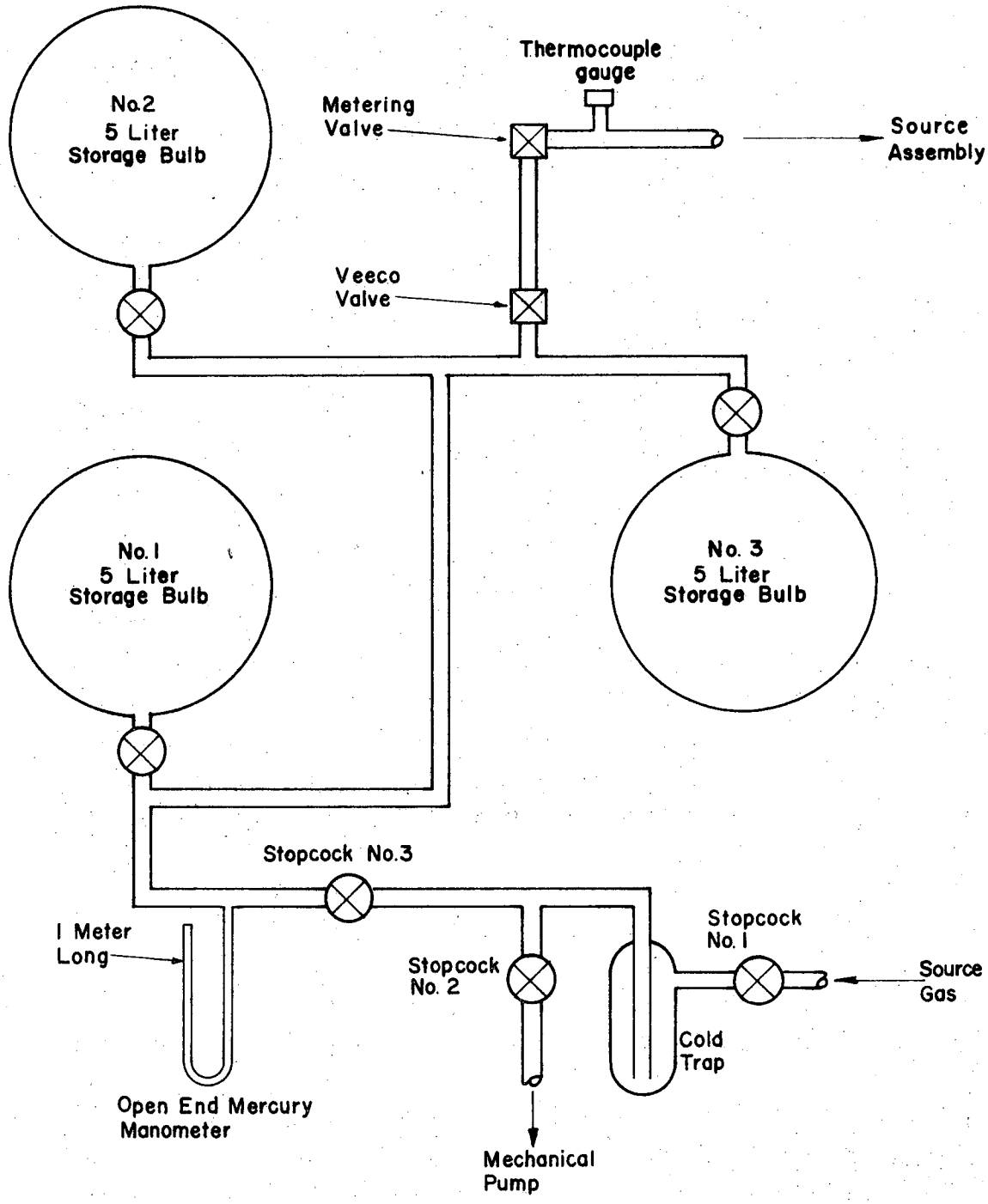

XBL 7011-6966

Fig. 6. Schematic illustration of the gas handling system. Total capacity is approximately 16 liters at one atmosphere.

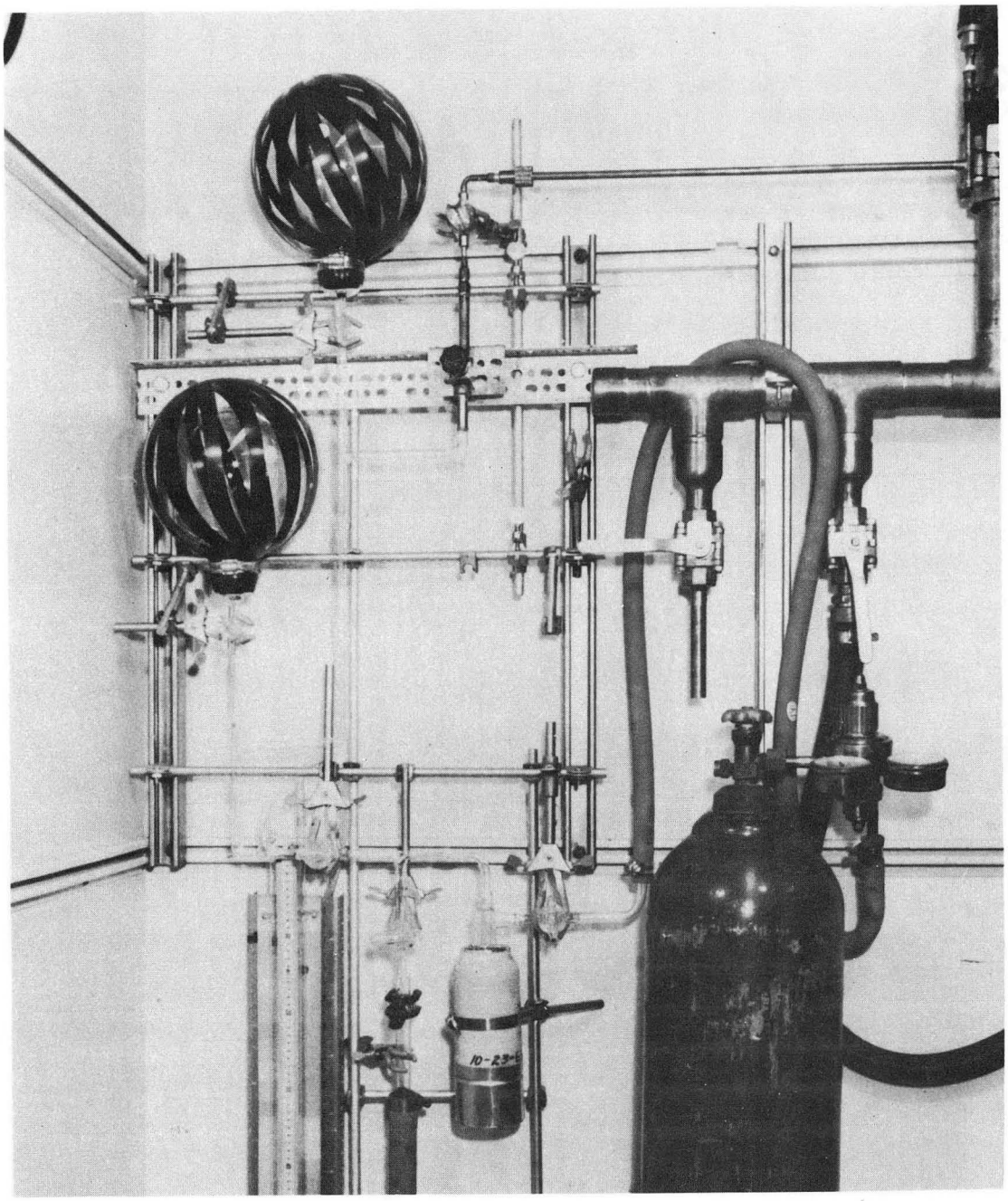

XBB 7010-4705

Fig. 7. Photograph of the present gas handling system. Total capacity is approximately 11 liters at one atmosphere.

uously from the large storage tank into the bulbs for need of very high flow rates. On this occasion, the high-pressure regulator malfunctioned, producing a large overpressure in the bulbs. The mercury overflowed and the gas was subsequently vented harmlessly into the room, preventing damage to the glassware.

The gas system as illustrated in Fig. 6 is of all-glass construction up to the Veeco valve which provides complete shutoff when necessary. The valve used to adjust the final flow rate in this experiment is a Vacoa Model MV-25-XL precision gas metering valve and could be very accurately adjusted to give almost any desired count rate. Typical running conditions might give a source chamber pressure of $1 \cdot 10^{-6}$ torr for helium (uncorrected) with the metering valve open to 7 turns. Since VHS-6 pumping speed is 3000 liters/sec (at STP) for helium, the flow rate is $\approx 2 \cdot 10^{-2}$ cc/sec for a corrected helium pressure of $6 \cdot 10^{-6}$ torr (VAR 65). As can be seen from the graph in Fig. 8, seven turns is to be expected for this flow rate. Viewed in a different way, the flow rate is 0.09 liters/hr; hence it would take approximately 11 hrs of continuous running to use 10% of the stored gas. The storage volume is thus sufficient for many runs, each lasting between 1 and 2 hours. The adjusted flow rate is usually the highest that can be tolerated (which is desirable for obtaining large signal-to-noise) in order to keep the count rate less than 10% of that which would saturate the output amplifiers.

Following the metering valve is a thermocouple gauge used to monitor the source line pressure, mainly to assure that the source line

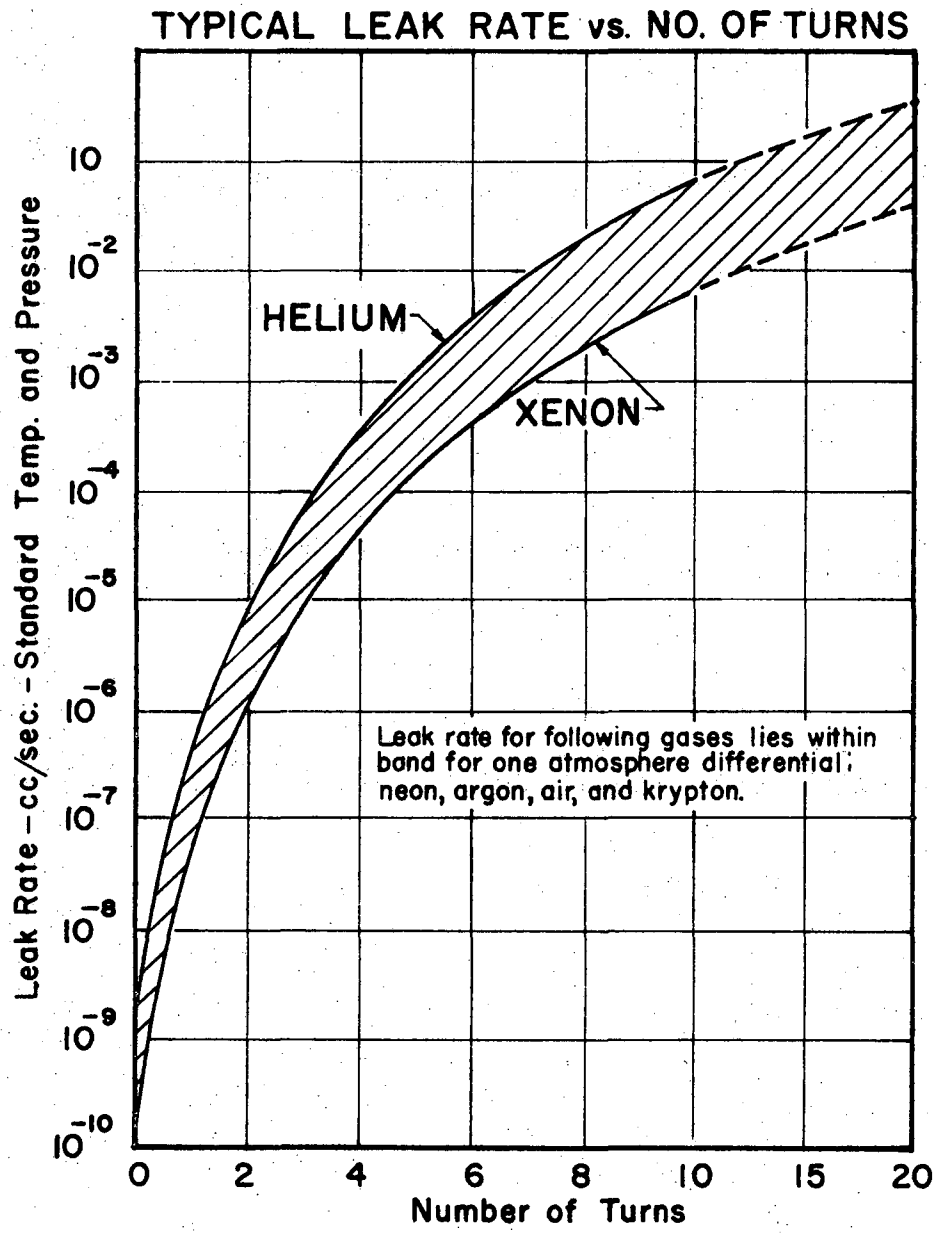

XBL 7011-6949

Fig. 8. Graph of leak rate versus number of turns on the precision metering valve for various gases according to manufacturers' specifications.

does not leak. Copper tubing with 3/8-inch O.D. and total length of 11 feet is used to connect the metering valve to the 4-foot-long, 1/8-inch O.D. stainless steel tubing in the source assembly. These lengths and diameters obviously create a sizeable impedance to the source gas flow. Thus a long delay usually ensues after any change of the metering valve. In the past, not only helium but H_2, N_2, Kr, and Ne have been used as source gases, and all can be made to have reasonable flow rates.

D. Source Assembly

In order to measure the decay of the beam over an appreciable fraction of the mean life of the singlet state, a cold beam is needed. Originally the goal was to obtain a liquid-helium-cooled beam. The source assembly thus designed and built is shown in Fig. 9. The inner dewar can be filled with either liquid nitrogen or liquid helium and the outer jacket normally contains liquid nitrogen. The source gas is first cooled to liquid nitrogen temperature by having the 1/8-inch O.D. stainless steel tubing wind around inside this outer jacket before passing into the heat exchanger (copper block) attached to the bottom of the inner dewar. A long copper tube with 3/16-inch O.D. is attached to this heat exchanger to bring the cooled gas onto the axis of the beam machine. In order to allow for shrinkage and minor line-up, the top two plates of the source assembly chamber slide upon each other at right angles to give the source slit at the end of the long copper tube a two-dimensional transverse movement across the beam axis. Usually, movement

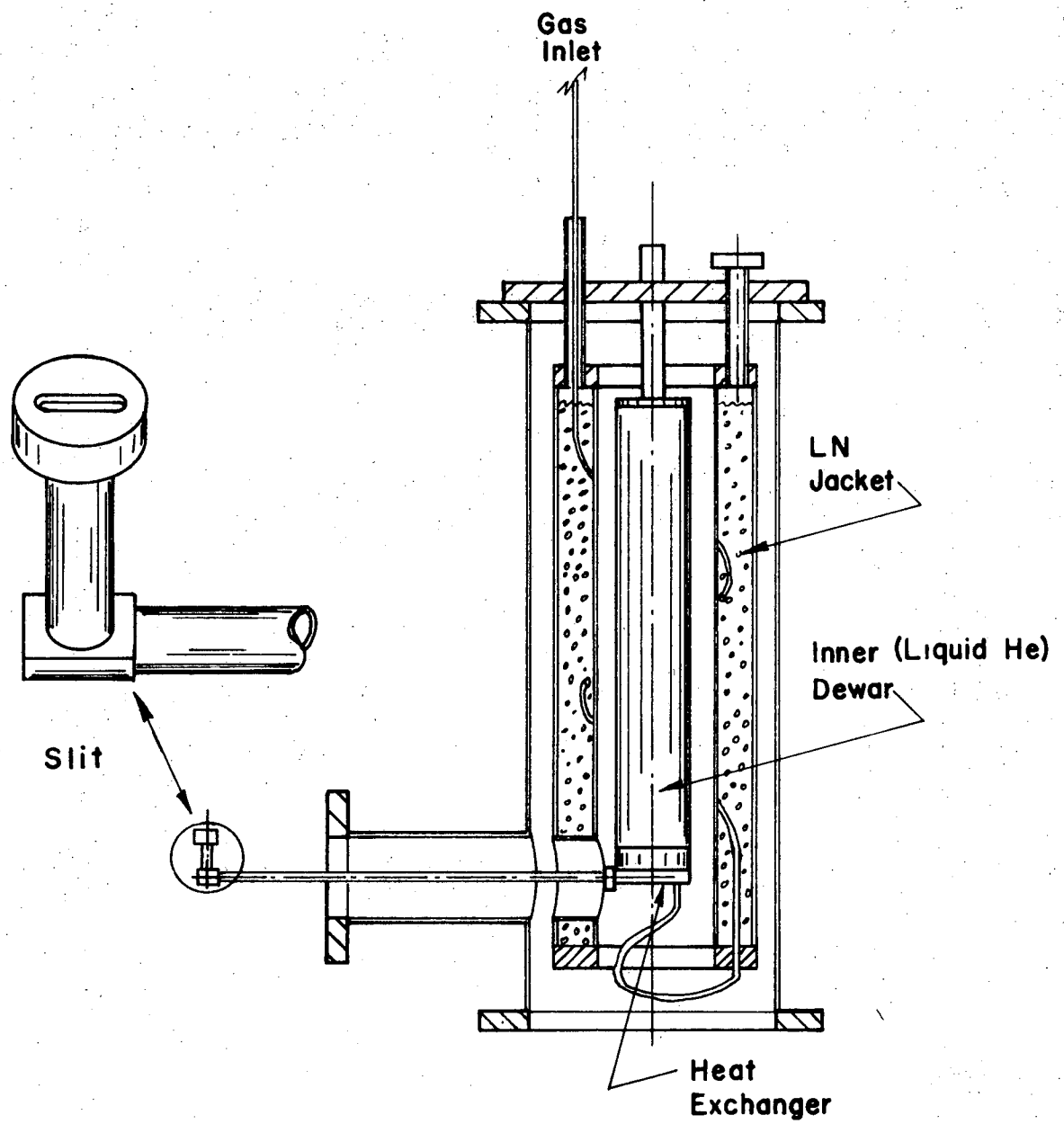

XBL 7011-7017

Fig. 9. Source assembly. Allows the neutral beam to be cooled by a coolant placed in the central dewar. Heat radiation from the electron gun is transferred by a long copper tube to the heat exchanger.

is limited to ±0.15 inch in either direction. When liquid helium is put into the inner dewar, a radiation shield is placed over the long copper tube. The slit at the end of this tube is oriented parallel to the long direction of the tube and is approximately 0.15 inch in length. The pressure P_s in the long copper tube depends on the flow rate desired or, equivalently, the pressure P_{sc} in the source chamber. At $P_{sc} = 2 \cdot 10^{-6}$ torr, P_s = 37 microns for a liquid-nitrogen-cooled source (see Appendix C).

In general, the full benefit of this elaborate source has never been realized, since it was found that the electron gun modifies the thermal speed distribution emanating from the source.

E. Metastabilizer

The task of raising atoms from the ground state to the 2^1S_0 metastable energy level was one of the most important experimental problems to solve. Of the two common possibilities, rf discharge and electron bombardment, the latter choice was settled upon. A discharge can give very large metastable populations but does not always turn off as cleanly as the electron gun. Also, in the final experimental arrangement, it was possible to produce all the metastable atoms that the counting equipment could handle, using electron bombardment.

Basically, the metastabilizer, placed immediately after the source slit, is a type of sheath electrode gun designed by Lamb and Retherford (LAM 51). Fig. 10 shows the first version of this gun, having two side electrodes 100 mils apart, each of which is 1.0 inch high, 5/8 inch

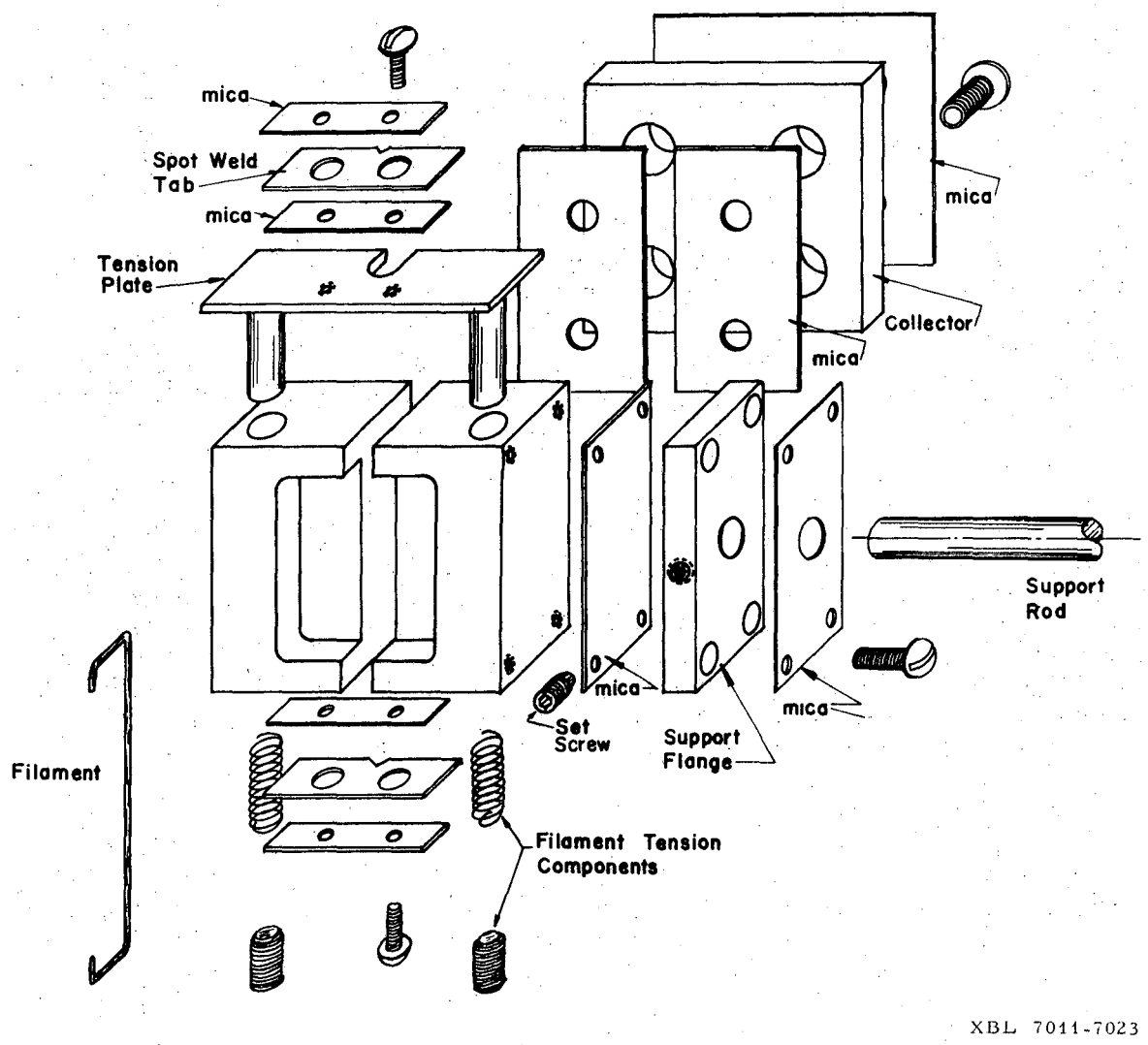

Fig. 10. Exploded view of the sheath electrode gun described by Lamb and Retherford (LAM 51). A 10-mil thoriated tungsten filament is spot-welded to stainless steel tabs and kept taut by a spring-loaded tension plate. The filament is located lengthwise in the 100-mil gap, flush with the depressed region of the side electrodes. The helium beam passes between the sheath electrodes, parallel to the filament. The entire stainless steel assembly is placed in a uniform magnetic field, aligned perpendicular to the filament within the gap.

wide, and 1/2 inch thick. Both electrodes, together with the collector plate attached to the back of the side electrodes, constitute the sheath and each carries the same positive potential to attract electrons into the 100-mil gap. For this purpose, a hot 10-mil thoriated tungsten filament is held near ground potential and centered lengthwise in the gap. The electrons are guided onto the collector, 1 cm from the filament, by a permanent Alnico magnet with 2-inch-square pole faces, 1-inch gap, and a field strength of about 1500 G. The atomic beam then passes through the center of the gap between the electrodes and parallel to the hot filament. In order to keep the filament taut, one end is attached to a bar that slides in parallel holes bored into each side electrode. A stainless steel spring placed in each hole provides the necessary tension. Sections of mica are used to provide the electrical insulation where necessary. The collector is also electrically isolated from the side electrodes to allow emission current reaching the collector to be monitored independently from that which strays to the side electrodes. Externally adjusting the position of the permanent magnet allows this collector current to be maximized, thus requiring most electrons to travel the full length of the gap, and increasing the probability of creating useful metastable atoms in the collimated atomic beam.

This particular arrangement of the electron gun led to a serious systematic error in the lifetime measured, by creating a dependence on the type and position of the source exit. The elimination of most of this unwanted source dependence was accomplished by rotating the gun by 90 degrees so that the filament is oriented parallel to the source slit.

A photograph showing the final form of the gun is found in Fig. 11. The gun is essentially the same as the first version except that the collector is almost entirely eliminated by cutting a slot in it for the beam to pass through the gun, perpendicular to the filament. Now, all electrons must eventually strike the sheath. Also, a solenoid is used to obtain a focusing magnetic field oriented parallel to the beam axis, constructed by wrapping many layers of 3.0-inch wide, 3-mil-thick strip aluminum between layers of 3.25-inch mylar upon a 2-inch diameter Pyrex tube.

The gun support system is illustrated in Fig. 12a and 12b. The system in Fig. 12a was sufficient for the first version of the gun, but the piece shown in Fig. 12b was necessary in the final version in order to support the gun in the center of the solenoid. This support system also allows a one-dimensional movement from outside the vacuum via a micrometer whose rotational motion is changed into longitudinal in-and-out motion. This movement is perpendicular to the less critical source slit direction, and is used basically for initial lineup of the machine, and to check that the gun's position gives the maximum collimated metastable beam. Electrical isolation at the point of connection to the gun is again achieved with mica.

The circuit which supplies the power to the gun filament is shown in Fig. 13. In order to keep the filament from shorting to the sheath because of the focusing magnetic field, the power circuit must supply a large audiofrequency (≈3 kc) current to the filament. A variable clock on a digital Flip Chip circuit board, followed by a flip flop

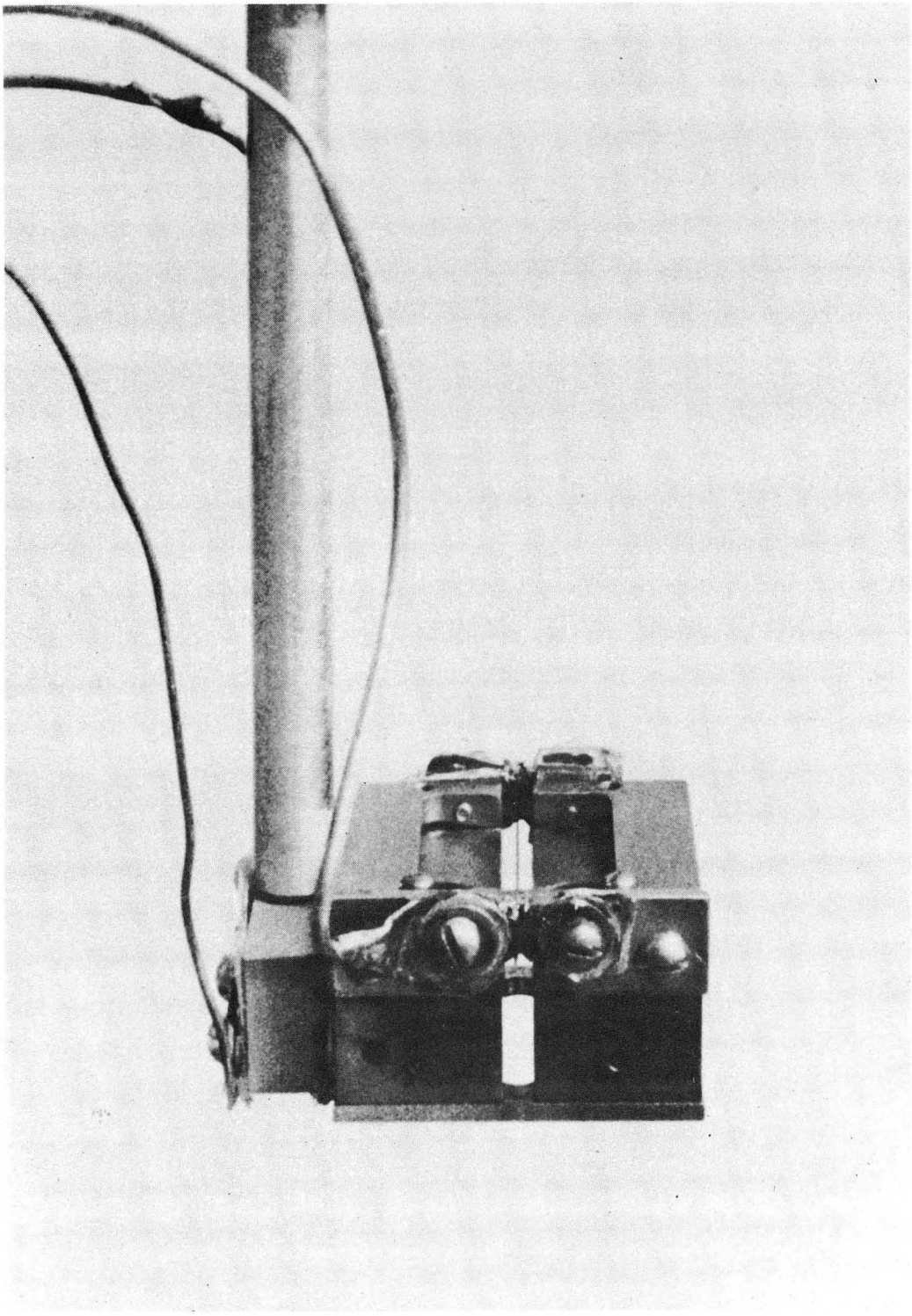

XBB 7010-4708

Fig. 11. Photograph of the electron gun in the final configuration, with collector plate eliminated for the atomic beam to pass between the sheath electrodes, perpendicular to the filament.

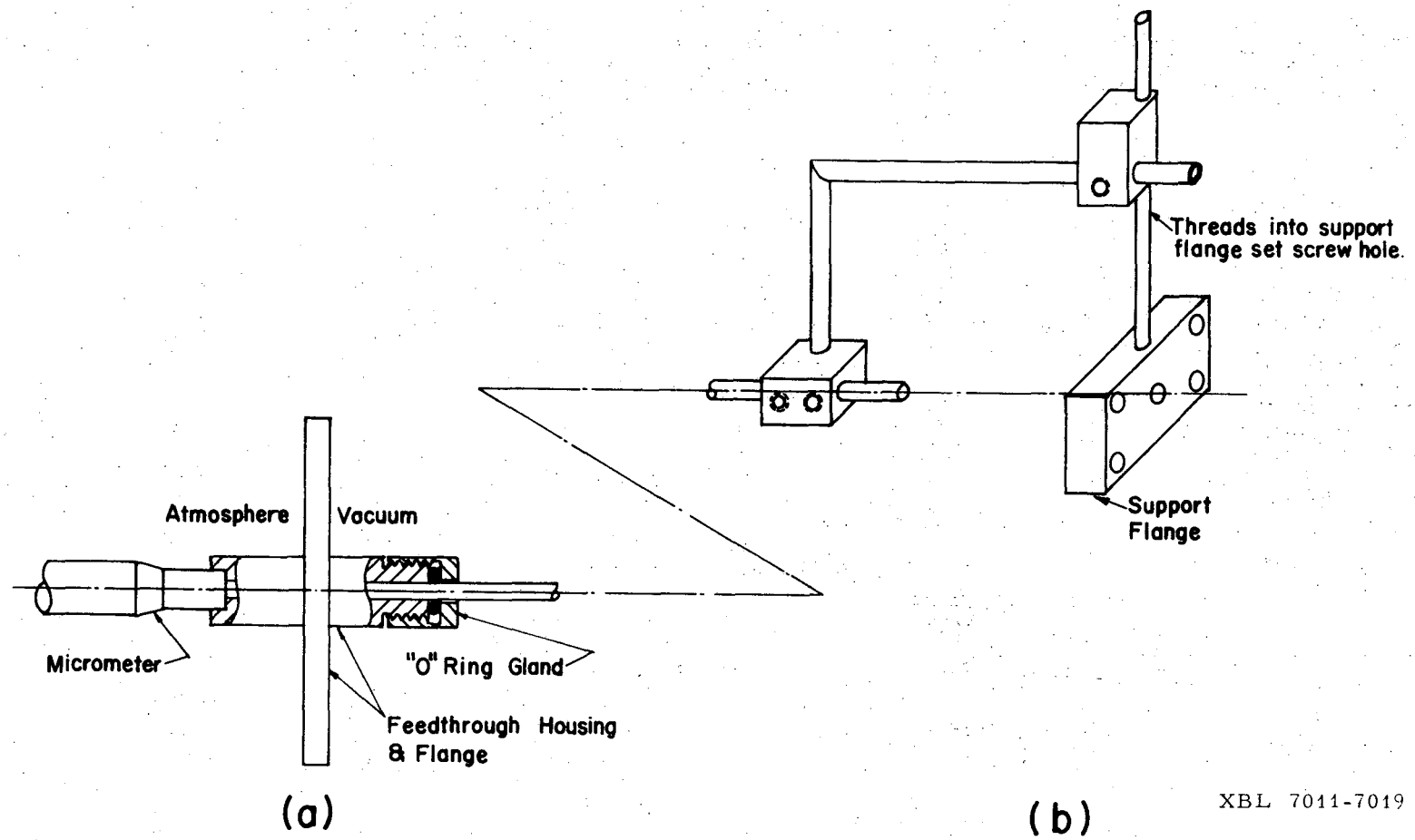

Fig. 12. Part (a) shows the movable gun support system which converts rotational motion to longitudinal motion. This system was sufficient for the first version of the electron gun. Part (b) shows the additional section needed to support the final version of the electron gun in the center of the solenoid.

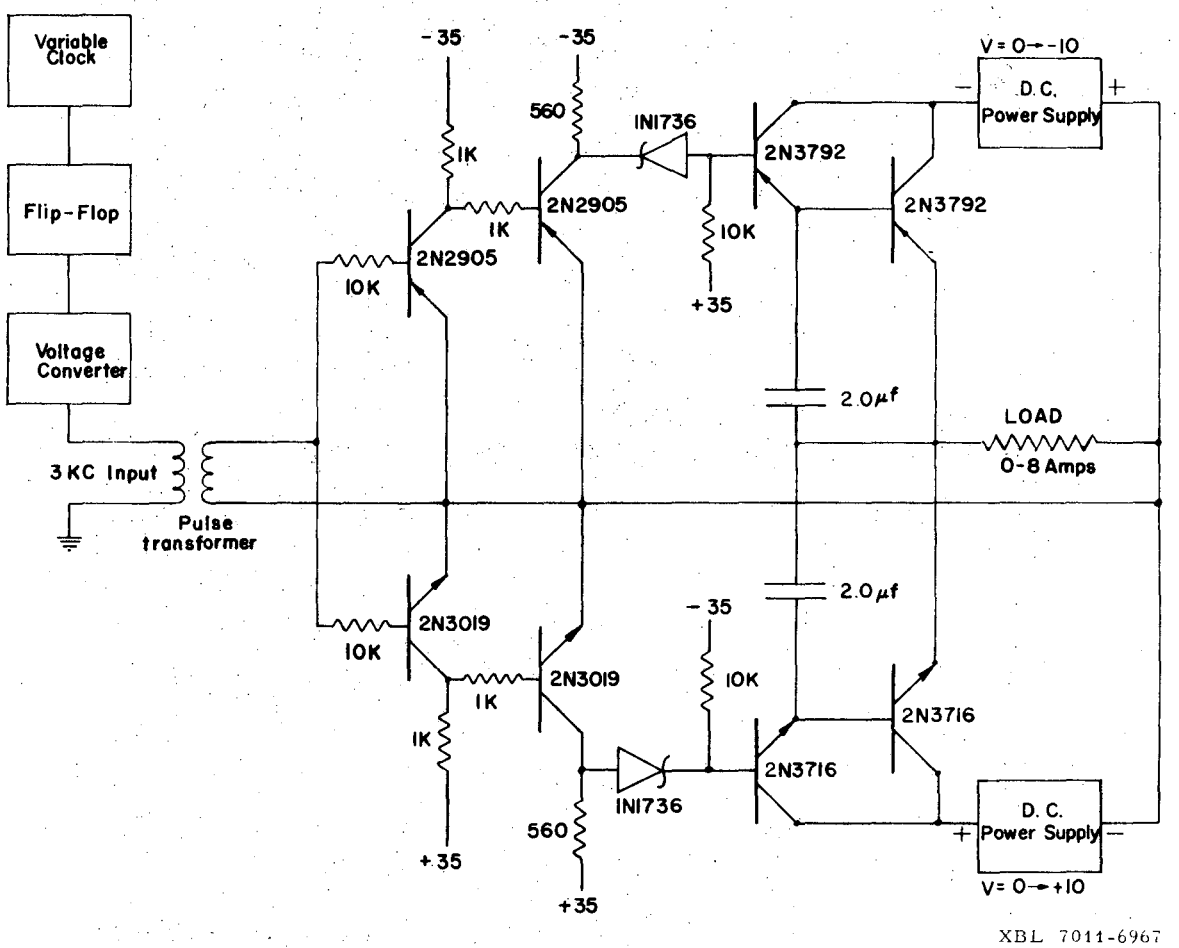

Fig. 13. Filament heater circuit. This power switch supplies a large plus-minus square wave current to the electron gun filament, with a frequency of approximately 3000 cps in order to prevent the filament from shorting to the sheath because of the focusing magnetic field.

and a voltage converter, provides a ±10 V audiofrequency, low-current input signal for the high-current plus-minus power switch. Note that the filament is able to float above ground, which is necessary in order to pulse the emission current during regular operation. Under normal conditions, the filament receives 7.5 amps at 6 volts, thus giving approximately 20 ma of emission current with 50 volts applied to the sheath.

The pulsing circuit for the emission current is shown in Fig. 14 with input signal controlled by a PDP-8 computer. When no pulse arrives the filament is biased +5 volts, preventing any electrons from leaving the filament. When a pulse arrives, the filament is grounded and electrons are accelerated toward the positive sheath. Normally the emission flows only for 80 to 100 μsec and remains off for 30 to 35 msec, during which time data are collected.

By varying the voltage to the sheath it was found that 50 V gives the greatest number of metastables. The actual accelerating potential is less than 50 V, though, because of the effect of space charge in the gap (HAE 39). As can be seen from the plots of 2^3S_1 and 2^1S_0 excitation functions in Fig. 15, the probability of producing metastable helium by electron impact maximizes near 30 V. Estimation of the fraction of 2^1S_0 atoms in the collimated beam is treated in Appendix D.

When a solenoid was substituted for the permanent magnet, it was found that a large amount of power was needed to energize the magnet and to maximize the number of metastable atoms in the beam. Thus, it was decided to pulse the magnet on a few milliseconds before the electron

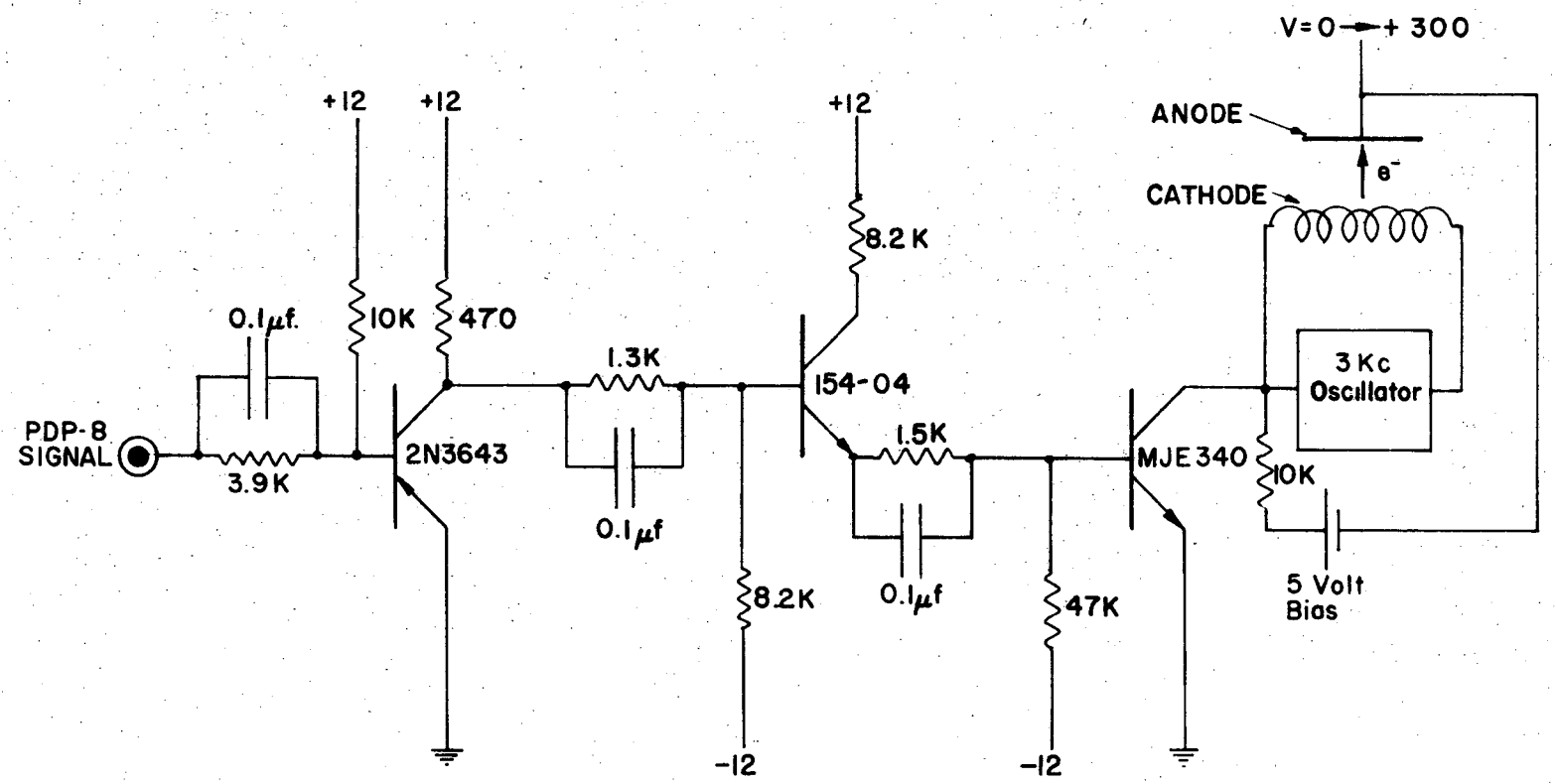

Fig. 14. Emission current pulsing circuit. When a positive going -3 volts-to-ground pulse arrives from the PDP-8 computer, the cathode is held at ground potential, allowing electrons to be accelerated to the anode. When a pulse does not arrive (input is at -3 volts), the cathode is biased +5 volts with respect to the anode, and no electrons can flow.

XBL 7011-6962

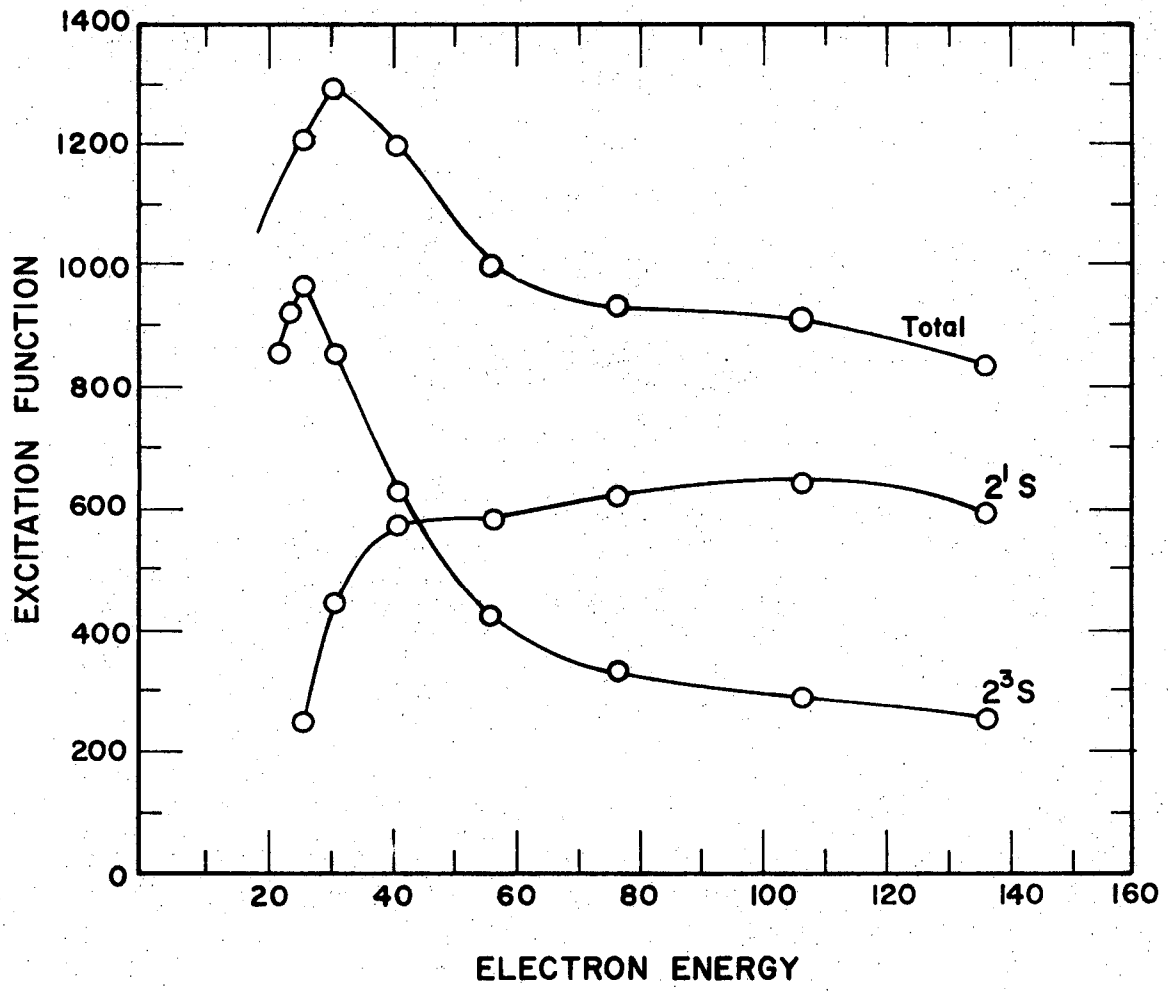

XBL 7011-6948

Fig. 15. Excitation functions for the 2^3S_1 and 2^1S_0 metastable atoms by electron impact versus electron energy. Also, the total excitation function is shown as the sum of the excitation functions for the individual metastable states (DUG 67).

gun is turned on in order to let the field rise to a stable value of approximately 200 G, and then turn the magnet off when the gun is turned off. With such a small duty cycle, the magnet coils are prevented from overheating. The circuitry for pulsing the solenoid is shown in Fig. 16. The PDP-8 computer again supplies the properly-timed input pulses to the power switch, capable of providing 15 to 20 amps through the coil windings when on.

The method for activating the thoriated filaments, found to give high emission current and long filament life, is to start at 2 V and slowly increase audiofrequency voltage, each time allowing the emission to rise and level off before further increasing the voltage. Finally, a point is reached beyond which further increases do not increase emission, as expected from a space charge limited situation. Final emissions of 40 ma at 8 V (with sheath potential = 50 V) have been attained, but filament temperatures never reach more than 2000°C, much less than the 2800°C recommended for the "flash" type of activation procedure (LAN 23).

F. Discharge Lamp

The electron gun must excite the 2^3S_1 metastable state in order to produce the 2^1S_0 metastable state, because of the higher onset potential for exciting the 2^1S_0 state. And, since the detection system is unable to differentiate directly between the singlet and the triplet metastable atoms, the following method was devised to effectively separate the two components.

A discharge is created in a small amount of helium gas contained

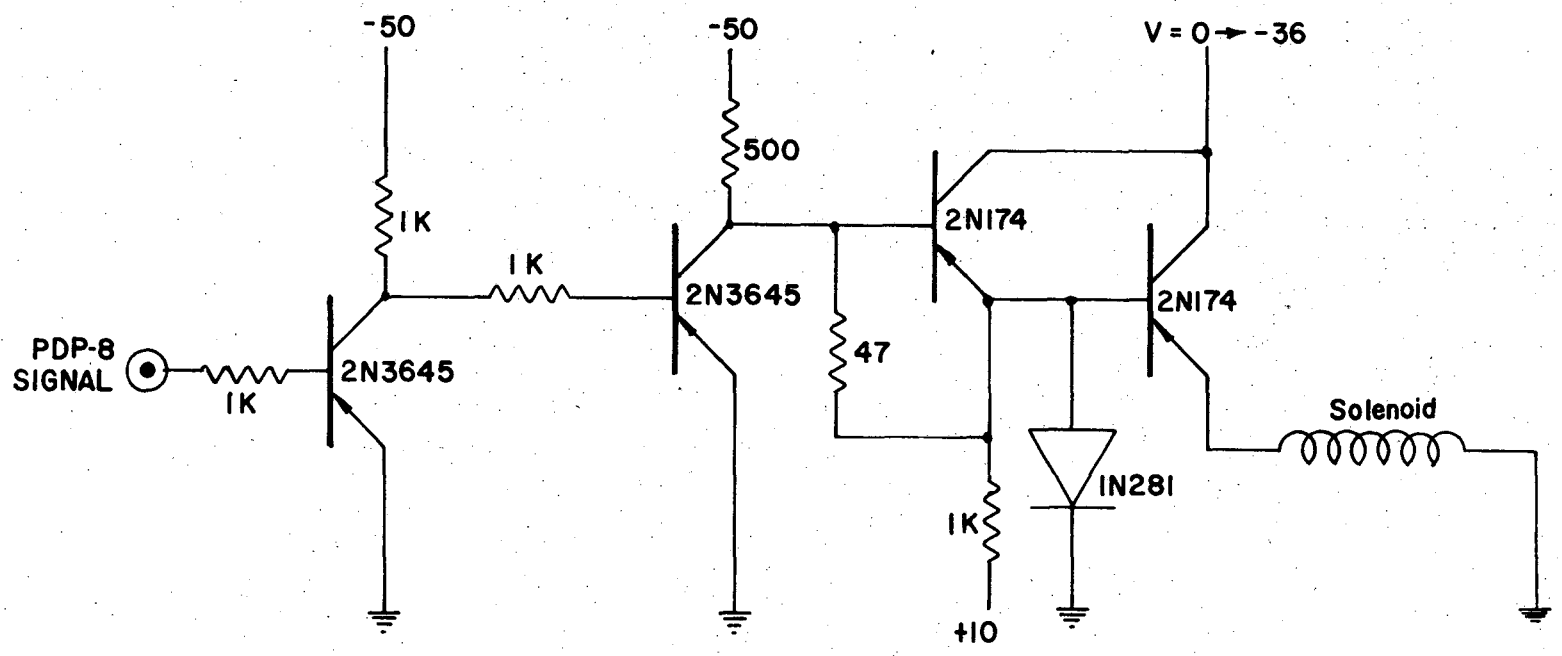

XBL 7011-6963

Fig. 16. Solenoid pulsing circuit. This power switch provides a large negative current to the solenoid, producing the uniform focusing magnetic field for the electron gun. The input modulation consists of a -3-volt potential which drives current through the solenoid and a ground potential for turning the solenoid off.

in a thin Pyrex tube during alternate data collection cycles. Data collected with the lamp on are stored in a different memory location in the PDP-8 computer than data collected with the lamp off. Now, referring to Fig. 17, it can be seen that, when 20581 Å radiation falls on an atom in the 2^1S_0 state, the atom can make a transition to the 2^1P_1 state, whereupon the atom may immediately decay by highly allowed electric dipole radiation to the 1^1S_0 ground state. The branching ratio between the transition back to the 2^1S_0 and the transition down to the 1^1S_0 state is 1:1000 (FRY 69a). Hence, by shining an intense beam of 20581 Å light on the metastable beam, most of the singlet component will be quenched. The probability for quenching depends on the time spent in the area of the radiation, and thus directly upon the velocity of the atom. In contrast, the 2^3S_1 state will be raised to higher triplet states, but will immediately return to the 2^3S_1 ground state for the orthohelium triplet system. There are some intercombination lines ($2^3P_1 \leftrightarrow 1^1S_0$, λ = 591 Å; $3^3D_2 \leftrightarrow 2^1P_1$, λ = 6680 Å; and $2^3P_1 \leftrightarrow 3^1D_2$, λ = 5874 Å), but they are extremely weak (HER 58). Thus, with the lamp on, the resulting metastable beam contains triplets almost entirely. The difference between these two beams is effectively a pure singlet beam, with a slightly modified velocity distribution.

Fig. 18 is a photograph of the lamp and its tuning circuit, all of which is kept outside the vacuum where air can be continuously applied to the discharge tube to prevent it from overheating and changing the quality of the light emitted. The tube is brought to within 3/4 in. of the metastable beam by way of a vacuum re-entrant port with 5-1/2 in.

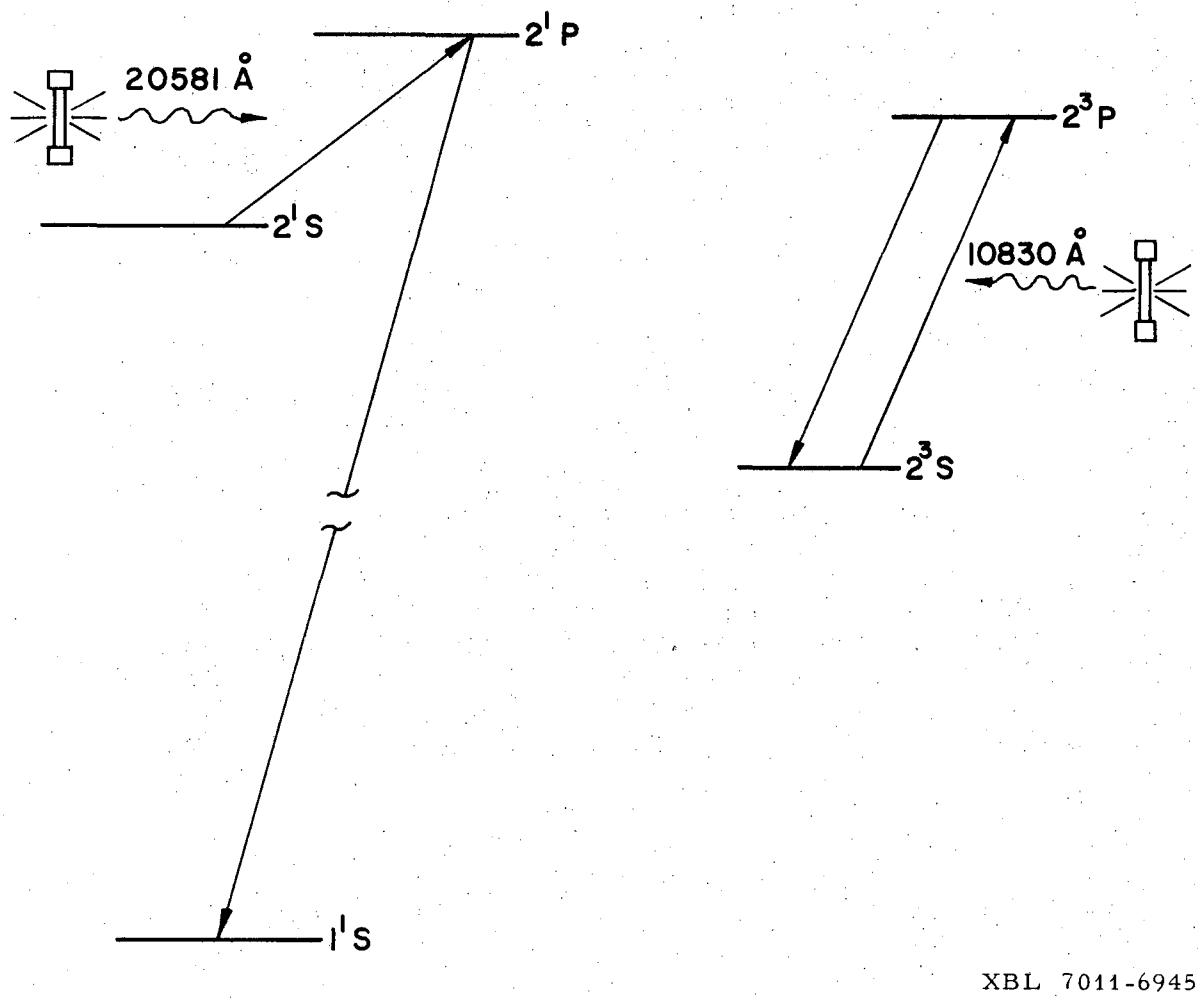

Fig. 17. Illustration of the quenching mechanism. The 20581 Å radiation raises the 2^1S_0 state to the 2^1P_1 state, which immediately decays to the ground state. But any radiation which raises the atom from the 2^3S_1 state does not affect the final triplet population, as all triplet states decay back to the triplet metastable state immediately.

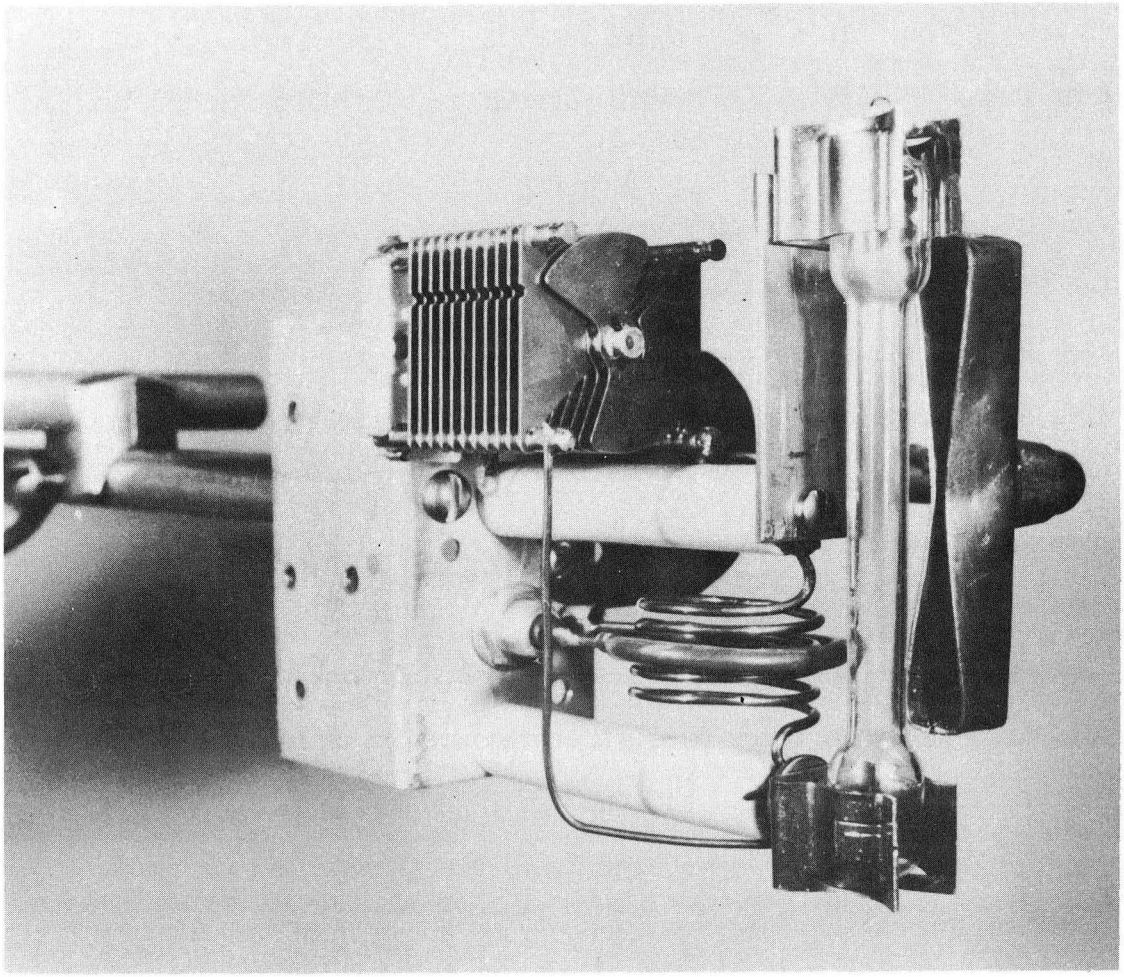

XBB 7010-4706

Fig. 18. Photograph of the helium discharge lamp and tuning circuit. Facility is made for cooling the lamp by continuously applying a stream of air directly to the discharge tube.

I.D. A Pyrex glass window allows the discharge light to pass into the vacuum region. In general, the lamp is positioned as close to the electron gun as possible, so that uv-quench photons have a small probability of reaching the detectors.

The circuit which drives the discharge lamp is shown in Fig. 19. The input modulation is supplied by the PDP-8 computer, as usual.

The lamps are made from a 2.25-inch long, 6 mm capillary tube with a small bulb at each end, and are prepared with special emphasis on cleanliness and purity of gas sample. These lamps are first baked at approximately 200°C and then allowed to cool while one end is attached to a clean vacuum system with pressure less than 10^{-5} torr. When the tubes are clean, pure helium gas is passed through a liquid nitrogen cold trap into the tubes until the pressure is approximately 3 microns. Then the tubes are sealed off and are ready for use.

These specially prepared lamps are then able to separate the singlets from the triplets, as described above. In this way, it is found that the singlet metastable component constitutes at least 20% of the total metastable beam.

G. Collimation

The main purpose of the collimation and subsequent lineup of the source slit, electron gun, and collimators is to assure that any atom that can be seen by the lower detector can also be seen by the upper detector. Collimation is achieved by use of the stainless steel separation plates between the various chambers. Each plate has a 1-inch-

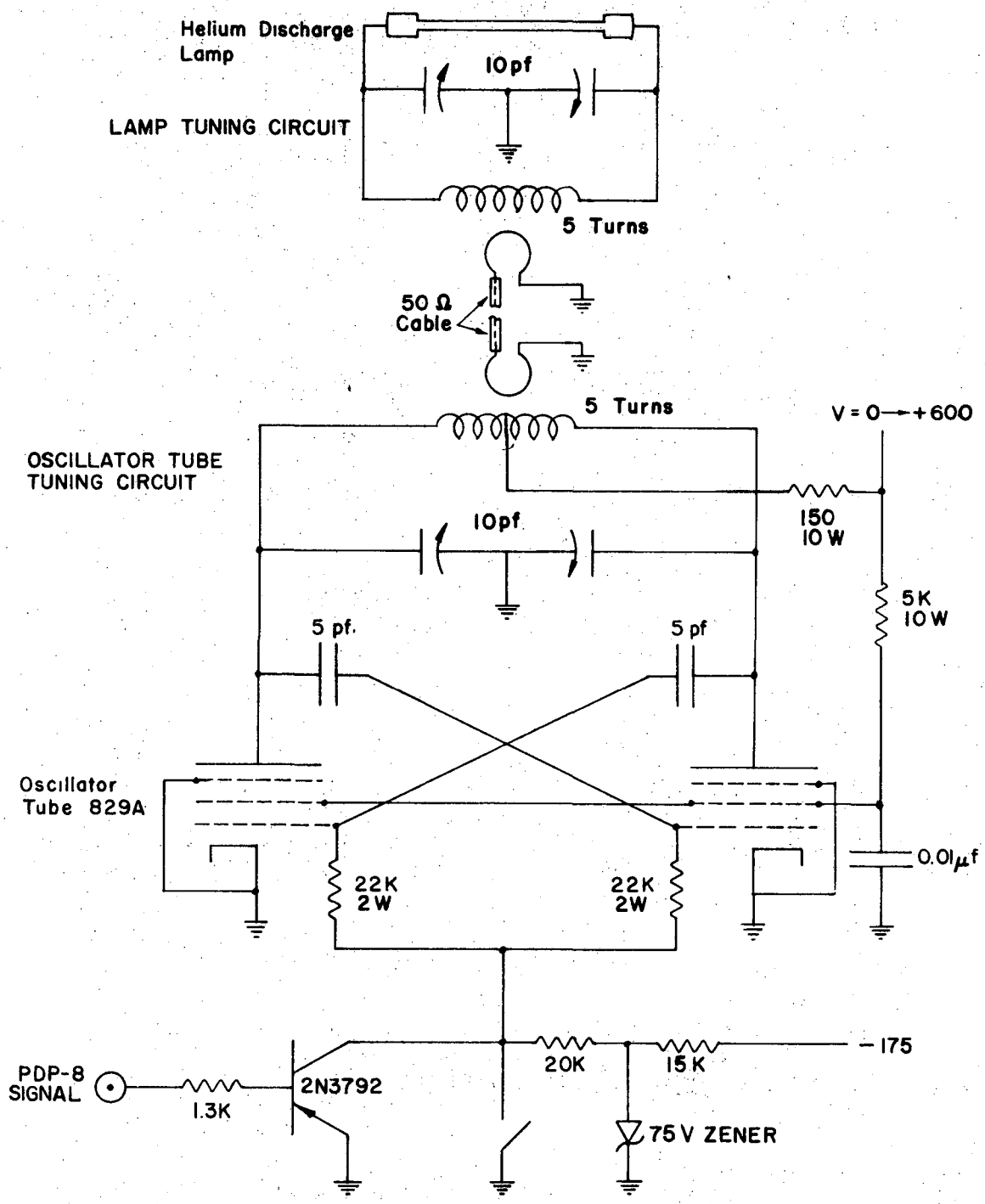

XBL 7011-6960

Fig. 19. Discharge lamp circuit. The input modulation consists of a -3-volt potential for turning the lamp on and a ground potential for turning the lamp off. The oscillator tube and the discharge lamp may be separately tuned by a variable capacitor in each tank circuit.

square hole in the center, over which is placed a 2-inch-square, 1/16-inch thick copper plate with a 1/4-inch diameter hole counter bored from above to present a knife edge to the beam. This combination, as shown in Fig. 20, allows the 1/4-inch hole to be moved until centered on the beam axis (which is not necessarily the exact center axis of each individual chamber).

To determine how good the collimation is, one takes the worst possible situation. Assume the source area is determined by the collimator directly above the electron gun. From Fig. 21, it can easily be found that the linear dimension subtended across the lower detector is 0.29 inches and the corresponding dimension on the upper detector is 1.75 inch. This case roughly approximates the projection of the long dimension of the slit in the source tube upon the detectors; the narrow source dimension will project smaller linear dimensions. Since each detector target is approximately 3.5 inches in diameter, both detectors necessarily see the same metastable beam, And the maximum solid angle subtended by the beam will be $5 \cdot 10^{-5}$ steradians.

Distance measurements are made by drawing a steel wire through the entire machine, cutting the wire at the appropriate places, and finally measuring the piece of wire outside the machine with a steel tape which is more accurate than 1/16 inch in 20 feet. Lineup of the machine is similarly done by drawing a thread through the machine and attaching a plumb bob to the end.

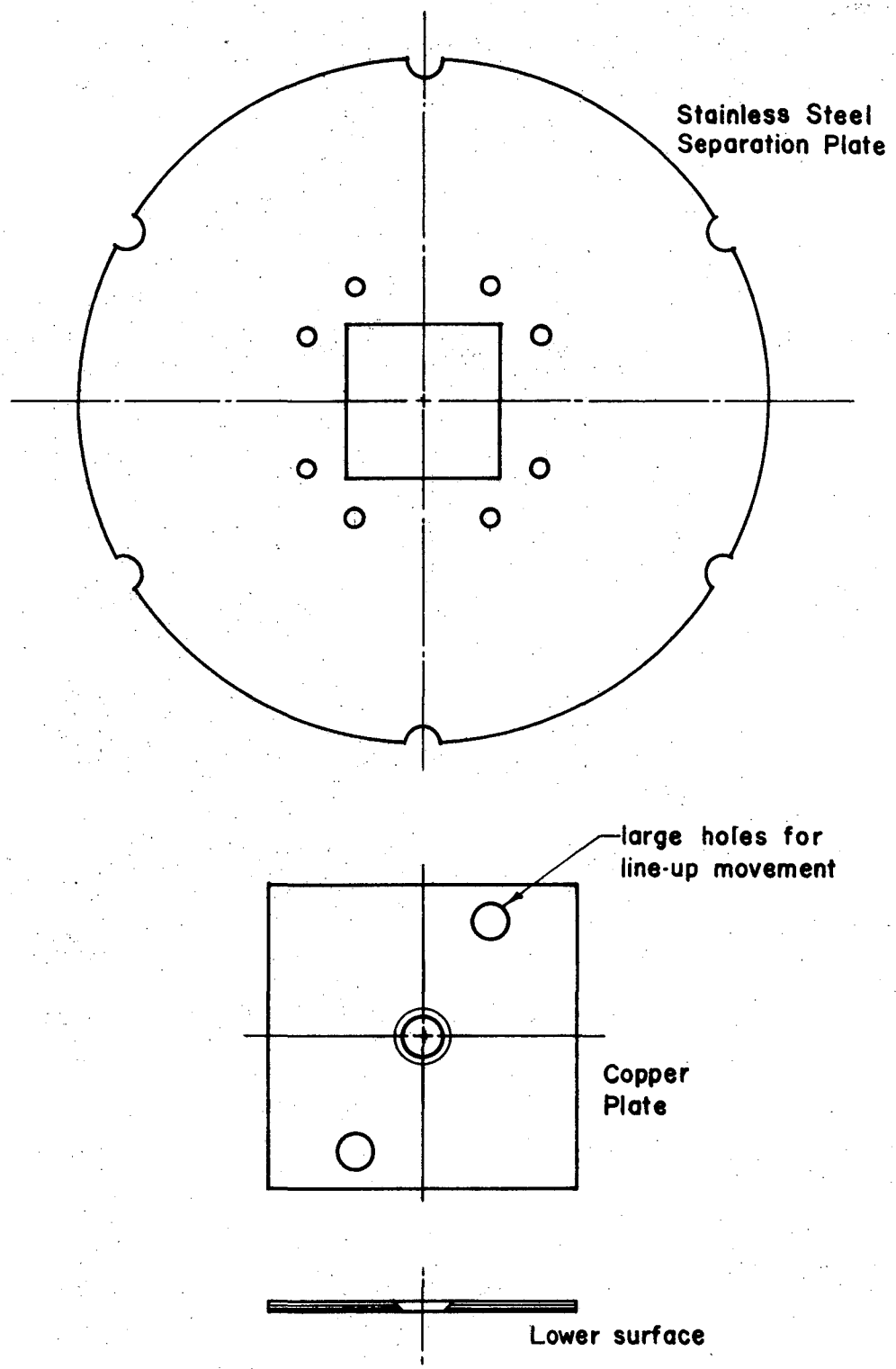

XBL 7011-6946

Fig. 20. Collimator - separation plate. A small 2-inch-square copper plate is moved around on the large separation plate for aligning the collimator hole with the beam axis.

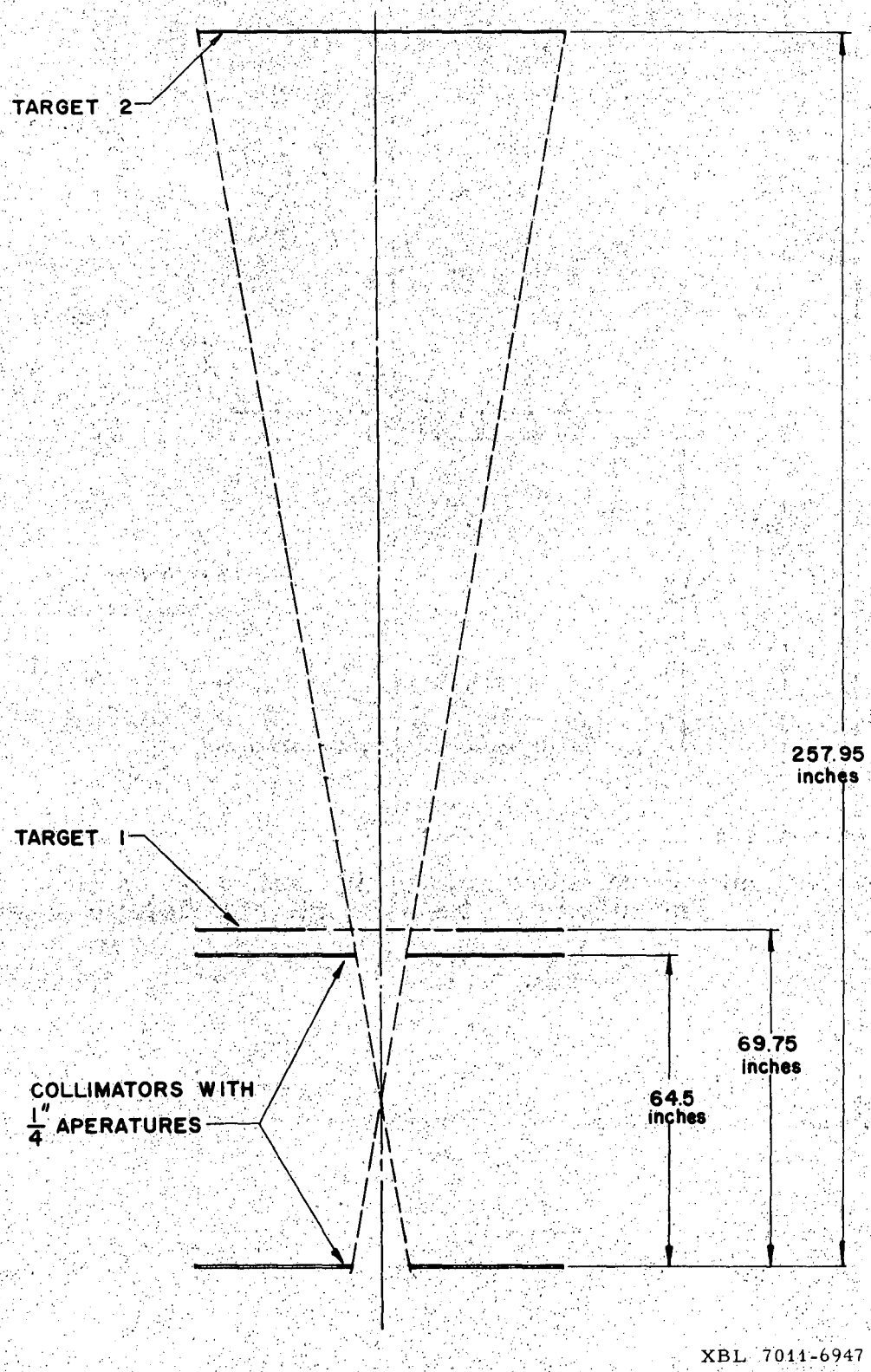

Fig. 21. Collimation scheme. The worst case arises when the collimation is determined by the first and last collimators.

H. Deflection Plates

The deflection plates, 1 cm apart and 14 cm high, located in the first buffer chamber, are not used during an actual run since they produced no observable effect. As shown in Appendix E, room temperature ions are unable to pass through all collimators and subsequently reach the first detector, because of the earth's magnetic field. Assuming a field of 0.5 G, perpendicular to the beam axis, an ion with velocity less than $7.7 \cdot 10^4$ m/sec cannot pass through both the first and last collimators. For this experiment on helium, atoms with velocities greater than 2000 m/sec are not analyzed primarily because there are so few of them. Nevertheless, the plates are useful with other gas samples, such as H_2. Also, in Appendix E, it is shown that, if a potential of 500 V is applied to the plates, any helium ion with velocity less than $2 \cdot 10^6$ m/sec is bent out of the beam. In this way, it was found that the present helium beam does not contain any detectable ground state ions that might be seen at the lower detector (hydrogen-like metastable helium ions would be easily quenched to the ground state).

I. Magnet

An inhomogeneous magnet of the usual two-wire type was constructed (but not used) with an especially high magnetic field gradient. A cross section of this magnet is displayed in Fig. 22. The convex surface (the bead) has a radius of 0.575 inch and the concave surface has a radius of 0.325 inch. The gap between these two surfaces is 0.250 inch. The magnet is totally 12 inches long and is spaced inside a 2-inch O.D.

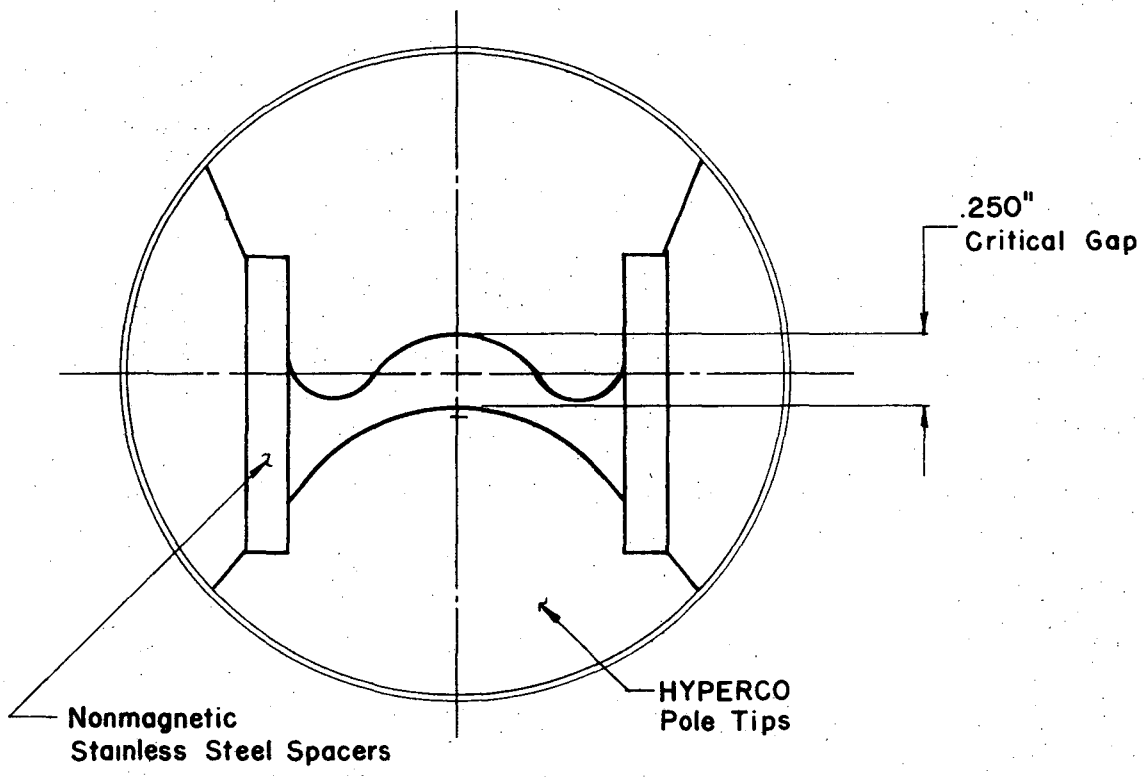

XBL 7011-6965

Fig. 22. Magnet cross section of the typical 2-wire type.

stainless steel tube. The pole tips are made of high-saturation Hiperco 35 magnetic steel with an expected field of 20,000 G in the gap.

Dimensions and gradients are such that, with only 10,000 G in the gap, all atoms with non-zero magnetic substates and velocities less than 2000 m/sec would be deflected from the beam and thus not reach the first detector. This is partly due to the large distance between the last collimator and the exit end of the magnet. The original purpose for the magnet was to change the relative populations of singlet and triplet metastable atoms in the beam in order to separate the effects of the two. The 2^1S_0 state does not have a magnetic moment, whereas the 2^3S_1 state does. Hence the $M = \pm 1$ substates of the 2^3S_1 metastable atoms would be deflected from the beam, leaving only 2^1S_0 $M = 0$ and 2^3S_1 $M = 0$ atoms. Analysis of the decay patterns should then allow the two components to be separated, because the 2^3S_1 atoms have a much longer lifetime. But, after discovering that a helium discharge lamp could do the same thing more easily and more completely, any plans to use the magnet were abandoned.

However, information can be gained from using the magnet. It can determine the ratio of singlets to triplets in the beam, providing equal populations among magnetic substates exist. Magnet-on would give $N_{on} = N(^1S_0) + 1/3\, N(^3S_1)$, whereas magnet-off would give $N_{off} = N(^1S_0) + N(^3S_1)$. Hence

$$\frac{N(^1S_0)}{N(^3S_1)} = \frac{N_{on} - \frac{2}{3} N_{off}}{N_{off} - N_{on}} .$$

Also, $N(^1S_0) = \frac{3}{2} N_{on} - N_{off}$.

More importantly, the magnet-on would allow singlet data to be collected nearly twice as fast. By throwing away 2/3 of the triplets, one throws away approximately 1/2 the metastable counts, but only triplet counts. Since higher count rate presently might produce uncertainty from dead-time correction for the amplifiers, eliminating a large number of triplets would allow increasing the source pressure, hence singlet count rate, without the necessity of any dead-time corrections.

J. Detection System

The basic goals of the detection system are: (a) to detect the 2^1S_0 metastable atoms (2^3S_1 atoms are also seen), (b) not to detect any ground state helium atoms, (c) to differentiate between lamp-on data and lamp-off data, and (d) to gate off light pulses occurring during excitation. The system consists of: (1) the targets to convert He^* to electrons, (2) the electrostatic electron multipliers to collect these electrons, (3) the high-rate linear amplifiers and 10 MHz discriminators to amplify the signal and discrimate against low-level noise, and (4) the computer network which properly stores the signal and synchronizes the lamp, the electron gun, and the solenoid with the data collection channels.

1. Targets

Originally, the targets were designed to intersect the atomic beam at a 45° angle and still appear circular when viewed along the beam axis. Thus the targets, cut from a 1/16-inch thick oxygen-free copper

plate, are elliptically shaped with a 3-1/2-inch minor diameter. This allowed the detector target to fill most of the area across the 4-inch O.D. drift tube, which is most important at the upper detector where the beam has a 1.75-inch diameter. At the lower detector, where the beam diameter is 0.29 inch, a 1-inch-square hole is cut in the target, over which is attached a 60%-transparent Buckbee Mears electroformed copper mesh. After it was found that distance (even changes as small as 0.25 cm) was very critical to the analysis of the data, the targets were placed horizontal , hence perpendicular to the atomic beam, in order to eliminate the 0.75-cm difference in height existing across the tilted detector surface.

The targets are mounted on ceramic stand-off insulators connected to 1/2-inch diameter aluminum rods in order to bias the targets positive (≈ +10 V) with respect to the ground potential of the drift tube's stainless steel surfaces. The electrons ejected from the target come off with 5 to 15 eV and, if it were not for the bias, many would be lost to the walls. In this respect, a more positively biased focus ring (≈20 to 50 V above ground) with an approximate 3-1/2-inch O.D., surrounds the first dynode of the electron multiplier and helps guide the ejected electrons toward the highly positive first dynode (≈500 to 700 V above ground). Potentials applied to these elements are varied to give a maximum count rate.

The principle by which metastables are detected by ejection of an electron from a metal surface was first discovered by Webb in 1924 with mercury metastables (WEB 24). In 1929, Oliphant showed that helium

metastables would also eject electrons from metal surfaces (OLI 29). The theory is based on the Auger process, in which an atom in an excited state of energy I above the ground state approaches the potential well of the metal, with work function ϕ (see Fig. 23). If $I > \phi$, then a conduction electron can be captured from the metal into the ground state of the helium atom and the excited electron will be ejected, without radiation. Excess energy $I - \phi$ is taken up in kinetic energy of recoil of the helium atom and of the freed electron. With I = 20.6 eV and ϕ = 4.46 eV for a copper surface (HOD 55), Auger ejection of electrons can readily occur near the copper surface for He^*, but not for $He(1^1S_0)$. Conceivably, some auto-ionization could also occur, however, because I_p(ionization) - I [= 4.0 eV] is less than the metal's work function. An excited atomic electron could be captured by the metal, resulting in a helium ion being evaporated from the surface. Actually, oxygen-free copper probably has a work function less than 4.46 eV, and conceivably lower than 4.0 eV, because of surface contaminates. Success of the present detection system is proof that sufficient Auger electrons are ejected for metastable helium on a copper surface.

The efficiency of this electron ejection process from copper has apparently not been measured, though He^+ on tantalum and molybdenum has an efficiency of 0.22 (HAG 53). Since each has a work function of 4.20 which might be close to that of our targets, it is reasonable to expect that He^+ on copper also has an efficiency of about 0.22. Also, the theory of this Auger ejection process suggests that neutrals and ions have identical efficiencies on the same target (HAG 54). Thus, a good

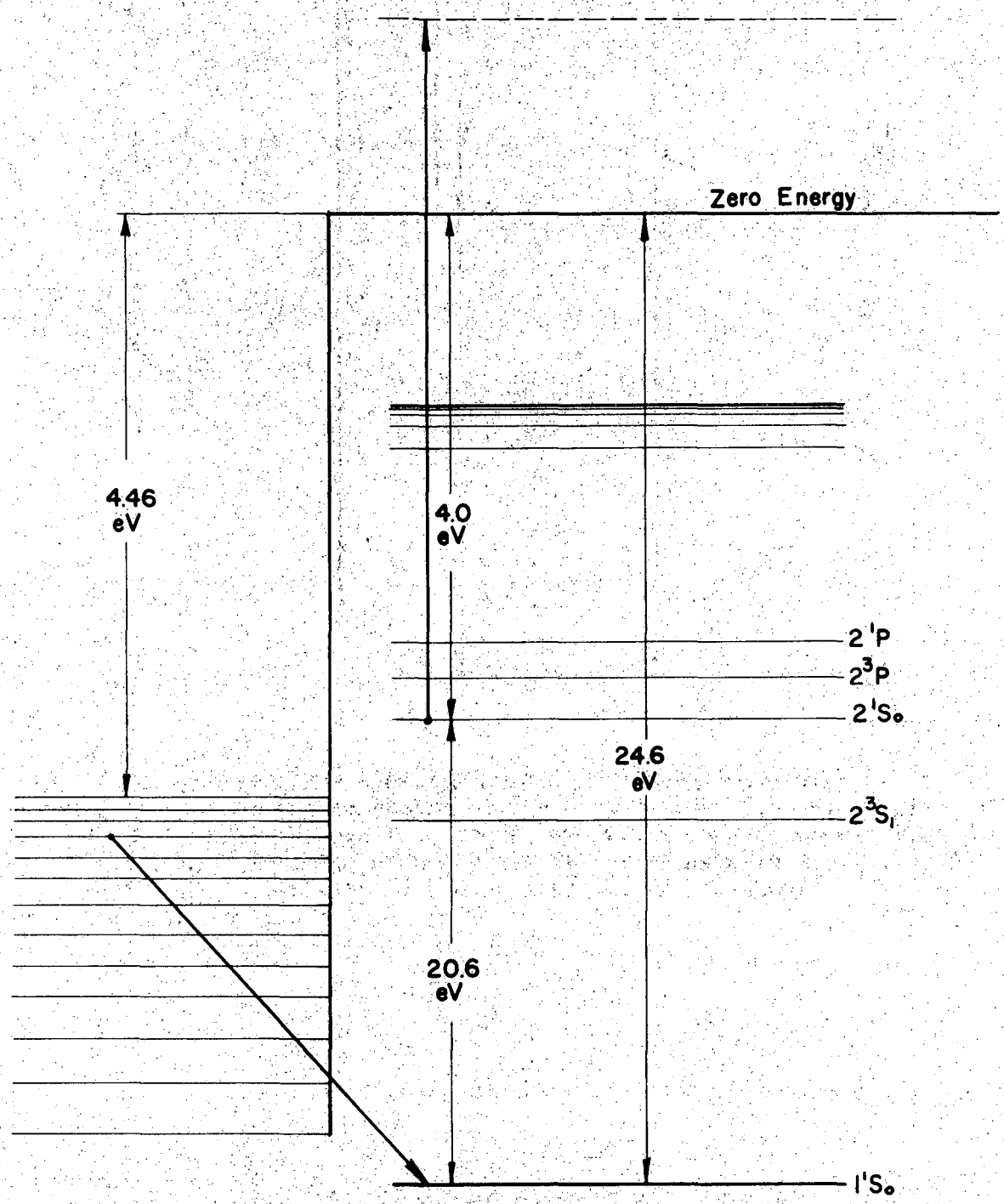

XBL 7011-7022

Fig. 23. Auger electron ejection mechanism. When the energy of the 2^1S_0 state minus the energy of the 1^1S_0 state (20.6 eV) is greater than the metal's work function (4.46 eV), a conduction electron can be captured into the ground state of the metastable atom with the simultaneous ejection of the excited electron without radiation.

estimate of the efficiency for electron ejection on copper by He^* is 0.22 ± 0.03, which represents a reasonable electron yield from copper.

2. Electron Multiplier

Originally, a Bendix Model 310 bakeable magnetic electron multiplier (MEM) was used to collect the ejected electrons. The detector was shielded with mu-metal in hopes of quenching the fringing magnetic fields. Unfortunately, the entrance window still contained fringing fields too large to allow many electrons to be collected. Thus the MEM was abandoned, though it could count neutral He^* very efficiently. Substituting an ordinary electrostatic electron multiplier for the MEM gave very good success. The multiplier, purchased from EMI with 24 venetian-blind-type dynodes, was adapted for use in the bakeable drift tube, with the first dynode parallel and 2 inches from the atomic beam, as illustrated in Fig. 24. The gain for these tubes is typically 10^6, depending on prior history. When the gain is too low, the tube can be partly reactivated by baking the drift tube or by placing the multiplier in an oxygen discharge for 15 to 30 min. Typically, 10 to 100 nsec wide negative pulses a few mv high are obtained, but after activation it is possible to have 50 to 100 mV high pulses. One-megohm resistors, used in the resistor chain, are spot-welded directly onto the dynodes, as can be seen in the photograph in Fig. 25, where both front and back views are shown with the transmitting target attached. Typically, 3000 V occurs across the resistor chain, giving a 1.5-mA current through each resistor. This current is much greater than typical μA currents produced by electrons absorbed into the dynodes. The anode potential is usually

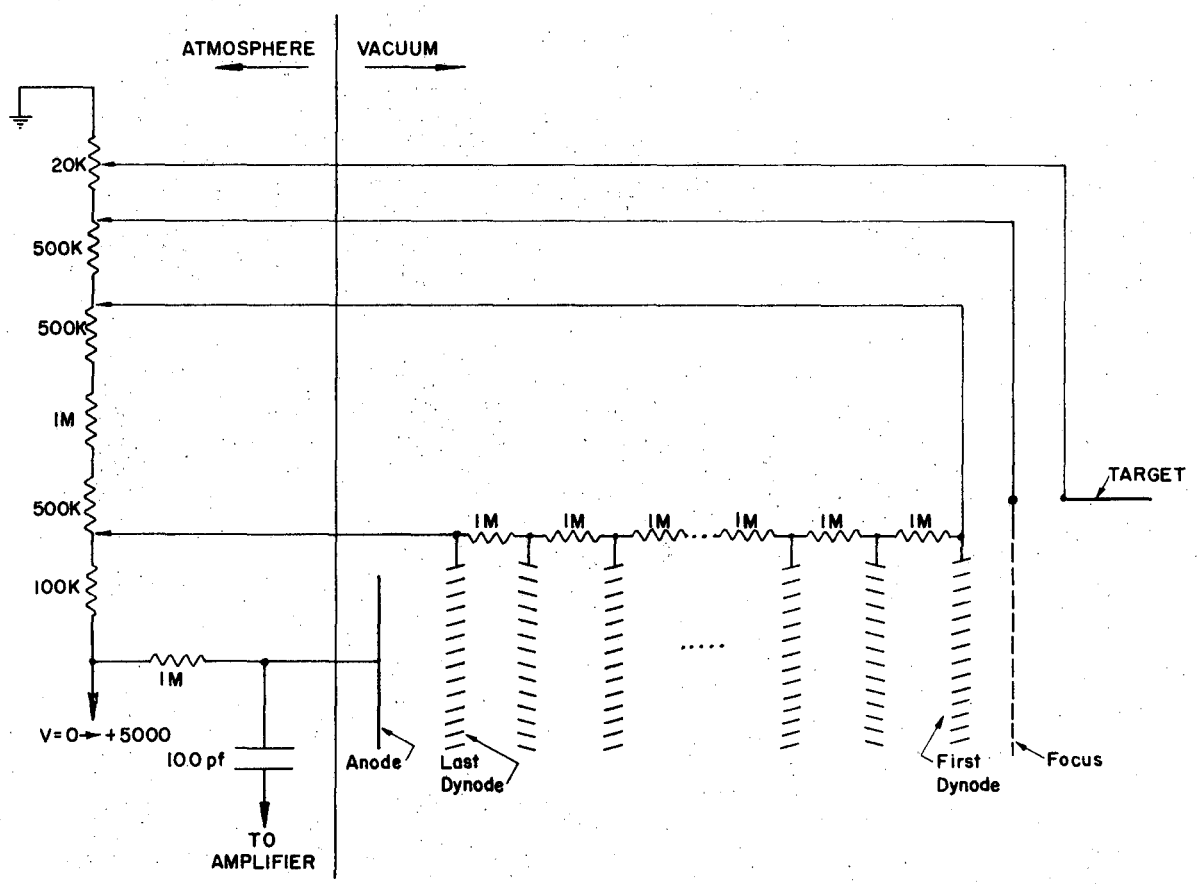

Fig. 24. Detection system, consisting of a target, an electron multiplier, a potential divider, and a capacitive output to the amplifier.

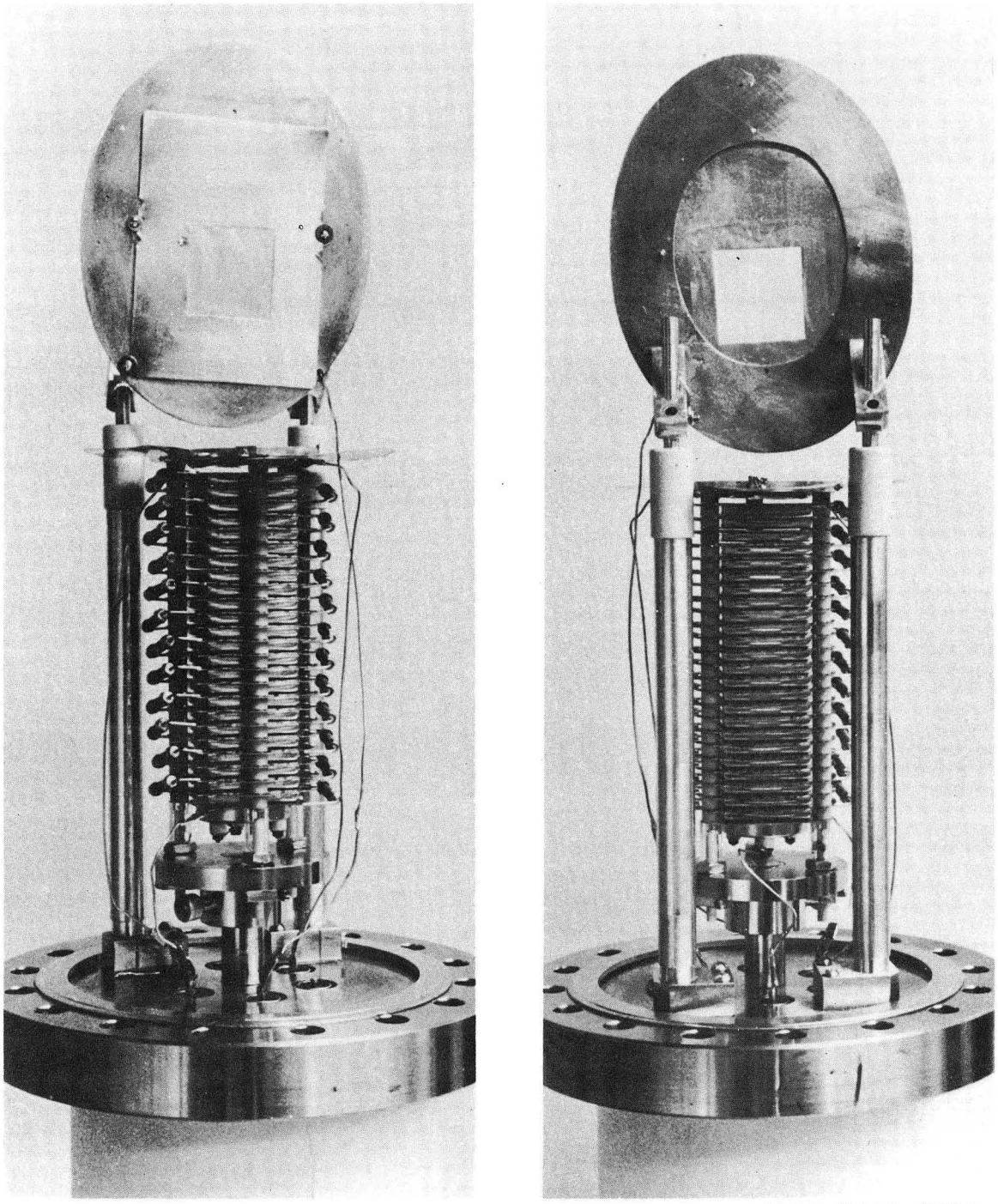

XBB 7010-4703

Fig. 25. Photograph, front and back views, of the electron multiplier and target with a 60% transmitting copper mesh.

200 volts higher than the last dynode's potential.

3. Amplifiers and Discriminators

A high-rate linear amplifier, Model 11X5501, with a 50-ohm input load to ground, is used to amplify the negative input pulses, giving out positive, 100 nsec-wide, 0.25-volt-high pulses on 125-ohm cable. Hence, two input pulses must not come closer than 100 nsec; otherwise they will appear as one pulse in the output of the amplifier. Theoretically, 10 MHz counting rates could be handled as a maximum if all pulses were equally spaced. Because real pulses are not equally spaced but actually arrive completely at random about any instant in time, the Poisson distribution must be invoked (EVA 55). That is, if the count rate observed is N_o and the actual count rate is N_A, then $N_o = N_A e^{-N_A \rho}$ where ρ = minimum resolution time (100 nsec). Hence,

$$N_A = -10 \text{ MHz } \ln \frac{N_o}{N_A} . \tag{38}$$

Thus, 99% of the real counts will be observed if the count rate is ≤100 kHz, and 99.9% will be detected if this count rate is ≤10 kHz. A further limitation occurs because the registers in the PDP-8 interface overflow if more than 64 counts arrive per channel time (≈80 μsec). In this experiment, the 100 kHz maximum is subsequently imposed in all runs. Actually, the integrated pulse count rate is ≤10 kHz, though the count rate for some peak channels may become as high as 70 kHz.

The output pulses from the 10-MHz discriminators (Model 3X9994) are given a rectangular shape of 40 nsec width and +6 volts height. The

only requirement on the pulse height is that it be greater than +3 V, necessary to trigger the PDP-8 interface logic circuitry. The discrimination level is set for the minimum 0.1 V to cut off only low-level noise pulses.

4. Computer Network

A block diagram of the total collection network is shown in Fig. 26. The central component of this network is the PDP-8 digital computer, programmed to control the solenoid and gun-pulsing circuits, the lamp oscillator circuit, the output keypunch, and the data collection system. The interface network properly gates and registers the count rate for lamp-on and lamp-off, gating out light pulses received when the electron gun is on. The time base circuitry is shown in Fig. 27 and consists of a series of flipflops to divide a standard 100 kc frequency, supplied by a Hewlett-Packard electronic counter, in multiples of 2. Thus, channel widths of 10, 20, 40, 80, and 160 μsec (or of 100, 200, 400, 800, and 1600 μsec if a standard 10 kc frequency is used) are available to the experiment. The time base circuit automatically shapes the standard input signal to give a -3 volt-to-ground square wave following the flipflops. This signal then triggers another pulse amplifier to produce uniform -3 volt-to-ground channel advance pulses used by the PDP-8 interface circuits.

The timing aspects of the experiment are shown in Fig. 28. The computer is programmed to determine this sequence of events, but the frequency of events is determined by the time base circuit. Channel 0 corresponds to the duration of the emission pulse created when the elec-

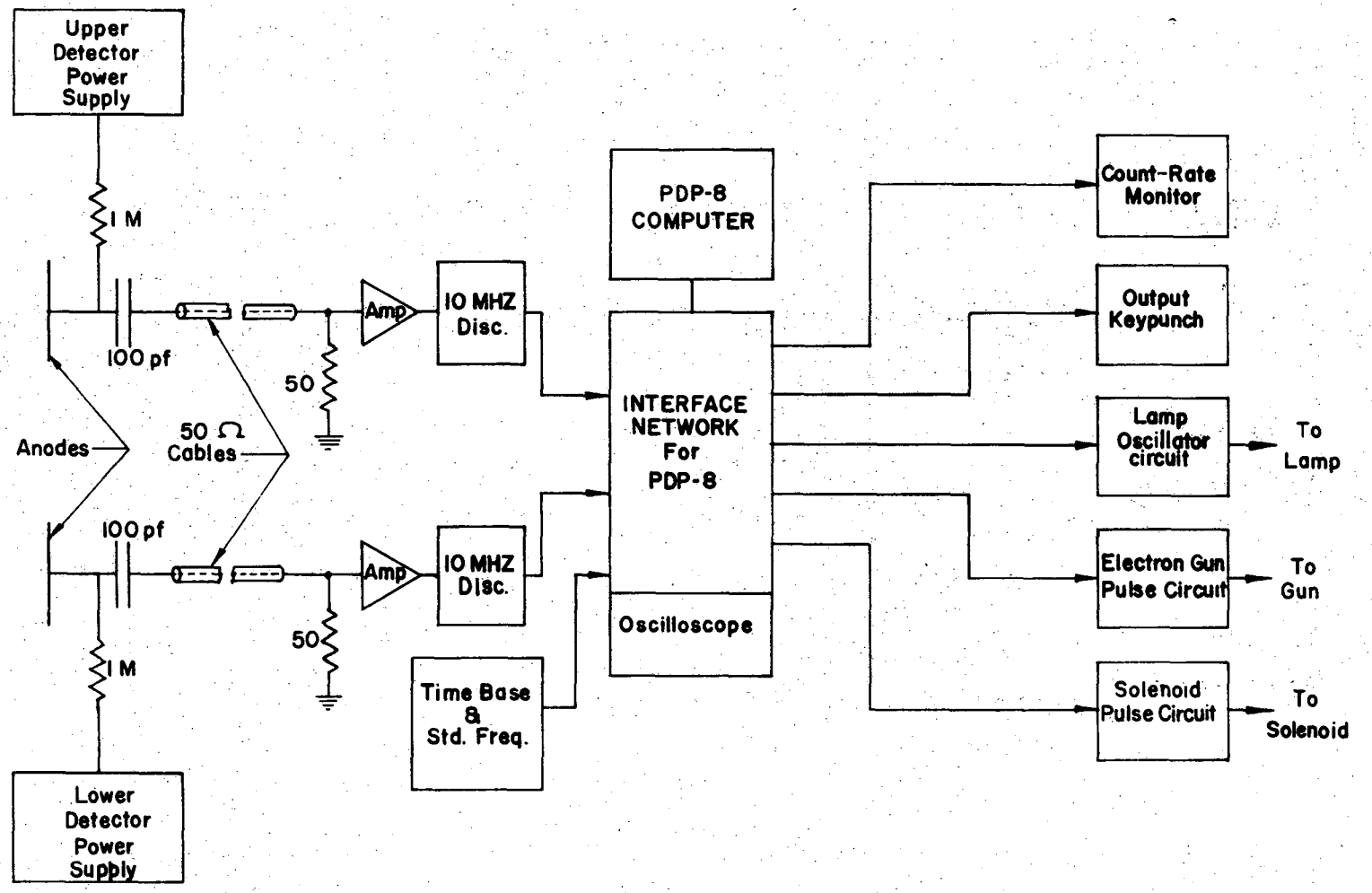

Fig. 26. Block diagram of the total collection network. Two identical systems, one for the lower detector and one for the upper, feed pulses into the PDP-8 interface network. Data collected is output on IBM cards.

XBL 7011-6961

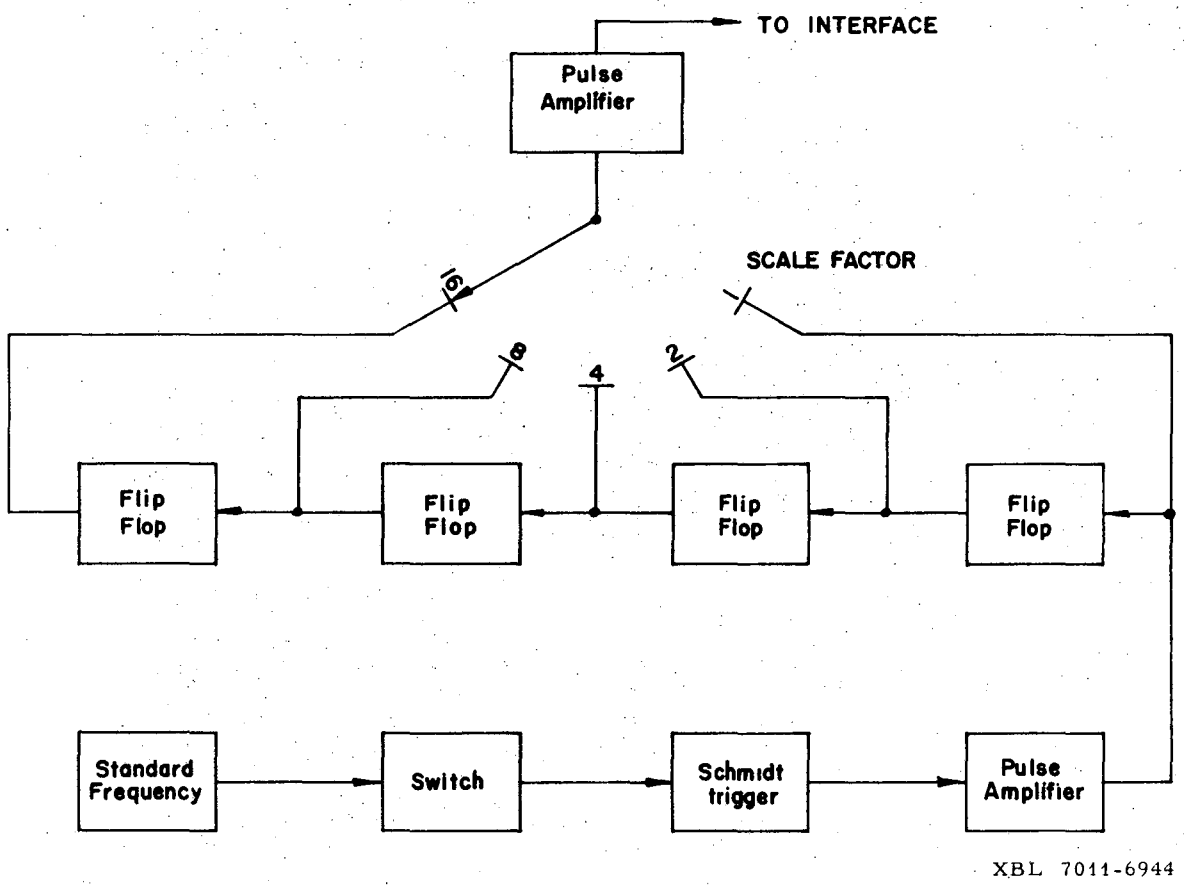

Fig. 27. Time base circuit. A standard frequency is divided by multiples of 2 to produce the basic channel advance pulses.

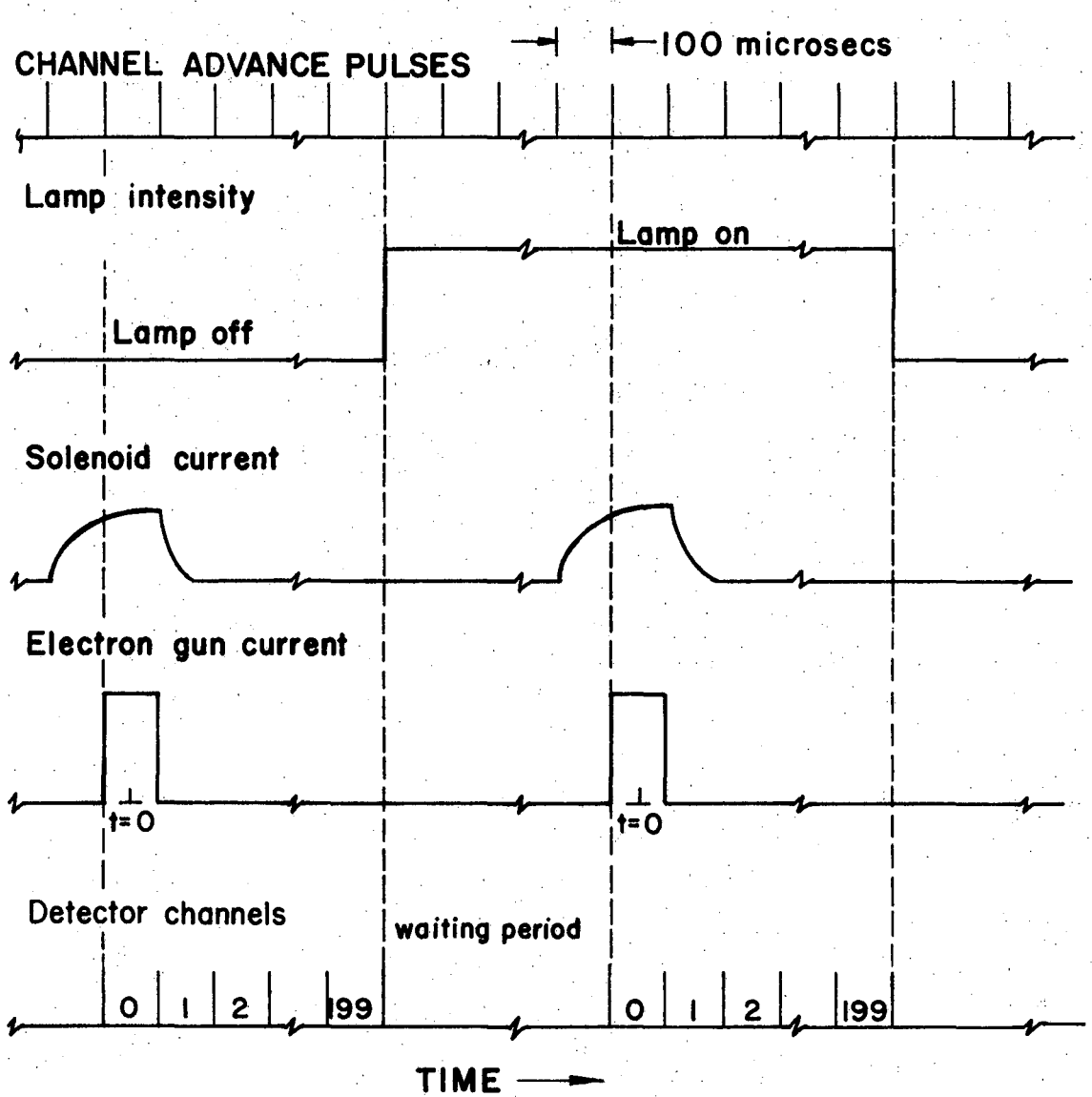

XBL 7011-6950

Fig. 28. Timing scheme, used to obtain the time-of-flight spectrum of the metastable helium atoms. Timing and data collection are controlled by the PDP-8 computer.

tron gun is pulsed on. Time t = 0 is marked by the center of Channel 0. The focusing solenoid is pulsed on a few milliseconds before Channel 0. In order to be stable when data counts are collected, the lamp is turned on (and off) only at the beginning of the waiting period – 16 msec –, at which time the computer is adding data collected in buffer registers to that already stored from previous sweeps and preparing for the next sweep. The critical timing provided by the channel advance pulses from the time base circuit is also shown in Fig. 28.

K. Experimental Procedures

The running procedure is a very simple one. When needed, traps are immediately filled with liquid nitrogen, since they can take up to an hour to cool down. Then instruments are turned on and valves are opened to let pressures equalize.

The count rate need not be maximized before each run, since the rate desired can be controlled through the precision metering valve. The gain on the multipliers and amplifiers is also set only once, to give maximum count rate without increasing the background noise. The system is also aligned only once by maximizing the count rate, to insure that all active components, besides the lamp, are positioned on the beam axis. Usually the electron gun filament remains on continuously in order to eliminate burn-out, since filaments usually break only when turning them on. Also, the emission likewise remains very stable.

When the electronics was first assembled, checks were made with a fast Tektronics oscilloscope to be sure that small timing errors did

not exist. During a run, only the lamp timing is monitored by the oscilloscope, through the use of a light-sensitive diode, thus allowing gross errors (such as factors of 2) to be detected easily if they exist, and providing a simple check to see if the lamp is turning on and off correctly. The drift tube pressure is usually checked before or after a run but never while a run is being taken, except in the source chamber, because the ion gauges can throw many counts into the detectors. Much care is usually taken not to introduce any spurious counts into the system, even those from turning on a light switch. Also, the PDP computer was found to very sensitive to any sparks accidentally created in the lab, tending to cause the computer to malfunction.

The following is a list of all the parameters which needed to be varied to check for effects on the lifetime $\tau(^1S_0)$. Also stated is the way these parameters are varied and the range of each.

(a) Source pressure: This pressure is varied by changing the flow rate through the precision metering valve starting from a base pressure of $5 \cdot 10^{-8}$ torr (with LN), increasing to a maximum of $3 \cdot 10^{-5}$ torr, at which point the diffusion pump foreline pressure would reach about 50 microns. The usual operating pressure is $(1 \text{ to } 2) \cdot 10^{-6}$ torr. The only criterion is that the amplifiers should not saturate, as discussed in Section III-J(3).

(b) Source position: The source assembly can be moved in two directions, but only the direction parallel to the slit is important. The center position is 300 mils, with movement possible from 150 mils to 450 mils.

(c) Source slit-to-gun distance: This can be varied only by removing the source assembly and changing the length of the tube which comes up to the gun. The distance ranges from 1/8 inch to 2 inches below the gun. Normally this distance is made as small as possible for obtaining the highest count rate, but a decrease by a factor of 10 can easily be obtained by increasing the distance to 2 inches.

(d) Beam temperature: This is changed by running with the source assembly's inner dewar at room temperature, filled with liquid nitrogen or filled with liquid helium. Usually, liquid nitrogen is kept in the center dewar. Unfortunately, the beam temperature never becomes the temperature of the source because of the effect of the colliding electrons and the heat radiation due to the filament.

(e) Gun voltage: Acceleration voltage can be varied from 0 to 300 V, though the best count rate is obtained at +50 V. These are not the voltages felt by the electrons, though, because of space charge effects.

(f) Lamp intensity: It can be lowered either by moving the lamp further away or by placing a screen mesh between the lamp and the reentry port. Normally the lamp is as close as possible for maximum intensity. Care is taken not to put too much power into the lamp since that would change the quality of the light by broadening the wings of the spectrum and possibly self-reversing the needed central frequency (KUH 62).

(g) Target and focus voltage: Target voltage is changed from 0 to +15 V but is normally set for maximum count rate (about +10 V). Focus

voltage can be set from +15 V to +500 V, but usually is placed at +15 V to maximuze the signal.

(h) Background pressure: This pressure depends on whether or not the drift tube is baked and the traps filled with LN. The pressures obtained are given in Table 2. Usually, runs are made after a bake, since there is a small pressure effect.

(i) Channel Width: This width may be 20, 40, 60, 80, 100, 160, 200, 400, 800, or 1600 μsec, but it was found that 80 μsec/channel gives the greatest number of useful points and still assures that almost all the slow atoms of the previous pulse have passed before the next pulse arrives at the upper detector. With the 16-msec waiting period and 200 channels of collection, the resulting 32 msec/sweep was found sufficient to prevent this overlap.

(j) Duration of run: Although the computer memory holds $16 \cdot 10^6$ counts/channel, the punch-out phase was designed to output data up to 6 digits only. Overflow rarely occurs, though, because it usually takes between 4 and 8 hours to collect 10^6 counts/channel. The usual run time is between 1 and 2 hours, with an integrated count rate of 4000 counts/sec. When a run is finished, the data counts collected are punched out on IBM cards, which are then analyzed by a CDC 6600 computer as required according to the analysis program.

IV. ANALYSIS AND CONCLUSIONS

A. Analysis Program ANALZ

As displayed by the interface oscilloscope, a typical example of the data collected and stored by the PDP-8 computer is shown in Fig. 29. Essentially, pulses from both detectors have been collected as counts into equally wide time-sequenced channels (Δ = 80 μsec). These data are punched onto IMB cards and analyzed by a larger computer. A program called ANALZ, designed to analyze these data, carefully matches the data from detector 1 with the data from detector 2.

Two means of approaching the analysis have been considered. The first possibility allows one to decide upon the size of δt at time t in the time-of-flight domain such that Eq. 28 remains valid. Then one determines the number of channels $\delta t_i/\Delta$ at time t_i which corresponds to δt for detector i. The advantage of this method is that δt may be varied in size, but the important disadvantage is that a time distribution of metastable atoms must be determined from the integrations that have occurred naturally by the collection process for each detector. This is easy to do at the upper detector because of the excellent resolution of the curve. Unfortunately, the spectrum is too sharp and narrow at the lower detector to obtain a reasonable distribution. Hence the problem is turned around and the program takes advantage of the natural integrations by the collection process at the lower detector. Thus $\delta t_1 = \Delta$, which then determines δt in the time-of-flight domain as well as δt_2 at the upper detector.

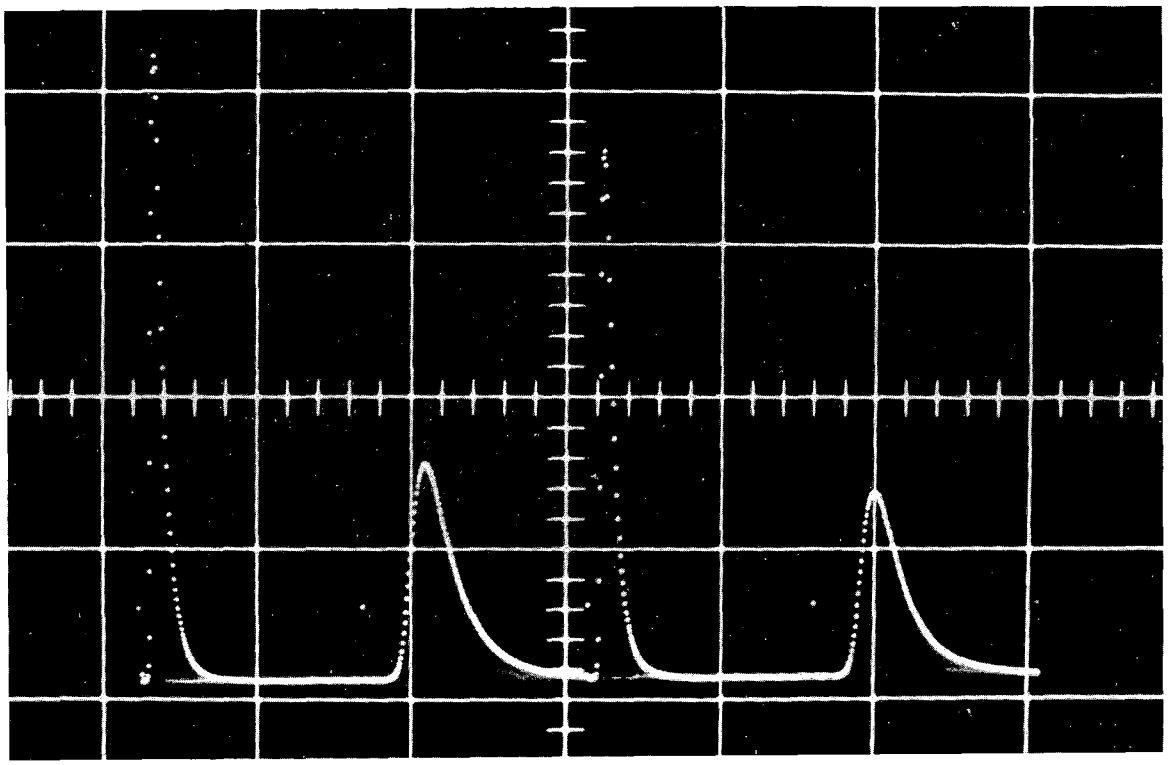

XBB 7010-4956

Fig. 29. Oscilloscope photograph of typical data collected. The tall narrow peaks are the time distributions for the lower detector; the small broad peaks are those for the upper detector. The left two distributions are lamp-off data, containing counts from both triplet and singlet metastable atoms. The right two distributions are lamp-on data, containing counts primarily from the triplet metastables.

In Appendix F, the size of δt_1 is investigated and is found to be sufficiently small as required by Eq. 28 if $t_1 > 12\Delta$ for a Maxwellian distribution.

The only other significant problem is to make sure that the atoms collected in δt_2 at time t_2 correspond exactly to atoms of the same speed at t_1 in δt_1. This task is controlled by subroutine SUMMAT. A five-point Lagrange interpolation method (ABR 64) is used by subroutine ENTGRL to determine a good approximation of the integral of the time distribution between t_2 and $t_2 + \delta t_2$. A seven-point Lagrange interpolation method was also tried with no detectable increase in accuracy.

The first thing program ANALZ does is to analyze the lamp-on data, which should consist of triplets only. The lifetime obtained is greater than one second, but because of the flatness of the curve, the error is often as large as the value of τ obtained. This analysis is important, though, because the triplets with their long lifetime provide a good indication of when something is not correct. For instance, the slope of the resulting plot is very sensitive to the exact distances d_1 amd d_2. These triplet plots were also used early in the experiment to see that scattering from the beam was insignificant within 10% accuracy.

Next, program ANALZ subtracts the lamp-on data from the lamp-off data. A typical singlet spectrum as a function of the time of flight for the upper detector, arising from this difference, is shown in Fig. 30. The program then analyzes the singlet data, taking the proper ratio of detector 2 to detector 1 data, and then fitting the resulting

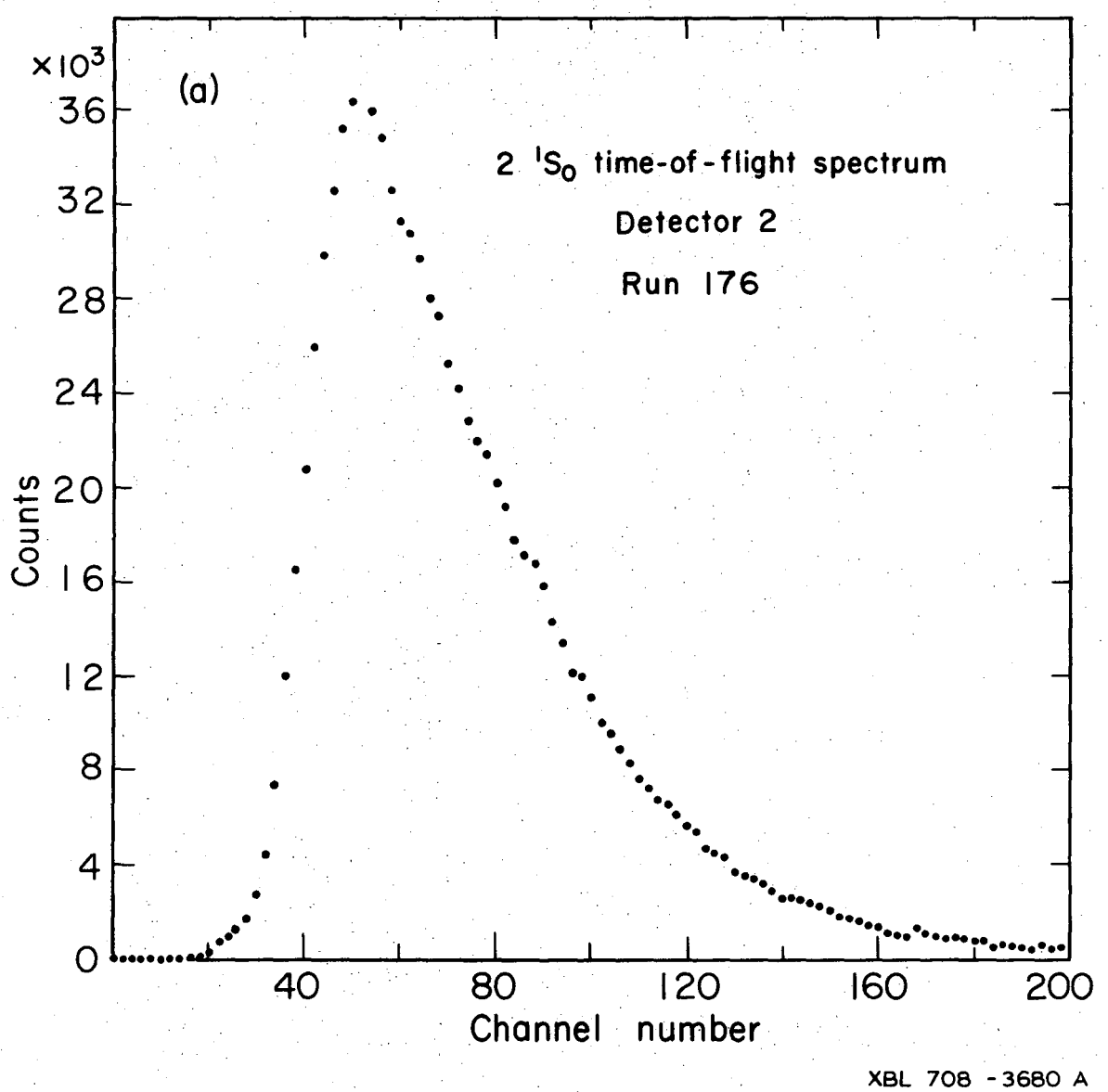

Fig. 30. Metastable singlet time-of-flight spectrum for detector 2 arising from the atoms quenched when the lamp is on.

log R(t) to a straight line between certain limits, giving the slope of this line as $-1/\tau$. Figure 31 is a typical logarithmic plot of R(t) and the resulting fitted straight line for a 2^1S_0 time-of-flight spectrum.

The entire program can be found listed in Appendix G. The following is a series of tests and checks which pertain only to the effectiveness of the program ANALZ.

(a) Accuracy of ENTGRL: This subroutine was tested on the discontinuous step function $F(x) = 1$ for $0 \leq x \leq 1$, and zero everywhere else. The integral

$$\int_0^1 F(x)\,dx$$

should have the value of unity, but was found instead to equal 1.00986, giving rise to an error of 1% resulting from the discontinuities at the endpoints. A more significant test of the subroutine was made using $F(x) = \sin x$. Then, in intervals between x and $x + \frac{\pi}{20}$, the result is good to 9 significant decimal places.

(b) Dependence on speed distribution: Test data were produced using a Maxwell distribution and assuming a decay lifetime of 10.00 msec. The resulting fit by program ANALZ gives $\tau = 10.05$ msec, giving rise to a 0.5% error. Similar test data were constructed using a simple triangle distribution and similar accuracy was obtained.

(c) Time/channel: This was changed in the program from the true values by 1%, 10%, and 100% for various runs, and in each case τ scaled by the same percentages.

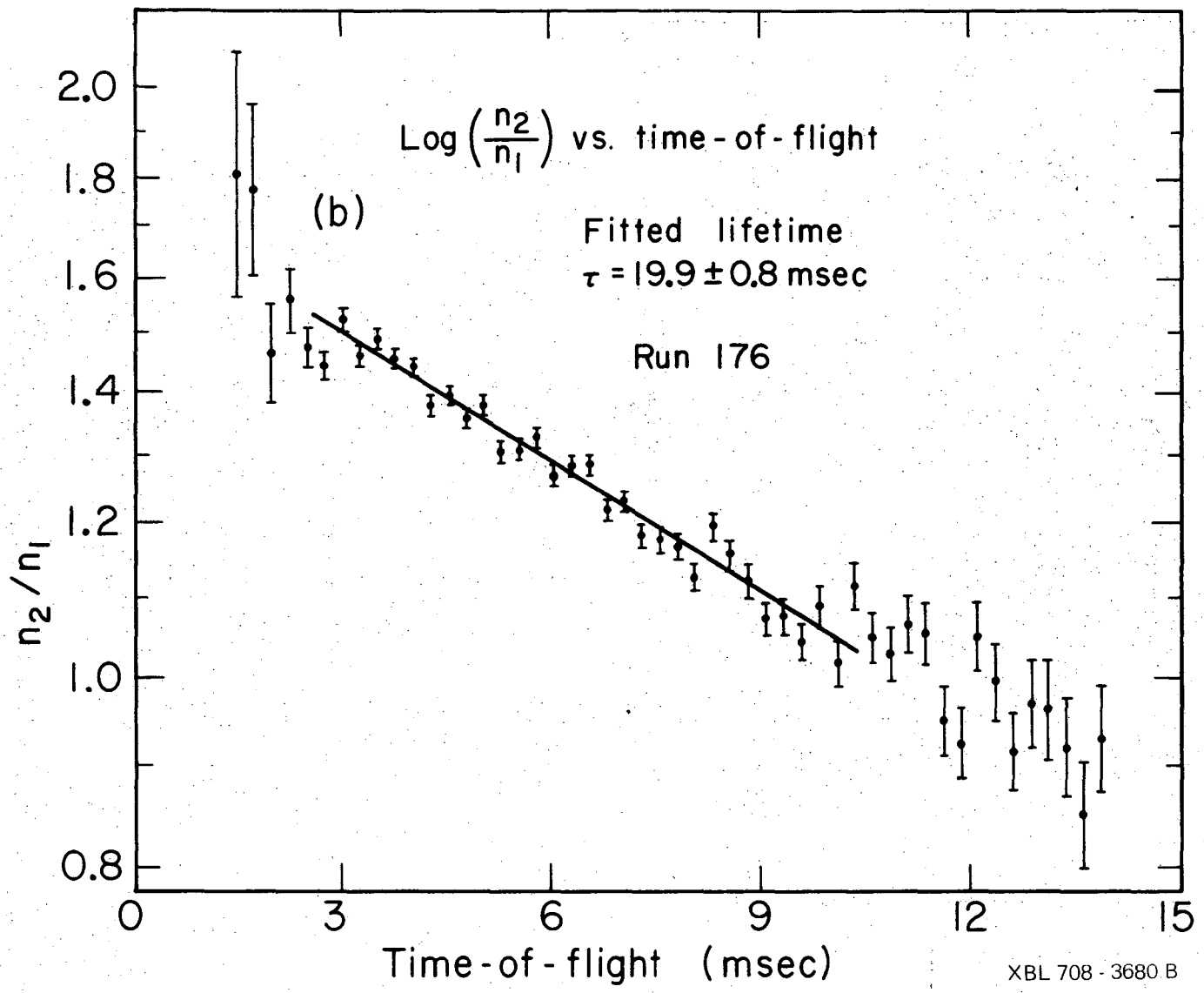

Fig. 31. Logarithmic plot of $R(t) = n_2/n_1$ versus time of flight t. The slope of the least-squares-fitted straight line is $-1/\tau$; only points with a number of counts $\geq$ 5% of the peak count are included in the fit.

(d) Background subtraction: It is assumed that detector i has the same background whether the lamp is on or off. The only mechanism that might increase the background for the lamp-on data would be the existence of some uv-quench photons in the beam. Because of the collimation of the machine, this effect has been minimized as much as possible. Also, the actual separate determinations of background have always suggested that they should be equal to within 5% at any one detector. Thus the difference data should always be independent of background, which may not be exactly uniform, because of shot noise. One test in which it was assumed that the upper detector had a background 20% higher for lamp-on data than lamp-off data indicated that τ would increase on the average by 0.35 msec. Since the backgrounds are probably not more than 5% different, the measured lifetime will not be increased more than 0.10 msec above the actual lifetime because of this effect.

(e) Limits for the straight-line fit: After the data have been analyzed, and the log of the ratio plotted, one then determines how much of the curve to fit to a straight line. The initial few points correspond to very few counts and should be neglected. There are, however, about 6 points on the time-of-flight plot beyond those first few which do not lie on the straight line, within their statistical errors. These are the points in which the size of δt_1 is too large for Eq. 28 to be valid and they too must be neglected. The points on the tail have large errors and may also be susceptible to low-velocity scattering. Table 3 summarizes a systematic check of the effect of the length of fit in the time-of-flight domain where

Table 3. Check on limits of straight-line fit.

Limits of K (Eq. 39)	Run	$\tau(^1S_0)$ (msec)
12-40	199	20.05(1.06)
	202	20.19(0.95)
	233	19.60(1.13)
	Average =	19.98(0.17)
12-50	199	19.74(0.95)
	202	19.51(0.78)
	233	19.80(0.90)
	Average =	19.66(0.09)
6-40	199	20.67(1.12)
	202	20.76(1.02)
	233	20.22(1.15)
	Average =	20.57(0.16)
12-26	199	21.66(2.46)
	202	19.58(1.85)
	233	24.13(3.48)
	Average =	20.91(1.17)
26-40	199	15.27(1.79)
	202	17.27(2.11)
	233	17;38(2.68)
	Average =	16.37(0.72)
19-33	199	20.10(2.42)
	202	25.59(2.47)
	233	17.71(2.02)
	Average =	20.64(2.31)

$$t = K\ \delta t + \text{constant} \tag{39}$$

with δt determined from $\delta t_1 = \Delta$. The table shows that, on the average, adding points too far into the tail or too soon at the beginning can cause an error of $\approx$0.5 msec in the lifetime. And any attempt to use fewer points simply increases the uncertainty in the fitted value.

(f) Convolution: In general, the spectrum obtained for detector i is not the true distribution involved in Eq. 28, but is a composite of those distributions created at any time during which the electron gun is on and anywhere in the electron gun region. Also, the integration which occurs because of the finite channel width as discussed in the first part of Appendix F is a convolution effect. These problems are studied in depth in the second part of Appendix F, where it is shown that, for a Maxwell distribution, convolution is not important beyond channel 12 of the lower detector.

(g) Distances to detectors: The distances which are used in program ANALZ must be known as accurately as possible. The sensitivity to distance can be seen by examining Table 4. There are two main reasons for this dependence: (1) changing the distances changes the size of δt_2 over which the integration is performed, and (2) the entire integration, taken at t_2, is shifted in position; hence, the wrong part of the curve is used for integration as well as the wrong size of δt_2 at t_2. Upon examining the weighted averages of the three runs in Table 4 for each change of the distances, and assuming that $\delta\tau' = \frac{\delta\langle\tau\rangle}{\langle\tau\rangle}$ is linear in δd_i, the following derivatives are found to fit the data:

Table 4. Check on sensitivity to distance measurement.

δd_1 (cm)	δd_2 (cm)	Run	$\tau(^1S_0)$ (msec)	$\tau(^3S_1)$ (msec)
0.0	0.0	199	20.05(1.06)	-467(139)
0.0	0.0	202	20.19(0.95)	-228(38)
0.0	0.0	233	19.60(1.13)	-222(42)
		Average =	19.98(0.17)	
0.5	0.0	199	21.53(1.22)	-172(25)
0.5	0.0	202	21.66(1.08)	-123(15)
0.5	0.0	233	20.98(1.32)	-119(17)
		Average =	21.43(0.20)	
-0.5	0.0	199	18.76(0.92)	952(516)
-0.5	0.0	202	18.93(0.86)	-955(514)
-0.5	0.0	233	18.41(0.97)	-969(543)
		Average =	18.72(0.15)	
0.0	0.5	199	19.67(1.02)	-723(307)
0.0	0.5	202	19.81(0.92)	-282(53)
0.0	0.5	233	19.25(1.08)	-274(57)
		Average =	19.61(0.16)	
0.0	0.0	239	21.17(0.99)	-2539(>1000)
0.0	0.0	250	19.54(1.14)	-206(31)
0.0	0.0	254	16.54(1.02)	-767(367)
		Average =	19.10(1.40)	
0.75	0.75	239	22.43(1.07)	-285(71)
0.75	0.75	250	20.71(1.37)	-126(16)
0.75	0.75	254	17.50(1.23)	-226(45)
		Average =	20.41(1.49)	
-0.75	-0.75	239	19.12(0.77)	396(64)
-0.75	-0.75	250	17.87(0.93)	-507(114)
-0.75	-0.75	254	15.70(0.87)	638(175)
		Average =	17.69(1.02)	

$$\frac{\partial\tau'}{\partial d_1} = 0.134/\text{cm}$$

$$\frac{\delta\tau'}{\delta d_2} = 0.039/\text{cm} \ . \qquad (40)$$

Thus, to find the actual change $\delta\tau$ for a computed change $\delta\tau'$, it is necessary to multiply this normalized change by the average lifetime. These formulas will be useful in Section IV-C for calculating the error in $\tau(^1S_0)$ due to distance uncertainty.

The triplet "lifetimes" are also listed in Table 4 for each change of d_i. Very large changes can occur in this lifetime for small changes in the slope of the $\ln[R(t)]$ curve because the slope is very close to zero.

B. Data

1. Helium

In total, 169 runs were taken using helium as a source gas, starting at number 100. Because of instrumental errors, runs 100 to 126 had to be discarded. After run 116, it was discovered that the counting system was saturating and had to be redesigned. Then, after run 126, it was found that the channel advance pulses were jittering. All runs taken after these conditions were corrected are listed in Table 5. The standard conditions for a run, after making final apparatus alterations to decrease systematic errors, consists of the following:

(a) Source pressure $P_s = 2\cdot10^{-6}$ torr representing $\approx$4000 cps inte-

Table 5a. First set of variable changes.

Run	$\tau(^1S_0)$ (msec)	$\tau(^3S_1)$ (msec)	P_D(torr)	Changes*	
127	18.69(0.78)	106(5)	$5\cdot10^{-8}$	Reduced lamp intensity	
128	18.32(0.73)	151(10)	$5\cdot10^{-8}$		
129	17.29(0.99)	99(5)	$1\cdot10^{-7}$		Far source hole
130	17.10(0.84)	107(7)	$1\cdot10^{-7}$		Far source hole
131	18.43(0.96)	100(7)	$1\cdot10^{-7}$		Far source hole
132	18.54(0.98)	93(5)	$5\cdot10^{-8}$		Far source hole
133	17.98(1.21)	101(10)	$5\cdot10^{-8}$		Far source hole
134	17.58(1.02)	103(6)	$5\cdot10^{-8}$		Far source hole
135	18.80(0.66)	263(52)	$1\cdot10^{-7}$	T_s = 4°K	Far source hole
136	18.31(1.07)	282(78)	$5\cdot10^{-8}$	T_s = 4°K	Far source hole
137	21.05(1.10)	176(25)	$5\cdot10^{-8}$	T_s = 4°K	Far source hole
138	18.73(0.97)	203(34)	$5\cdot10^{-8}$	T_s = 4°K	Far source hole

* The exceptions to standard conditions are:

1. Cross electron beam
2. Hole-type source
3. Δ = 100 μsec
4. d_1 = 1.918 meters; d_2 = 6.712 meters.
5. Target angle to beam = 45°

Table 5b. First source dependency check.

Run	$\tau(^1S_0)$ (msec)	$\tau(^3S_1)$ (msec)	Changes*	
			x_s (mils)	Lower peak channel for $^1S_0$
148	21.06(1.60)	73(4)	150	16
146	16.39(1.15)	77(3)	200	16
141	15.50(0.76)	96(7)	250	17
149	15.62(0.84)	105(7)	250	17
145	20.30(1.03)	213(34)	300	17.5
144	20.80(0.93)	264(54)	300	18
143	21.42(0.82)	222(41)	300	18.5
139	19.87(0.96)	666(>1000)	350	18
147	26.95(1.85)	723(>1000)	350	18
142	31.63(1.96)	-208(50)	400	18.5
140	37.87(3.51)	-128(20)	450	19

* The exceptions to standard conditions are the same as those in Table IV-3a, with the addition of:

6. Source hole close to gun
7. $P_D \approx 5 \cdot 10^{-8}$ torr

Table 5c. Second set of variable changes.

Run	$\tau(^1S_0)$ (msec)	$\tau(^3S_1)$ (msec)	Changes*	
			P_D (torr)	
150	17.04(0.57)	884(438)	$5\cdot10^{-8}$	
151	16.79(0.58)	523(123)	$5\cdot10^{-8}$	. . . x_S = 200 mils
152	21.17(0.87)	288(44)	$5\cdot10^{-8}$	. . . x_S = 400 mils
153	19.41(0.82)	214(24)	$5\cdot10^{-8}$	. . . V_T = 0.0 turns
154	17.62(0.65)	548(134)	$5\cdot10^{-8}$	
155	15.88(0.59)	993(418)	$1\cdot10^{-7}$	
156	16.82(0.69)	357(71)	$1\cdot10^{-7}$	
157	19.00(0.86)	2599(>1000)	$5\cdot10^{-8}$	
158	20.64(1.16)	-489(147)	$5\cdot10^{-8}$	. . . x_S = 400 mils
159	14.92(0.84)	2469(>1000)	$5\cdot10^{-8}$	. . . x_S = 200 mils
160	19.53(1.05)	446(109)	$5\cdot10^{-8}$	
161	21.01(1.86)	927(508)	$5\cdot10^{-8}$	. . . x_S = 400 mils
162	19.14(1.39)	398(106)	$5\cdot10^{-8}$	. . . x_S = 200 mils
163	19.13(0.66)	224(30)	$1\cdot10^{-7}$	
164	16.50(0.71)	277(46)	$1\cdot10^{-7}$	
165	19.82(0.88)	514(120)	$5\cdot10^{-8}$	
166	19.39(0.86)	527(125)	$5\cdot10^{-8}$	

* Common exceptions to standard conditions are:

1. Hole-type source
2. Δ = 100 μsec
3. d_1 = 1.895 meters; d_2 = 6.676 meters
4. Target angle to beam = 45°

Table 5d. Third set of variable changes.

Run	$\tau(^1S_0)$ (msec)	$\tau(^3S_1)$ (msec)	Changes*
167	20.57(1.19)	780(356)	x_s = 400 mils
168	20.55(1.05)	907(332)	x_s = 400 mils
169	20.78(1.11)	-3491(>1000)	
170	18.71(0.87)	>10,000	x_s = 200 mils
171	21.42(0.85)	700(254)	T_s = 4°K
172	21.36(0.90)	488(87)	T_s = 4°K
173	20.52(0.71)	863(340)	
174	20.39(1.56)	1316(957)	
175	19.74(0.76)	1926(>1000)	T_s = 4°K
176	19.75(0.84)	1557(>1000)	T_s = 4°K
177	19.85(0.82)	2255(>1000)	
178	20.70(0.87)	546(120)	
179	19.60(0.93)	-8902(>1000)	x_s = 200 mils
180	21.24(0.60)	573(199)	V_g = 75 volts
181	17.75(0.96)	1978(>1000)	
182	23.42(1.62)	-1083(654)	V_g = 35 volts
183	21.49(0.79)	2480(>1000)	$P_s = 1\cdot10^{-6}$ torr
184	16.97(0.62)	-647(221)	Solenoid current divided by 2
185	20.42(1.02)	312(38)	
186	23.47(1.07)	2838(>1000)	Δ = 200 μsec
187	18.98(0.70)	573(140)	
188	19.72(1.16)	403(71)	V_T = 0 turns
189	17.87(1.02)	299(52)	Reduced lamp intensity
190	17.93(1.17)	349(54)	Reduced lamp intensity
191	21.55(1.09)	608(160)	x_s = 200 mils Source far from gun
192	21.80(0.64)	-1226(>1000)	T_s = 4°K x_s = 200 mils Source far from gun

* Exceptions to standard conditions are:

1. $P_D \approx 5\cdot10^{-8}$ torr
2. Δ = 100 μsec
3. Target angle to beam = 45°
4. d_1 = 1.895 meters; d_2 = 6.676 meters

Table 5e. Pressure dependency check.

Run	$\tau(^1S_0)$ (msec)	$\tau(^3S_1)$ (msec)	Run	$\tau(^1S_0)$ (msec)	$\tau(^3S_1)$ (msec)
$P_D = 1\cdot10^{-7}$ torr			$P_D = 2\cdot10^{-9}$ torr		
193	18.61(0.79)	274(35)	213	20.41(1.10)	-274(52)
194	20.01(2.13)	828(449)	214	22.51(1.13)	-310(66)
195	22.32(1.69)	1526(>1000)	215	22.35(1.26)	-329(70)
196	20.49(1.04)	-890(442)	216	21.28(1.05)	-390(81)
197	18.82(0.99)	-1245(598)	217	18.87(0.85)	-293(58)
198	18.82(1.03)	-569(181)	218	19.71(1.04)	-342(81)
199	20.05(1.06)	-1022(578)	219	20.63(0.92)	-335(58)
200	18.94(1.07)	-550(153)	220	20.35(0.84)	-289(45)
			221	22.12(1.03)	-337(71)
$P_D = 4\cdot10^{-8}$ torr			222	20.05(0.99)	-297(53)
			223	21.60(1.07)	-280(49)
201	20.95(0.91)	-382(76)	224	18.84(0.81)	-340(61)
202	20.19(0.95)	-319(61)	225	19.33(0.75)	-411(97)
203	21.88(0.82)	-451(101)	226	19.35(0.92)	-319(64)
204	19.79(1.60)	-442(87)	227	20.17(1.10)	-342(64)
205	19.28(1.42)	-434(120)	228	19.29(1.01)	-371(78)
206	21.72(1.64)	-295(37)	229	19.23(1.19)	-322(65)
207	20.90(1.28)	-367(61)	230	20.43(1.00)	-339(59)
208	20.88(1.20)	-439(111)	231	20.33(0.82)	-308(59)
209	19.27(1.12)	-354(66)	232	20.63(0.92)	-265(44)
210	20.39(0.97)	-419(81)	233	19.60(1.13)	-299(55)
211	22.17(0.97)	-331(51)	234	21.58(1.26)	-292(49)
212	22.84(1.20)	-432(100)	235	19.93(1.02)	-296(49)
			236	23.16(1.39)	-380(81)

Table 5f. Second source dependency check.

Run	$\tau(^1S_0)$ (msec)	$\tau(^3S_1)$ (msec)	Changes	
237	21.28(1.16)	-1279(907)	x_s = 300 mils	V_T = 0 turns
238	21.21(1.06)	-1316(970)	300	0
239	21.17(0.99)	-2539(>1000)	300	0
240	18.73(0.98)	-837(434)	300	0
241	19.13(0.81)	-1369(>1000)	300	0
242	21.40(1.16)	-9327(>1000)	300	0
243	22.26(1.56)	-1503(>1000)	300	0
244	19.98(1.24)	-880(544)	300	0
245	18.97(1.06)	-512(133)	150	
246	18.05(0.92)	-281(36)	150	
247	19.53(1.24)	-259(37)	150	
248	18.69(1.03)	-263(45)	150	
249	24.41(1.40)	-271(53)	150	
250	19.54(1.14)	-206(31)	150	
251	20.60(0.90)	-233(44)	150	
252	21.11(1.14)	-251(43)	150	
261	20.67(1.30)	-294(70)	400	
262	21.73(1.38)	-265(52)	400	
263	20.54(0.78)	-251(55)	400	
264	24.21(1.77)	-265(56)	400	
265	22.50(1.49)	-226(42)	400	
266	22.55(1.37)	-238(42)	400	
267	19.60(1.09)	-204(32)	400	
268	21.55(1.06)	-222(39)	400	

Table 5g. Reduced lamp intensity check.

Run	$\tau(^1S_0)$ (msec)	$\tau(^3S_1)$ (msec)	Changes
253	18.93(1.35)	6710(>1000)	Reduced lamp intensity
254	16.54(1.02)	-767(367)	Reduced lamp intensity
255	21.84(1.44)	-976(546)	Reduced lamp intensity
256	20.07(1.60)	-1155(791)	Reduced lamp intensity
257	20.74(1.32)	-841(503)	Reduced lamp intensity
258	20.53(1.42)	-607(229)	Reduced lamp intensity
259	20.03(1.97)	-524(185)	Reduced lamp intensity
260	21.98(1.43)	-1319(>1000)	Reduced lamp intensity

grated count rate at the upper detector.

(b) Type of source = slit.

(c) Source-to-gun distance = minimum possible.

(d) Source position x_s = 300 mils.

(e) Electron beam direction = antiparallel.

(f) Source assembly temperature T_s = 77°K.

(g) Gun voltage V_g = 50 volts.

(h) Lamp intensity = maximum possible.

(i) Target angle to beam = 90°.

(j) Target and focus voltages (turns on helipot) at upper detector V_T = 6.3 turns and V_F = 0.0 turns.

(k) Detector distances d_1 = 1.9275 meters and d_2 = 6.7075 meters.

(l) Background pressure in drift tube $P_D = 2 \cdot 10^{-9}$ torr.

(m) Channel width Δ = 80 μsec.

(n) Duration of run = 1.5 hrs.

When conditions are different from these standard conditions, they will be indicated in the tables by the symbols defined above; all lifetimes are measured in milliseconds.

The triplet lifetimes of runs listed in Table 5a reflect inaccurate distance measurements which have been refined for latter runs upon discovery of the sensitivity of program ANALZ to d_1 and d_2. But some information can still be obtained from these runs. For instance,

$$\langle \tau(^1S_0) \rangle = 17.56 \pm 0.41 \text{ msec for } P_D \approx 1 \cdot 10^{-7} \text{ torr}$$

$$\langle \tau(^1S_0) \rangle = 18.05 \pm 0.29 \text{ msec for } P_D \approx 5 \cdot 10^{-8} \text{ torr.} \qquad (41)$$

This is only weak evidence for the existence of a pressure effect, though runs taken later verify its existence. Also,

$$\langle\tau(^1S_0)\rangle = 19.29 \pm 0.82 \text{ msec for } T_s = 4°K \,, \tag{42}$$

and this was the first evidence of a possible source dependence, since the slower beam of atoms created the effect of the off-centered source hole dependence (for positions $x_s > 300$ mils) found in runs listed in Table 5b. The explanation for this effect as explained in Section II-G(2) depends on the electron impact excitation process discussed in Appendix B. The quench lamp intensity may also affect the lifetime by a small amount since

$$\langle\tau(^1S_0)\rangle = 18.49 \pm 0.19 \text{ msec for reduced lamp intensity,} \tag{43}$$

though later runs will prove there is no detectable effect.

The runs in Table 5b are listed in order of increasing x_s, such that the general increase of $\tau(^1S_0)$ from 16 msec at $x_s = 200$ mils to 38 msec at $x_s = 450$ mils is readily visible. Also clear from this ordering is a shift towards more slow-speed atoms being excited into the metastable beam as the source hole moves away from the gun filament. This is evidenced by the shift in the $^1S_0$ peak channel of the time distribution to longer times, and this effect is consistent with that shift in $\tau(^1S_0)$ predicted from the $T_s = 4°K$ runs listed in Table 5a.

An attempt to remedy this condition by making the electron beam pass antiparallel to the atomic beam is evidenced by the runs in Table 5c. The relevant averages are:

$$\langle\tau(^1S_0)\rangle = 16.50 \pm 0.87 \text{ msec at } x_s = 200 \text{ mils}$$

$$\langle\tau(^1S_0)\rangle = 18.30 \pm 0.49 \text{ msec at } x_s = 300 \text{ mils}$$

$$\langle\tau(^1S_0)\rangle = 20.98 \pm 0.53 \text{ msec at } x_s = 400 \text{ mils.} \tag{44}$$

Clearly, a sizeable source dependence still remains. Also,

$$\langle\tau(^1S_0)\rangle = 17.03 \pm 0.72 \text{ msec for } P_D \approx 1\cdot10^{-7} \text{ torr,} \tag{45}$$

which now gives much stronger evidence of a pressure effect. Initially it was found that varying detector voltages also reflected the source dependence, but a $V_T = 0$ run now gives only weak evidence of this effect.

In hopes of further reducing the source dependence, a slit-type source is introduced, with the long direction parallel to the gun filament. Preliminary evidence for the reduction of the source effect can be found in Table 5d, from which it follows that:

$$\langle\tau(^1S_0)\rangle = 19.13 \pm 0.44 \text{ msec for } x_s = 200 \text{ mils}$$

$$\langle\tau(^1S_0)\rangle = 19.84 \pm 0.36 \text{ msec for } x_s = 300 \text{ mils}$$

$$\langle\tau(^1S_0)\rangle = 20.56 \pm 0.40 \text{ msec for } x_s = 400 \text{ mils}$$

$$\langle\tau(^1S_0)\rangle = 20.49 \pm 0.47 \text{ msec for } T_s = 4°K\ . \tag{46}$$

Other changes in variables such as source-to-gun distance, V_g, and V_T, are related to this source dependence, and are expected to affect $\tau(^1S_0)$ indirectly.

Because so few runs were taken for each variable change up to

this point, the results cannot be considered very conclusive. Hence the runs listed in Tables 5e-g are meant to remedy this deficiency. These runs were all taken using horizontal detectors, in hope of further reducing the source dependency effect. In Table 5e, only drift pressure is varied, with the result that:

$$\langle\tau(^1S_0)\rangle = 19.39 \pm 0.39 \text{ msec for } P_D = 1\cdot10^{-7} \text{ torr}$$

$$\langle\tau(^1S_0)\rangle = 20.96 \pm 0.31 \text{ msec for } P_D = 4\cdot10^{-8} \text{ torr}$$

$$\langle\tau(^1S_0)\rangle = 20.22 \pm 0.22 \text{ msec for } P_D = 2\cdot10^{-9} \text{ torr.} \qquad (47)$$

For the last two pressures, there is no clear evidence of a remaining pressure effect. The runs in Table 5f do show a remaining source dependency effect, though, as shown by the following averages:

$$\langle\tau(^1S_0)\rangle = 19.45 \pm 0.42 \text{ msec for } x_s = 150 \text{ mils}$$

$$\langle\tau(^1S_0)\rangle = 21.04 \pm 0.39 \text{ msec for } x_s = 400 \text{ mils,} \qquad (48)$$

where the mean of these two averages is near that expected for the standard source position. And, because

$$\langle\tau(^1S_0)\rangle = 20.36 \pm 0.44 \text{ msec for } V_T = 0, \qquad (49)$$

it follows that the singlet lifetime is no longer sensitive to target voltage of the upper detector (use of V_T at detector 2 for monitoring purposes follows from the larger target area employed in detection). From Table 5g it follows that

$$\langle\tau(^1S_0)\rangle = 20.61 \pm 0.42 \text{ msec} \qquad (50)$$

when lamp intensity is reduced. Thus, the singlet lifetime is not dependent on the speed distribution of the singlets as determined by the quenching factor f(v).

When necessary, runs in Tables 5e-g which differ by more than 3 msec (i.e., much greater than 3 standard deviations) from the computed average are rejected as having contained some anomalous fluctuation of the experimental conditions. The runs rejected are numbers 236 (>3 msec), 249 (>5 msec), 264 (>3 msec), and 254 (<4 msec).

Finally, it can be concluded that further simple modifications of the existing apparatus cannot eliminate the remaining systematic error. Since the electron gun is the direct cause of the source dependence, a major revision of that component will be necessary.

2. Helium Lifetimes

The best data available for determining a final value for $\tau(^1S_0)$ is found in Table 5e for $P_D = 2\cdot10^{-9}$ torr. These runs were generally fit between limits K = 12 and K = 40 in program ANALZ, and gave $\langle\tau(^1S_0)\rangle = 20.22 \pm 0.22$ msec, according to Eq. 47. To understand further the experiment, the same runs were fit between limits K = 18 and K = 38 and limits K = 25 and K = 55. The results of the first refitting are found in Table 6a, giving an average lifetime of

$$\langle\tau(^1S_0)\rangle = 19.34 \pm 0.32 \text{ msec} \tag{51}$$

and for every run, the triplet lifetime becomes a larger negative number. The second refitting is found in Table 6b and gives

Table 6a. Helium data fitted between K = 18 and K = 38.

Run	$\tau(^1S_0)$ msec	$\tau(^3S_1)$ msec
213	22.56(2.02)	-1031(721)
214	22.36(1.92)	-465(160)
215	21.35(1.91)	-1127(842)
216	20.24(1.40)	-387(101)
217	18.89(1.51)	-347(104)
218	22.07(1.97)	-1930(3281)
219	21.09(1.45)	-399(125)
220	19.57(1.22)	-632(226)
221	21.36(1.23)	-638(220)
222	19.37(1.39)	-715(348)
223	21.36(1.76)	-439(155)
224	17.50(1.07)	-514(129)
225	18.21(0.99)	-1172(868)
226	18.28(1.27)	-833(369)
227	18.93(1.27)	-876(482)
228	17.35(0.90)	-540(266)
229	20.38(1.94)	-596(237)
230	19.81(1.56)	-748(416)
231	19.64(1.22)	-502(145)
232	20.13(1.26)	-823(299)
233	17.92(1.38)	-545(205)
234	20.32(1.55)	-773(420)
235	17.79(1.02)	-275(52)
236	22.12(1.95)	-793(400)

Table 6b. Helium data fitted between K = 25 and K = 55.

Run	$\tau(^1S_0)$ msec	$\tau(^3S_1)$ msec
213	19.85(1.39)	-1181(1028)
214	20.70(1.36)	2665(5986)
215	19.95(1.83)	-1100(939)
216	22.50(1.77)	1926(2203)
217	19.22(1.61)	-843(677)
218	20.86(1.87)	-2232(4603)
219	18.54(1.18)	-593(270)
220	17.42(1.03)	-430(115)
221	19.81(1.58)	-1536(1534)
222	18.36(1.24)	-791(498)
223	20.25(1.49)	-1226(1188)
224	21.34(2.00)	-1345(1464)
225	21.10(1.22)	34,708(>10,000)
226	19.01(1.55)	-1084(823)
227	18.98(1.21)	-1099(938)
228	17.51(1.08)	-999(915)
229	21.66(2.41)	1683(2391)
230	18.73(1.15)	-876(534)
231	18.05(1.28)	-1163(1146)
232	18.22(0.91)	-1802(1414)
233	19.36(1.57)	-1343(1530)
234	17.65(1.13)	-519(213)
235	20.83(1.41)	18,339(>10,000)
236	20.65(1.53)	-5768(>10,000)

$$\langle\tau(^1S_0)\rangle = 19.16 \pm 0.28 \text{ msec} \tag{52}$$

where some triplet lifetimes now have very large positive values.

a. Triplets. A small convolution effect still disturbs the near-zero slope of the $\ln R(t)$ curve even beyond point K = 12, causing these initial points to lie below the straight horizontal line. Distance and background uncertainties account for the existence of the remaining negative values of $\tau(^3S_1)$ in Table 6b. A reasonable lower limit for the triplet lifetime, therefore, would be

$$\tau(^3S_1) \geq 1.0 \text{ sec.} \tag{53}$$

b. Singlets. It is possible that a lingering pressure effect still exists for very slow singlet metastables. That is, the scattering cross section might increase with decreasing speed for a beam atom, thus increasing the probability of scattering from a residual helium gas atom; the effective lifetime therefore becomes shorter. Fitting the first and second halves of the data, shown in Table 3, also verifies the shorter lifetimes for slower atoms. Because of this additional complication, the data points fitted between K = 12 and K = 40, emphasizing fast atoms, are used to extract the true radiative lifetime.

3. Neon

Neon has two long-lived metastable states. Since j-j coupling applies to neon (though equivalent LS notation is used), only the general selection rules in Table 1 apply. The usual order of states above the 2^1S_0 ground state is 3^3P_2, 3^3P_1, and 3^3P_0, respectively. Thus, the

$^3P_0$ state can decay either by M1 radiation to the $^3P_1$ state or by E2 radiation to the $^3P_0$ state. Classical arguments (STE 68, p.7) show: the lifetime of the $^3P_0$ state decaying by the above mechanisms is approximately 1000 seconds. Similarly, the $^3P_2$ state, decaying by M2 radiation, has a lifetime of approximately 77 seconds. In both cases, two-photon decay is impossible because of parity conservation.

Preliminary experimentation suggests that neon has a single detectable lifetime (within the limits of investigation of the present apparatus) with a lower limit of 1/2 second. Because of its almost constant metastable beam, neon was useful as a source gas during the early testing of the machine, when little was known about the systematic effects. All early neon runs were devoted to understanding the extent of systematic errors, and only those runs taken with the antiparallel electron beam are listed in Table 7. The standard neon run consists of the following:

(a) Integrated count rate $\approx$ 2000 counts/sec at the upper detector.

(b) Electron beam direction = antiparallel.

(c) Source-to-gun distance Z_s = minimum possible.

(d) Type of source = slit.

(e) Source position x_s = 300 mils.

(f) Gun voltage V_g = 50 volts.

(g) Target and focus voltages at upper detector: V_T = 17 volts and V_F = 43 volts.

(h) Source assembly temperature T_s = 77°K.

(i) Background pressure in drift tube $P_D = 1 \cdot 10^{-7}$ torr.

Table 7. Neon data with antiparallel electron beam.

Run	τ (msec)	Lower Peak Channel	Changes		
			x_s (mils)		
157	480(68)	19	200	large Z_s	
158	681(107)	19	300	large Z_s	
159	545(87)	18.5	200	large Z_s	V_T = 0 V
160	1743(874)	18	200	large Z_s	V_F = 150 V
161	547(81)	18	200	large Z_s	
162	1567(760)	19.5	400	large Z_s	
163	2763(2821)	18.5	300	hole source	no magnet current
164	504(66)	19.5	300	hole source	
165	456(52)	19	200	hole source	
166	533(91)	19.5	400	hole source	
167	687(124)	19.5	300	hole source	V_T = 0 V
168	465(47)	19.5	300	hole source	

(j) Channel width Δ = 200 μsec.

(k) Detector distances d_1 = 1.895 meters and d_2 = 6.676 meters.

The usual weighted average with standard deviation of all runs listed in Table 7 is

$$\tau = 507 \pm 23 \text{ msec} . \tag{54}$$

This value is stated as a lower limit, since it is very difficult to determine any lifetime greater than one second with any accuracy using only the attenuation measured in the initial 15 milliseconds of the beam's time of flight. Such limits of the machine will be discussed in Section IV-D(2). The effect on the speed distribution of changing the source position is indicated by the shift in the peak of the distribution as listed in Table 7.

C. Error Analysis

The three main sources of error in the experiment are: (1) statistical error associated with the total number of counts per channel, (2) experimental uncertainty in measured parameters, and (3) systematic errors introduced by the basic design of some parts of the beam machine. The statistical error arises from the deviations of the individual lifetimes about the average, calculated for a series of 23 runs taken under the best of conditions. The experimental uncertainty results principally from the measured error in the detector distances d_1 and d_2, and the systematic error arises principally from the source dependency effect discussed in the previous section.

1. Statistical Error

Assuming a Poisson distribution of the number of counts about the average, the standard deviation σ_n for each channel is equal to $n^{\frac{1}{2}}$ where n is the total number of counts collected in the given channel (YOU 62, pp. 57-64). Then the error in the $\ln R(t)$ is

$$\sigma_L{}^2 = \frac{\sigma_{num}^2}{n_2{}^2} + \frac{\sigma_{den}^2}{n_1{}^2} \tag{55}$$

where, by Eq. 28, $R = n_2/n_1$ (YOU 62, p. 98). For the triplet analysis,

$$\sigma_{num} = [n_2(\text{lamp on})]^{\frac{1}{2}}$$
$$\sigma_{den} = [n_1(\text{lamp on})]^{\frac{1}{2}} . \tag{56}$$

And for the singlet analysis,

$$\sigma_{num} = [n_2(\text{lamp off}) + n_2(\text{lamp on})]^{\frac{1}{2}}$$
$$\sigma_{den} = [n_1(\text{lamp off}) + n_1(\text{lamp on})]^{\frac{1}{2}} . \tag{57}$$

The values of σ_L, computed using Eq. 55, are then inserted into the straight line fitting program to compute the error σ_τ for the lifetime measured in a given run. The value of σ_τ according to Appendix H is

$$\sigma_\tau = \tau^2 \left[\frac{(\sum_i w_i)(\sum_i w_i [y_i - y_i(\text{fitted})]^2)}{N(\sum_i w_i)(\sum_i w_i x_i^2) - N(\sum_i w_i x_i)^2} \right]^{\frac{1}{2}} \tag{58}$$

where N is the number of fitted points or observations and (y_i, x_i) is a particular observation of the parameters $\ln R(t)$ and t, respectively. The weights w_i are the inverses of the uncertainties σ_L^2 for the observation in question. All run errors are obtained in this way.

The average and uncertainty for a given set of runs are obtained from the usual statistical formulas for a weighted mean and its corresponding standard deviation of the mean (TOP 65). If a particular run is designated by the index i, then

$$\langle\tau\rangle = \frac{\sum_i w_i \tau_i}{\sum_i w_i}$$

and

$$\sigma_{\langle\tau\rangle} = \left[\frac{\sum_i w_i (\langle\tau\rangle - \tau_i)^2}{(N' - 1)\sum_i w_i}\right]^{\frac{1}{2}} \tag{59}$$

where

$$w_i = \frac{1}{\sigma^2_{\tau_i}} ,$$

σ_{τ_i} is given by Eq. 58, and N′ is the number of runs being averaged. These formulae were used to calculate all the averages and uncertainties appearing in the previous two sections.

2. Experimental Uncertainty

The uncertainty in d_1 and d_2, as the main source of experimental error, arises for two reasons. First, each distance separately measured

is accurate to ±1/16 inch, or equivalently, ±0.16 cm. Secondly, all distances are measured to the center of the electron gun, which need not be the center of the excitation region; that is, no precaution was taken to confine the electrons totally within the limits of the gun. Since the gun height is 1 cm, and since electrons probably do not stray more than 0.5 cm from either the collector end or the filament end of the gun, a reasonable upper limit on the certainty of the central position for excitation is ±0.25 cm. Taken in quadrature, these two errors give an uncertainty of ±0.30 cm. Now, one applies the derivatives defined in Eq. 40 to this uncertainty by means of the formula (YOU 62, p.98)

$$\sigma'_{\tau,d} = \left(\frac{\partial\tau'}{\partial d_1}\right)^2 (\delta d_1)^2 + \left(\frac{\partial\tau'}{\partial d_2}\right)^2 (\delta d_2)^2 \quad . \tag{60}$$

Assuming that $\delta d_1 = \delta d_2 = 0.30$ cm, it follows that, if $\langle\tau\rangle = 20.22$ msec,

$$\sigma_{\tau,d} = \langle\tau\rangle\sigma'_{\tau,d} = 0.85 \text{ msec} \ . \tag{61}$$

There is some reason to believe that the derivatives defined in Eq. 40 overestimate the distance effect, because a refitting similar to that listed in Table 6b, for $\delta d_1 = \delta d_2 = -0.25$ cm and K = 25 to K = 55, decreases $\langle\tau(^1S_0)\rangle$ by only 0.18 msec. The distance effect should be smaller, though, for slower atoms, because the distribution changes more slowly as time increases.

3. Systematic Error

The following facts have been established concerning the effect on $\tau(^1S_0)$ by the source-dependency effect:

(a) As x_s increases, τ increases;

(b) As x_s increases, the speed distribution includes more slow atoms;

(c) $T_s = 4°K$ for $x_s = 300$ mils affects τ in the same way that $T_s = 77°K$ does for $x_s = 400$ mils.

The conclusion is that a colder, slower source gas is affected more by the source dependency than a fast beam. This is shown by facts (b) and (c), where slow atoms have a higher probability of being excited into the collimated metastable beam than fast atoms. Then, to minimize the source dependency problem, a shift towards faster atoms should be taken. Because of fact (a), the claim is that the lifetime measured at the central position, $x_s = 300$ mils, is too long and should be corrected by subtracting a small amount $\delta\tau$ from $\langle\tau\rangle$ for $x_s = 300$ mils. Since $\delta\tau$ is is unknown, but would probably make $\langle\tau\rangle$ fall between the values of $\langle\tau\rangle$ for positions $x_s = 300$ mils and $x_s = 150$ mils, it is reasonable to assign one-half the difference between these two averages as the error due to the source-dependency effect, that is, ±0.37 msec.

One can also use the following argument to find this uncertainty. Since the slit is approximately 150 mils long, $x_s = 225$ mils represents the position for atoms coming from the edge of the slit farthest from the source assembly, and $x_s = 375$ mils represents the position for atoms coming from the nearest edge. By linear extrapolation, the average change in τ from either position is ±0.50 msec, using Eq. 48.

By assuming the larger of the two possible errors discussed,

$$\sigma_{\tau,s} = 0.50 \text{ msec} . \tag{62}$$

If this value happens to be somewhat small, it will be compensated for by the fact that $\sigma_{\tau,d}$ is somewhat large.

4. Total Error

From Eq. 47, the calculated statistical error is 0.22 msec for $\langle\tau\rangle$ = 20.22 msec. Taken together in quadrature with errors defined by Eq. 61 and Eq. 62, the total error becomes

$$\sigma_{\langle\tau\rangle} = 1.02 \text{ msec} . \tag{63}$$

D. Conclusions

1. Improvements

This experiment can be vastly improved by building a new electron gun which confines the electrons within the bounds of the gun and has electrons traveling only parallel or antiparallel to the atomic beam axis. By confining the electrons, one determines accurately the center of the excitation region. And by restricting the electron motion perpendicular to the beam axis, the source dependency should be eliminated. The present gun cannot prevent all transverse motion, mainly because the focusing magnetic field produces helical electron motion. Also, the new gun should not allow atoms to strike a hot surface and then be excited into the beam. A system of fine mesh grids, used in the place of solid surfaces, would probably reduce the number of fast excited atoms; and an accelerating grid structure surrounding an equipotential region would restrict most perpendicular electron motion.

Another improvement of the experiment would have the incoming

cold beam directed parallel to the beam axis to help reduce the source-dependency effect, and also to eliminate most of the beam which has little chance of entering the collimated metastable beam. Thus it would be possible to run a more intense beam without increasing the source chamber pressure.

Lastly, the analysis program could be improved by including a program which deconvolved the data. This program would simply calculate the convolved count total in a given channel for a given distribution and compare this sum with the actual total count collected. When the correct distribution is found, the two count totals must agree, channel for channel. In this way, more data points would be available for determining τ. Also, slight errors would not exist in the straight-line analysis as they presently do for the helium triplets.

2. Measurable Lifetimes

It is important to know the range of lifetimes that can be reasonably measured by this atomic beam machine. Then one can determine if a particular metastable lifetime of a given source gas is measurable with reasonable accuracy. The necessary assumptions are that the metastable atom will cause an electron to be ejected from a target and that the metastable state can be isolated by quenching, appearance potential, or other means.

First determine the channel width Δ such that an appreciable fraction of the time distribution lies between say, $t_1 = 10\Delta$ and $t_1 = 50\Delta$ at the lower detector. Generally, if K_{in} is the first usable channel and K_{fin} is the final usable channel at detector 1, then $n_1(t_1)$

must be greater than 5% of the peak value for t_1 between $K_{in}\Delta$ and $K_{fin}\Delta$. At the very minimum, $K_{fin} - K_{in} = 20$, since fewer points no longer give a reasonable statistical error to the measured lifetime.

Then the following two criteria must be met:

(a) The lower limit of τ is defined by

$$\tau \geq T_L \, \Delta \tag{64}$$

where, if K_p is the peak channel for detector 1,

$$T_L = \frac{d_2}{d_1} \cdot K_p \, .$$

(b) The upper limit on τ is determined from

$$\tau \leq T_U \, \Delta \tag{65}$$

where $$T_U = 10 \, \frac{d_2 - d_1}{d_1} \, (K_{fin} - K_{in}) \, .$$

Eq. 64 assures that a sufficient number of metastable atoms reach detector 2 before decaying. Since $\Delta = 1.5$ μsec is the minimum that could be programmed for the present apparatus, and since K_p is usually made to be ≈20, τ must be greater than 0.1 msec. If τ is greater than this limit, Eq. 64 may be turned around to determine possible values of Δ which can be used.

Eq. 65 assures that at least 10% of τ will be observed in the time-of-flight domain, which is necessary if τ is to be measured with reasonable accuracy. This upper limit can be approximated for $T_s = 77°K$ if one again assumes that $K_p = 20$ for detector 1. Then $\Delta \approx d_1/20\alpha$ where

α is the most probable speed; and if $K_{fin} - K_{in} \approx 60$, it follows that

$$\tau \leq 50\ M^{\frac{1}{2}}\ \text{(msec)} \tag{66}$$

where M is the molecular weight of the source gas and $\alpha \approx 1500$ m/sec for helium at $T_s = 77°K$. For helium, Eq. 66 implies that a lifetime greater than 100 msec cannot be reasonably measured.

It may be possible to realize both conditions 64 and 65 simply by cooling the beam down.

3. Summary

From data collected for helium and neon, it can be determined that $\tau(\text{neon}) \geq 0.5$ sec and $\tau(\text{helium } 2^3S_1) \geq 1.0$ sec. The final lifetime obtained for the helium singlet metastable is, from Eqs. 47 and 63:

$$\langle \tau(^1S_0) \rangle = 20.2 \pm 1.0 \text{ msec}\ , \tag{3}$$

which is well within the limits of measurable lifetimes defined by Eqs. 64 and 65. This value readily agrees with the theoretical lifetime of 19.5 msec (DRA 69). Table 8 summarizes all the theoretical predictions and previous experimental measurements of the singlet lifetime. The experimental lower limits are all in agreement (STE 69, PEA 68), but the last experimental value by Pearl disagrees by a factor of 2 (PEA 70).

Though this experiment did not verify the theory, it did prove to be consistent. This is the best that could be hoped for because of the large experimental and systematic errors still remaining in the experiment. These individual errors are also listed in Table 8.

Table 8. Helium 2^1S_0 lifetime.

$\tau(2^1S_0)$ msec	Reference
Experiment	
1 (lower limit)	PEA 68
9 (lower limit)	STE 69
38 ± 8	PEA 70
20.2 ± 1.0	Present experiment
0.22 (statistical error)	
0.50 (systematic error)	
0.85 (experimental error)	
Theory	
115 to 155	BRE 40
22	DAL 66
12	DAL 66a
20	VIC 67
19.5	DRA 69
19.6 and 20.2	JAC 70

APPENDICES

A. Transition Probability

The starting point for all transition probability computations is Fermi's Golden Rule (GOT 66, p. 444):

$$W = \frac{2\pi}{\hbar} |M_{fi}|^2_{av} \frac{dn}{dE} , \qquad (1)$$

where W is the transition probability per second, M_{fi} is the matrix element for the interaction energy H′, dn/dE is the density of accessible final states per unit energy, and the average is taken over photon directions and polarizations.

To observe two-photon emission from an electron in a bound state, which is necessarily a second-order process, the first-order interaction matrix element must be zero. The general perturbation expansion for the energy of interaction between an atom in state i with energy E_i^o and the electromagnetic field created by the emitted photons, resulting in the atom's making a transition to state f with energy E_f^o, is (SLA 60, p.124)

$$H'_{fi} + \sum_n \left[\frac{H'_{fn} H'_{ni}}{E_n - E_i^o} + \left(\begin{matrix}\text{Interchange} \\ \text{of photons}\end{matrix}\right) \right] + (\text{higher order terms}) \qquad (2)$$

where n represents the intermediate state with energy E_n, and the term requiring interchange of photons is necessary because one cannot differentiate between the photons. The expression (2) replaces the matrix element M_{fi} in Eq. (1), and since it is assumed that state i and state f cannot be connected by a single photon ($H'_{fi} = 0$), Eq. (1) becomes

$$W = \frac{2\pi}{\hbar} \left| \sum_n \frac{H'_{fn} H'_{ni}}{E_n - E_i^o} + \sum_n \left(\begin{matrix}\text{Interchange}\\ \text{of photons}\end{matrix}\right) \right|^2_{av} \frac{dn}{dE} \tag{3}$$

where one photon accompanies each interaction term in the energy matrix element. In particular, with reference to the first summation, let photon 1 with frequency ν_1 be associated with term H'_{ni}, and photon 2 with frequency ν_2 be associated with term H'_{fn}. Since the intermediate state consists of photon 1 and one real state of the atom with energy E_n^o (see Fig. 32),

$$E_n = E_n^o + h\nu_1 \ . \tag{4}$$

(Remember, energy is not conserved in the intermediate states.) Define the frequency ν_{ni} by

$$E_n^o - E_i^o = h\nu_{ni} \ . \tag{5}$$

Thus the energy denominator for the first summation in Eq. (3) becomes

$$h\nu_{ni} + h\nu_i \ . \tag{6}$$

The interaction operator which is treated as a perturbation is (GOT 66, p. 465)

$$H' = -\frac{e}{mc} \vec{P}\cdot\vec{A}(\vec{r}) \ . \tag{7}$$

As usual, time is not considered in this operator since it would only produce the phase factor

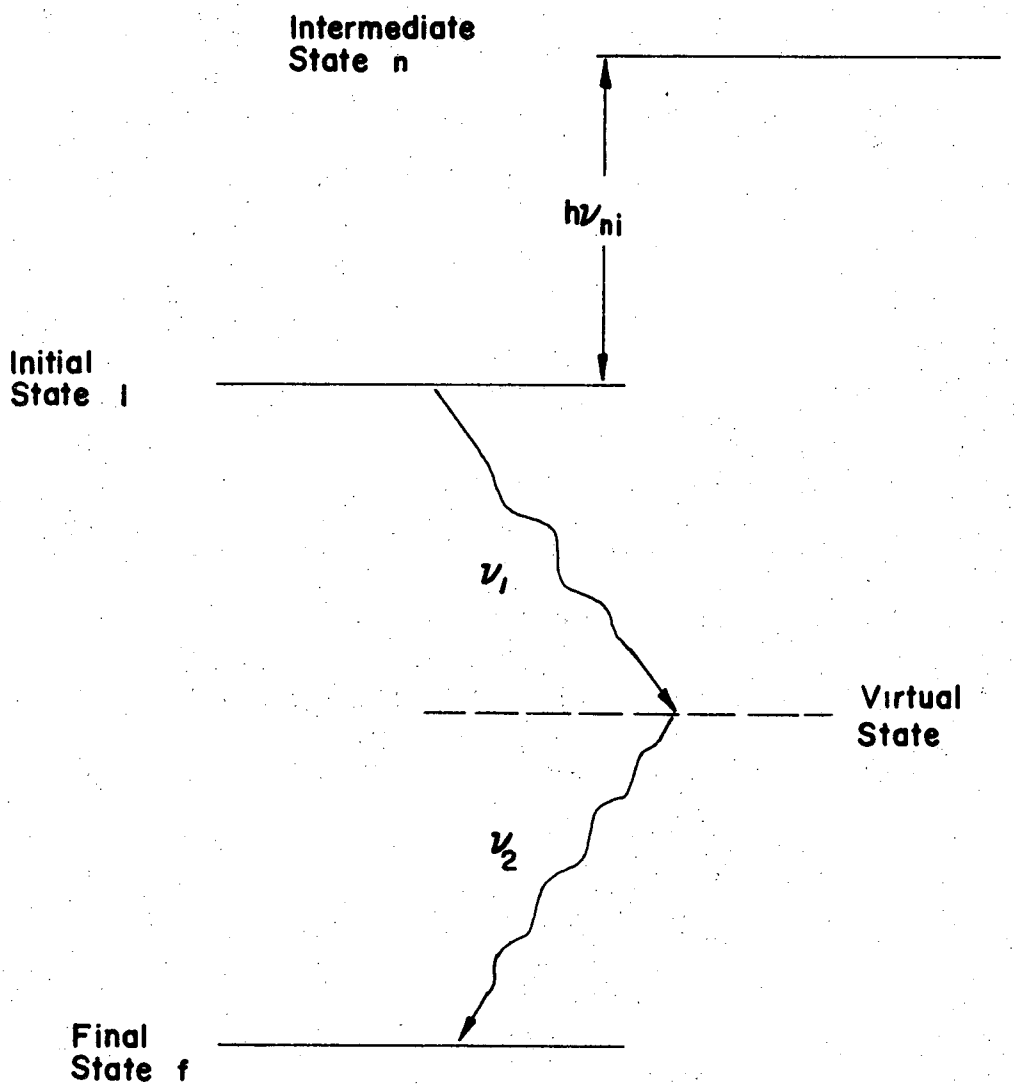

XBL 7011-7020

Fig. 32. Two-photon decay process. Photons 1 and 2, with frequency ν_1 and ν_2, respectively, are emitted simultaneously with total energy equal to $E_i - E_f$.

$$e^{-i2\pi(\nu_1+\nu_2)t} \tag{8}$$

which will be common to every term in both summations, and will disappear when the matrix element is squared.

To evaluate the individual matrix terms in the first summation, such as

$$H_{ni} = \langle n|H'|i\rangle \ , \tag{9}$$

H' will be considered a small perturbation between eigenstates of the unperturbed Hamiltonian $H_\gamma + H_A$, where H_γ and H_A are the Hamiltonians of the free electromagnetic field and the atom, respectively. The combined eigenstate is then a product of two eigenstates, one for each Hamiltonian:

$$|n\rangle = |\psi_n\rangle \ |\vec{k}_1\alpha_1\rangle \ , \tag{10}$$

where $|\psi_n\rangle$ is the eigenstate of the atom in state n and $|\vec{k}_1\alpha_1\rangle$ is the eigenstate of the free radiation field for photon 1 with momentum $\hbar\vec{k}_1$ and polarization component α_1. Equation (9) can now be evaluated by inserting the following Fourier expansion of the vector potential in terms of creation and destruction operators (GOT 66, p. 408):

$$\vec{A}(\vec{r}) = \sum_{\vec{k},\alpha} \left[\frac{hc^2}{\omega V} \right]^{\frac{1}{2}} e^{-i\vec{k}\cdot\vec{r}} \left[\hat{\varepsilon}_{-\vec{k}\alpha}\, a_{-k\alpha} + \hat{\varepsilon}_{\vec{k}\alpha}\, a^{\dagger}_{k\alpha}\right] \tag{11}$$

where $\omega = 2\pi\nu = ck$, V = very large finite normalization volume (always cancels out, but allows discrete values of k), $\hat{\varepsilon}_{\vec{k}\alpha}$ is a unit polarization vector for the photon with momentum $\hbar\vec{k}$ and component of polariza-

tion α, and $a^{\dagger}_{k\alpha}$ (or $a_{k\alpha}$) is the creation (or destruction) operator of the $k\alpha$-photon. For the creation operator

$$a^{\dagger}_{k\alpha}|0\rangle = |\vec{k}\alpha\rangle \tag{12}$$

where $|0\rangle$ is the vacuum eigenstate for the radiation field (no photons). Thus Eq. (9) becomes

$$H'_{ni} = -\frac{e}{mc} \sum_{\vec{k}',\alpha'} \left[\frac{hc^2}{\omega' V} \right]^{\frac{1}{2}} \langle \psi_n; k_1\alpha_1 | e^{-i\vec{k}'\cdot\vec{r}} \left[\hat{\varepsilon}_{-k'\alpha'}\cdot\vec{P}\, a_{-k'\alpha'} + \hat{\varepsilon}_{\vec{k}'\alpha'}\cdot\vec{P}\, a^{\dagger}_{k'\alpha'} \right] | \psi_i; 0\rangle \ . \tag{13}$$

Because of the orthonormality of the radiation field eigenstates

$$\langle k'\alpha' | k\alpha\rangle = \langle 0 | a_{k'\alpha'}\, a^{\dagger}_{k\alpha} | 0\rangle = \delta_{k'k}\, \delta_{\alpha'\alpha} \ , \tag{14}$$

only the creation operators need be considered in Eq. (13). The matrix element then becomes

$$\begin{aligned} H'_{ni} &= -\frac{e}{mc} \sum_{\vec{k}',\alpha'} \left[\frac{hc^2}{\omega' V} \right]^{\frac{1}{2}} \langle \psi_n | e^{-i\vec{k}'\cdot\vec{r}}\, \hat{\varepsilon}_{\vec{k}'\alpha'}\cdot\vec{P}\, \delta_{k_1 k'}\, \delta_{\alpha_1\alpha'} | \psi_i\rangle \\ &= -\frac{e}{mc} \left[\frac{hc^2}{\omega_1 V} \right]^{\frac{1}{2}} \langle \psi_n | e^{-i\vec{k}_1\cdot\vec{r}}\, \hat{\varepsilon}_{\vec{k}_1\alpha_1}\cdot\vec{P} | \psi_i\rangle \ . \end{aligned} \tag{15}$$

In the electric dipole approximation, which holds for wavelengths much greater than the characteristic dimensions of the atomic oscillator,

$$e^{-i\vec{k}_1\cdot\vec{r}} \simeq 1 \ . \tag{16}$$

Also, because the operator $\vec{P}$, acting upon the initial state ψ_i, induces

the emission of photon 1 as an electric dipole oscillator of mass m would,

$$\langle\psi_n|\vec{P}|\psi_i\rangle \rightarrow im\omega_1 \langle\psi_n|\vec{r}|\psi_i\rangle \tag{17}$$

where the commutation relation

$$[\vec{r},H_A] = \frac{i\hbar\vec{p}}{m} \tag{18}$$

is used to reduce the matrix element of $\vec{P}$ (GOT 66, p. 470). Thus Eq. (15) finally becomes

$$H'_{ni} = -ie\left[\frac{h\omega_1}{V}\right]^{\frac{1}{2}} \langle\psi_n|\hat{\varepsilon}_1\cdot\vec{r}|\psi_i\rangle \tag{19}$$

where $\hat{\varepsilon}_{\vec{k}_1\alpha_1}$ has been replaced by $\hat{\varepsilon}_1$ to denote the polarization vector of photon 1. A similar expression holds for H'_{fn}.

For single-photon decay, the number of modes of vibration with frequency less than ν in a finite volume V is (SLA 60, p. 136)

$$n(\nu) = \frac{8\pi V}{3c^3}\nu^3 \tag{20}$$

and because $E = h\nu$

$$\frac{dn}{dE} = \frac{8\pi V}{hc^3}\nu^2 . \tag{21}$$

For two-photon decay, the density of states is a product of phase space factors similar to Eq. (21); thus

$$\frac{dn}{dE} = \frac{1}{dE}\frac{8\pi V}{c^3}\nu_1^{\,2}\,d\nu_1\,\frac{8\pi V}{c^3}\nu_2^{\,2}\,d\nu_2 \tag{22}$$

where, by conservation of energy

$$\begin{aligned} E &= E_i^{\,o} - E_f^{\,o} \\ &= h\nu_1 + h\nu_2 \,. \end{aligned} \tag{23}$$

By fixing ν_1, Eq. (22) reduces to

$$\frac{dn}{dE} = \frac{2^6\pi^2V^2}{hc^6}\,\nu_1^{\,2}\,\nu_2^{\,2}\,d\nu_1 \,. \tag{24}$$

Now applying (6), (19), and (24), the transition probability in Eq. (3) for photon 1 to be emitted with frequency ν_1 in interval $d\nu_1$ is

$$W = A(\nu_1)d\nu_1 = \frac{2^{10}\pi^6e^4}{h^2c^6}\,\nu_1^{\,3}\,\nu_2^{\,3}\,|M_{fi}|^2_{av}\,d\nu_1$$

where

$$M_{fi} = \sum_n \frac{\langle\psi_f|\hat{\varepsilon}_2\cdot\vec{r}|\psi_n\rangle\langle\psi_n|\hat{\varepsilon}_1\cdot\vec{r}|\psi_i\rangle}{\nu_{ni} + \nu_1} + \sum_n \frac{\langle\psi_f|\hat{\varepsilon}_1\cdot\vec{r}|\psi_n\rangle\langle\psi_n|\hat{\varepsilon}_2\cdot\vec{r}|\psi_i\rangle}{\nu_{ni} + \nu_2} \,. \tag{25}$$

Finally, the total emission probability for this two-photon decay is obtained by integrating Eq. (25) over frequency ν_1,

$$A_T = \frac{1}{2}\int_0^{E/h} A(\nu_1)d\nu_1 \tag{26}$$

where the 1/2 factor comes from counting photon 1 twice in the energy

interval between 0 and E/h.

B. Inelastic Collisions

The important aspect of the inelastic collision of an energetic electron with a thermal atom is the effect on the atom's final speed. First, this speed will be calculated using only classical arguments. Then the results will be applied to a cross electron beam and an anti-parallel electron beam.

1. Final Speed

The relevant parameters are illustrated in Fig. 33. An atom of mass m, energy E_i, and momentum $\vec{P}_i$ makes a collision with an electron of mass m_e, energy E, and momentum $\vec{P}$. The electron recoils with energy E′ and momentum $\vec{P}'$ and the excited atom has final energy E_o and momentum $\vec{P}_o$. By conservation of momentum,

$$\begin{aligned} P - P_i \sin\psi_i &= P_o \sin\psi_o - P' \sin\psi_e \\ P_i \cos\psi_i &= P_o \cos\psi_o - P' \cos\psi_e \end{aligned} \tag{1}$$

where the energies and momenta are related by

$$\begin{aligned} P &= (2m_e E)^{\frac{1}{2}} \\ P_i &= (2mE_i)^{\frac{1}{2}} \\ P_o &= (2mE_o)^{\frac{1}{2}} \\ P' &= (2m_e E')^{\frac{1}{2}} . \end{aligned} \tag{2}$$

By conservation of energy,

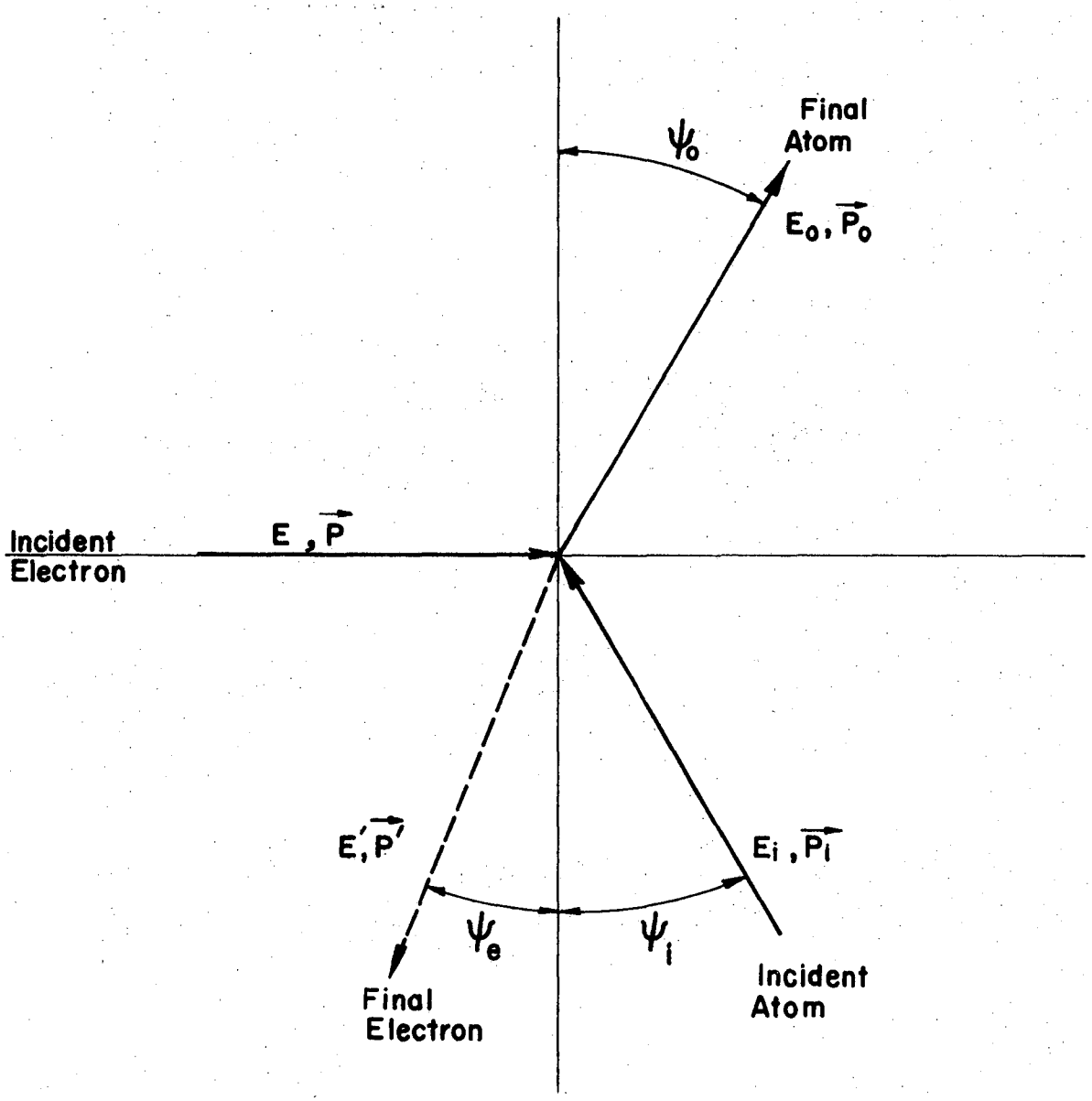

XBL 7011-7021

Fig. 33. Inelastic collision process. An atom and an electron collide, with the recoiling excited atom being observed.

$$E + E_i = E_o + E' + \Delta E \ , \tag{3}$$

where ΔE is the energy of excitation and is a positive quantity. Assume that E, E_i, ψ_i, ψ_o, and ΔE are known. Eliminate ψ_e by shifting all terms with known parameters to the left in Eq. (1) and squaring the resulting equations. E' can be eliminated by using Eq. (3). Thus,

$$2m_e(E+E_i-E_o-\Delta E) = [(2mE_i)^{\frac{1}{2}} \cos\psi_i - (2mE_o)^{\frac{1}{2}} \cos\psi_o]^2 + [(2m_eE)^{\frac{1}{2}} - (2mE_i)^{\frac{1}{2}} \sin\psi_i - (2mE_o)^{\frac{1}{2}} \sin\psi_o]^2 . \tag{4}$$

Upon expanding and simplifying, the following result is obtained:

$$E_o(1+\frac{m_e}{m}) - E_o^{\frac{1}{2}}[2E_i^{\frac{1}{2}} \cos(\psi_i+\psi_o) + 2(\frac{m_e}{m} E)^{\frac{1}{2}} \sin\psi_o] + (1-\frac{m_e}{m})E_i + \frac{m_e}{m} \Delta E - 2(\frac{m_e}{m} E_iE)^{\frac{1}{2}} \sin\psi_i = 0 \ . \tag{5}$$

Equation (5) is a quadratic equation in $E_o^{\frac{1}{2}}$. Using $E_o = mv_o^2/2$ and $E_i = mv_i^2/2$ where v_i and v_o are the atom's speeds before and after collision, respectively,

$$v_o = \frac{b}{a} \pm [(\frac{b}{a})^2 - \frac{c}{a}]^{\frac{1}{2}}$$

where

$$a = 1 + \frac{m_e}{m}$$

$$b = v_i \cos(\psi_i+\psi_o) + \frac{1}{m} (2m_eE)^{\frac{1}{2}} \sin\psi_o$$

$$c = (1 - \frac{m_e}{m})v_i^2 + \frac{2m_e}{m^2} \Delta E - \frac{2}{m} (2m_eE)^{\frac{1}{2}} v_i \sin\psi_i \ . \tag{6}$$

Now, approximate the quantity 'a' by unity since $m_e << m$ (0.01% error) and define the variable V equal to the expression

$$[\frac{2m_eE}{m^2}]^{\frac{1}{2}} . \tag{7}$$

Then Eq. (6) becomes

$$v_o = V \sin\psi_o + v_i \cos(\psi_o + \psi_i)$$
$$\pm \{[V \sin\psi_o + v_i \cos(\psi_o+\psi_i)]^2 - v_i^2 - V^2 \frac{\Delta E}{E} + 2v_iV \sin\psi_i\}^{\frac{1}{2}}. \tag{8}$$

Note that, in general, two speeds exist for each set of allowable angles (argument of the square root > 0).

2. Cross Electron Beam

The first special case considers a cross electron beam. Observation is made within such a small solid angle that ψ_o may be taken as zero. Then Eq. (8) becomes

$$\frac{v_o}{v_i} = \cos\psi_i \pm [\frac{2V}{v_i} \sin\psi_i - \sin^2\psi_i - \frac{\Delta E}{E} (\frac{V}{v_i})^2]^{\frac{1}{2}} . \tag{9}$$

Now consider an electron with 40 volts of energy colliding with a helium atom incident at angle ψ_i. Since the excitation energy is approximately 20 eV,

$$\frac{\Delta E}{E} = \frac{1}{2} \tag{10}$$

and because E = 40 volts,

$$V = 511 \text{ m/sec} . \tag{11}$$

There are two important characteristics of Eq. (9) worth noting. For a given incident speed there is a maximum and a minimum angle of incidence which will give $\psi_o = 0$; that is, for $v_i = 1000$ m/sec,

$$\psi_i(\text{min}) = 8°36' \text{ and } \psi_i(\text{max}) = 60°45' . \tag{12}$$

Also, for a given angle of incidence, there are two speeds possible for the atom traveling along the beam axis for each incident speed; that is, for $\psi_i = 12°$ and $v_i = 1000$ m/sec,

$$v_o = 782 \text{ m/sec and } 1175 \text{ m/sec} . \tag{13}$$

The important conclusion is that, even for small angles ψ_i, the observed speed v_o is different for different angles of incidence. One can now see why, if different parts of the electron gun have different sets of incidence angles available to them, that one part of the gun will have a speed distribution of metastable atoms different from that of another part of the gun with a different set of incident angles. The claim is that this characteristic of a cross electron beam accounts for the observed source dependency (see Section II-G (2)).

3. Antiparallel Electron Beam

For this configuration, let $\psi_o = -90°$ and ψ_i be replaced by $\psi_i + 90°$ (see Fig. 33). Then Eq. (8) becomes

$$\frac{v_o}{v_i} = \cos\psi_i - \frac{V}{v_i} \pm [(1 - \frac{\Delta E}{E})(\frac{V}{v_i})^2 - \sin^2\psi_i]^{\frac{1}{2}} . \tag{14}$$

Unlike Eq. (9), all small angles ψ_i are allowed, though a maximum angle still exists for each incident speed $\geq$ 360 m/sec under conditions specified by Eq. (10) and (11). More important, though, is the fact that, for small angles ψ_i, v_o is almost independent of this incident angle, thus greatly reducing the source dependency effect.

Also, using a slit source with long dimension parallel to the gun filament nearly equalizes each set of allowable incident angles associated with a given point in the gun to the set for any other point in the gun.

C. Pressure in Source Tube

From the perfect gas law, it follows that diffusion pump speed F can be defined as

$$F = \frac{1}{P_{sc}} \left(\frac{dn}{dt} \right)_{pump} kT \qquad (1)$$

where

k = Boltzmann's constant

T = equilibrium source chamber temperature

$\left(\frac{dn}{dt} \right)_{pump}$ = number/sec flowing into the diffusion pump

P_{sc} = source chamber pressure.

Since the number of atoms/sec emerging from the source chamber is generally much smaller than the number/sec flowing from the source slit (due to solid angle), it follows that, for equilibrium pumping,

$$\left(\frac{dn}{dt} \right)_{slit} = \left(\frac{dn}{dt} \right)_{pump} . \qquad (2)$$

Then, for molecular effusion, the rate at which atoms emerge from a source slit of area A_s is, by elementary kinetic theory (REI 65),

$$\left(\frac{dn}{dt}\right)_{slit} = \frac{P_s \, \bar{u} \, A_s}{4kT_s} \tag{3}$$

where

P_s = source tube pressure

T_s = source tube temperature

$\bar{u}$ = average speed of emerging atoms.

Now, combining Eq. (1), (2), and (3), and solving for source tube pressure,

$$\frac{P_s}{P_{sc}} = \frac{4F}{\bar{u}A_s} \cdot \frac{T_s}{T} \quad . \tag{4}$$

When both the source chamber and the source tube are at room temperature and

$$\begin{aligned} \bar{u} &\approx 10^5 \text{ cm/sec for helium} \\ A_s &\approx 0.01 \text{ cm}^2 \\ F &\approx 3000 \text{ liters/sec for VHS-6 pump} \end{aligned} \quad , \tag{5}$$

it follows from Eq. (4) that

$$\frac{P_s}{P_{sc}} \approx 12{,}000 \quad . \tag{6}$$

If the source chamber pressure is $2.0 \cdot 10^{-6}$ torr (read by gauge), the

actual helium pressure would be $1.25 \cdot 10^{-5}$ torr because of helium's lesser gauge sensitivity (VAR 65); thus,

$$P_s \approx 150 \text{ microns} . \tag{7}$$

And when liquid nitrogen is used in the source assembly, $T_s/T \approx 1/4$, giving

$$P_s \approx 37 \text{ microns} . \tag{8}$$

D. Fraction of 2^1S_0 Metastable Atoms in Beam

It is sufficient to calculate the fraction of atoms metastabilized to a given state in the electron gun. Assume the total inelastic collision cross-section for this process is σ. Using the well-known attenuation formula (SEG 65, p. 11),

$$I(x) = I(0)\, e^{-\sigma n x} \tag{1}$$

where $I(x)$ is an intensity at position x, in a media of density n. The probability of making the desired inelastic collision/electron in distance x is (for small argument of the exponential)

$$\frac{I(x) - I(0)}{I(0)} = \sigma n x . \tag{2}$$

If now n is the equilibrium density of atoms in the electron gun, x is the total path length for the electron, and I is the number of electrons per second crossing the gun, then the number of desired inelastic collisions/sec is

$$I\sigma nx \ . \tag{3}$$

Since n = equilibrium number of atoms in the gun/unit volume V, and the number of desired collisions/sec represents the number of atoms excited to the metastable state, the fraction per second f/sec is the following:

$$f/sec = I\sigma \cdot \frac{x}{V} \ . \tag{4}$$

This fraction/sec is better known as the transition probability per second for exciting the desired state, and is usually found in the form

$$\frac{J}{e} \cdot \sigma \ , \tag{5}$$

where J is the current density and J/e is the flux of particles per unit area producing the excitation. Since an atom of speed v will spend d/v time in the electron gun, the fraction metastabilized with speed v is

$$f = \frac{J}{e} \cdot \sigma \cdot \frac{d}{v} \tag{6}$$

where d is the length of the gun traversed by the atoms. One can now replace f by a fraction $\langle f \rangle$ averaged over a modified Maxwell speed distribution, giving

$$\langle f \rangle = (1.57) \frac{J\sigma d}{e\alpha} \tag{7}$$

where

$$\alpha = \left(\frac{3kT}{m} \right)^{\frac{1}{2}}$$

for a source gas of mass m and temperature T.

Some typical parameters for the gun used are:

$$J = 0.031 \text{ amps/cm}^2 \text{ (20 ma)}$$

$$d = 1 \text{ cm}$$

$$\alpha \approx 1500 \text{ m/sec} . \tag{8}$$

The excitation cross section for helium 2^1S_0 at 22 volts (near maximum) is (HOL 65)

$$\sigma(2^1S_0) = 1.7 \cdot 10^{-18} \text{ cm}^2 . \tag{9}$$

For higher voltages, the singlet state can be fed by higher excited states cascading down to the 2^1S_0 state. This effects tends to level off the singlet production, making Eq. (9) valid for a wide range of voltages. Thus,

$$\langle f \rangle = 3.5 \cdot 10^{-6} . \tag{10}$$

or, equivalently, 1 atom is excited to the 2^1S_0 state for every 300,000 atoms entering the electron gun.

E. Ion Deflection in Electric and Magnetic Fields

1. Magnetic Field

Assume a uniform magnetic field B_o is applied perpendicularly to the beam axis. Then, an ion of speed v and mass m will rotate in cyclotron fashion with radius (SEG 65, p. 125)

$$R = \frac{mc^2}{eB_o} \cdot \frac{v}{c} \tag{1}$$

where e = ion charge and c = speed of light. Now the criterion for determining that the ion just passes through both first and last collimators is that the distance 2L between collimators be the chord of the circle displaced a maximum distance s from the arc cut off from the circle, the distance s being the diameter of the collimator holes. The radius of the circle fitting this criterion is, for L >> s,

$$R = \frac{L^2 + s^2}{2s} \approx \frac{L^2}{2s} . \tag{2}$$

In particular, 2L = 71 inches and s = 0.25 inches, indicates that R = 64.0 meters. Solving Eq. (1) for the speed,

$$v = (4788)\ B_o\ R\ M^{-\frac{1}{2}} \text{ meters/second} \tag{3}$$

where B_o is in gauss, R is in meters, and M is the molecular weight of the ion. Thus, for helium, B_o = 0.5 gauss gives

$$v = 7.7 \cdot 10^4 \text{ m/sec} \tag{4}$$

as the minimum speed that an ion may have and still reach the first detector.

2. Electric Field

The equation of motion for an ion of mass m in a uniform electric field E_o, directed perpendicular to the beam axis, is

$$\frac{d^2x}{dt^2} \equiv \ddot{x} = \frac{eE_o}{m} \tag{5}$$

where e is again the ion charge and x is the transverse displacement. It is assumed that deflection plates, with a gap width d and length Z_p, create the uniform field. The intermediate distance between the plates and the last collimator (hole diameter x_c) is Z_c. Also, it is assumed that the ion entering the field region is initially traveling along a trajectory parallel to the axis and intercepting one edge of the collimator hole. The deflection x will project diametrically across the collimator hole. Now, if the ion has speed v, then at the exit edge of the field region

$$\dot{x}_p = \frac{eE_o Z_p}{mv}$$

$$x_p = \frac{eE_o Z_p^2}{2mv^2} \quad . \tag{6}$$

After passing out of the field region, the ion travels in a straight line with further transverse displacement = $\dot{x}_p Z_c/v$. The criterion for the ion to pass just through the last collimator is for the total transverse displacement = x_c. Thus

$$x_c = \frac{eE_o Z_p}{mv^2} (Z_c + \frac{Z_p}{2}) \quad . \tag{7}$$

In particular, solving for the speed from Eq. (7) assuming

$$E_o = 500 \text{ V/cm } (d = 1 \text{ cm})$$
$$x_c = 0.635 \text{ cm } (0.25 \text{ in})$$
$$Z_c = 137 \text{ cm}$$
$$Z_p = 14 \text{ cm} , \tag{8}$$

one finds that

$$v = (3.9)M^{-\frac{1}{2}} \cdot 10^6 \text{ meters/sec} \tag{9}$$

where M is the molecular weight of the ion. For helium (M = 4),

$$v = 1.95 \cdot 10^6 \text{ meters/sec} \tag{10}$$

is the minimum speed an ion may have and still reach the first detector.

F. Convolution Studies

1. Limit on the Size of δt

Let f(t) be the instantaneous time distribution at time t. Then for t anywhere in the interval $(t_o, t_o + \delta t)$

$$f(t) = f(t_o) + \left(\frac{df}{dt}\right)_{t_o} (t - t_o) + \cdots . \tag{1}$$

The accuracy of only the first two terms depends on the size of δt and on how fast f(t) changes in the interval. The count N collected in this interval is found by integration:

$$N = \int_{t_o}^{t_o+\delta t} f(t)dt = f(t_o)\delta t + f'(t_o) \frac{(\delta t)^2}{2} + \cdots , \tag{2}$$

where f′ denotes the first derivative. Since it is desirable to have only the first term contribute to N, the question is asked, when is

$$|f'(t_o)|\delta t << 2f(t_o) \ ? \tag{3}$$

Assuming a Maxwell time distribution with decay of the form

$$f(t) = Kt^{-4}\ e^{-A/t^2}\ e^{-t/\tau}\ , \tag{4}$$

it follows that the first derivative has the form

$$f'(t) = f(t)\left(\frac{2A}{t^3} - \frac{4}{t} - \frac{1}{\tau}\right)\ . \tag{5}$$

The constant K is for normalization, τ represents a decay lifetime, and $A^{\frac{1}{2}} = d/\alpha$ where d = distance to a detector and α is the most probable speed. Using Eq. (5), Eq. (3) becomes the following question:

$$\left|\frac{2A}{t_o^3} - \frac{4}{t_o} - \frac{1}{\tau}\right| \cdot \delta t << 2? \tag{6}$$

Because $\tau \approx 20$ msec and $\delta t = 80$ μsec, the term containing the decay lifetime may be ignored. And since δt is the channel width, t_o will be defined as a multiple of δt as follows:

$$t_o = K\ \delta t\ . \tag{7}$$

Using $d_1 = 1.9275$ meters, $d_2 = 6.7075$ meters, and $\alpha = 1500$ meters/sec,

$$A_1 = 256(\delta t)^2$$
$$A_2 = 3136(\delta t)^2\ . \tag{8}$$

Thus, the following are the conditions that δt be sufficiently small for analysis of the collected counts:

$$\Gamma_1 = \left| \frac{256}{K_1^2} - 2 \right| << K, \text{ for detector 1}$$

$$\Gamma_2 \equiv \left| \frac{3136}{K_2^2} - 2 \right| << K, \text{ for detector 2 .} \tag{9}$$

The values of Γ_1 and Γ_2 are listed in Table 9 for different values of K using the relation

$$K_2 = \frac{d_2}{d_1} K_1 = 3.5\ K_1 \tag{10}$$

since the sets (K_1, K_2) represent the atoms of the same speed compared in program ANALZ. From the table, it is clear that the extra term added to the integral in Eq. (2) is small for $K_1 > 12$ ($K_2 > 42$) but always remains a ∿6% correction (∿2% correction for detector 2). Thus, in the ratio N_2/N_1, there is the following correction:

$$\Lambda = \frac{1 + \frac{\Gamma_2}{K_2}}{1 + \frac{\Gamma_1}{K_1}} . \tag{11}$$

From the table, it can be seen that, for $K_1 > 12$, Λ is nearly constant and will not affect the slope by more than a few tenths of a percent.

It should also be remembered that the above analysis is carried out using a Maxwell distribution (REI 65, p. 267) to first order in the Taylor's expansion. The actual distribution in the experiment is not

Table 9. Corrections for size of δt.

K_1	Γ_1	$\frac{\Gamma_1}{K_1}$	K_2	Γ_2	$\frac{\Gamma_2}{K_1}$	Λ
6	5.11	0.852	21	5.11	0.2430	0.671
8	2.00	0.250	28	2.00	0.0715	0.857
10	0.56	0.056	35	0.56	0.0160	0.962
12	0.22	0.018	42	0.22	0.0052	0.987
14	0.69	0.049	49	0.69	0.0014	0.955
16	1.00	0.062	56	1.00	0.0180	0.959
18	1.21	0.067	63	1.21	0.0192	0.955
20	1.36	0.068	70	1.36	0.0195	0.955
22	1.47	0.067	77	1.47	0.0191	0.955
24	1.56	0.065	84	1.56	0.0186	0.956
26	1.62	0.062	91	1.62	0.0178	0.958
28	1.67	0.060	98	1.67	0.0170	0.959
30	1.72	0.057	105	1.72	0.0164	0.962
32	1.75	0.055	112	1.75	0.0156	0.963
34	1.78	0.052	119	1.78	0.0150	0.964
36	1.80	0.050	126	1.80	0.0143	0.966
38	1.82	0.048	133	1.82	0.0137	0.967
40	1.84	0.046	140	1.84	0.0131	0.969
42	1.86	0.044	147	1.86	0.0127	0.970
44	1.87	0.043	154	1.87	0.0121	0.971
46	1.88	0.041	161	1.88	0.0117	0.972
48	1.89	0.039	168	1.89	0.0113	0.973
50	1.90	0.038	175	1.90	0.0109	0.974

Maxwellian, but these results are expected to hold qualitatively.

2. Detailed Convolution

Let $g(s,v)dsdv$ be the number of atoms with speed v between v and v + dv, created in gun at time t = s in time interval ds. Then

$$g_d'(0,t) = g(0, \frac{d}{t}) \frac{d}{t^2} e^{-t/\tau} \tag{12}$$

is the instantaneous distribution at a detector, a distance d from the source, and at time t, due to atoms excited instantaneously at time t = 0, and allowing for decay. The convolution can be thought of as adding the same distribution to a given point in time, but shifted in position by a time s; that is,

$$g_d'(s,t) = g_d'(0,t-s) \ . \tag{13}$$

If F(T) is equal to the number of counts in a channel of width 2Δ where t = T is the center of the channel, due to metastable atoms created in the electron gun during a pulse of width 2λ centered at t = 0, then

$$F(T) = \int_{-\lambda}^{\lambda} ds \int_{T-\Delta}^{T+\Delta} g_d'(s,t)dt \ . \tag{14}$$

Then, using Eq. (13) and making a change of variables $s \to t-s$,

$$F(T) = \int_{T-\Delta}^{T+\Delta} dt \int_{t-\lambda}^{t+\lambda} g_d'(0,s)ds \ . \tag{15}$$

Now change the labels s and t to obtain a symmetric form of the integral

$$F(T) = \int_{T-\Delta}^{T+\Delta} ds \int_{s-\lambda}^{s+\lambda} g_d'(0,t)dt \ . \tag{16}$$

Also, define the ratio

$$\begin{aligned} R(T_2-T_1) &\equiv e^{-(T_2-T_1)/\tau} \\ &= \left[\frac{d_2}{d_1} \cdot \frac{g_{d_2}'(0,T_2)}{g_{d_1}'(0,T_1)}\right]_{\frac{T_1}{d_1} = \frac{T_2}{d_2}} \end{aligned} \tag{17}$$

where Eq. (12) was used to obtain the last relation.

The goal for the remainder of this appendix is eventually to compare this ratio with $F(T_2)/F(T_1)$.

Again, it is necessary to assume a Maxwell speed distribution, but modified by the probability/sec of exciting an atom as defined in Eq. (5) of Appendix D. Thus,

$$g_d'(0,t) \equiv f(t) = Kt^{-4}\ e^{-A/t^2}\ e^{-t/\tau}\ , \tag{18}$$

where

$$K = N\,\frac{d^3}{\alpha^3} \cdot \frac{J\sigma}{e} \quad \text{and} \quad A = \left(\frac{d}{\alpha}\right)^2$$

and N is a unitless normalization factor. Eq. (18) is therefore the same as Eq. (4), if σ is assumed to be a constant for atoms of all speeds.

Eq. (16) can now be put into the more useful form

$$F_T = \int_{T-\Delta}^{T+\Delta} ds \int_{-\lambda}^{\lambda} f(y + s)dy \ . \tag{19}$$

Taylor expand $f(y + s)$ about the time s, giving

$$f(y + s) = f(s) + f'(s)y + f''(s) \frac{y^2}{2} + \cdots \ . \tag{20}$$

After doing the first integration, repeat the Taylor's expansion for $f(y + T)$, $f''(y + T)$, and $f^{(4)}(y + T)$, keeping terms up to and including the fourth derivative of $f(t)$. The final result is

$$F(T) = 2\lambda 2\Delta[f(t) + f''(T)(\frac{\Delta^2+\lambda^2}{3!}) + \frac{\lambda^2 f^{(4)}(T)}{3!} (\frac{\Delta^2}{6} + \frac{\lambda^2}{20})]. \tag{21}$$

Upon expanding the derivatives using Eq. (18)

$$F(T) = 2\lambda 2\Delta \ f(T) \ \phi(T) \tag{22}$$

where

$$\phi(T) = 1 + \eta(T) \ .$$

The correction function $\eta(T)$ is as follows:

$$\begin{aligned}\eta(T) = {} & \frac{1}{6}(\Delta^2 + \lambda^2) \left[\frac{1}{\tau^2} + \frac{8}{\tau T} + \frac{20}{T^2} - \frac{4A}{\tau T^3} - \frac{22A}{T^4} + \frac{4A^2}{T^6}\right] \\ & + \frac{\lambda^2}{6} (\frac{\Delta^2}{6} + \frac{\lambda^2}{20}) \left[\frac{16A^4}{T^{12}} - \frac{A^3}{T^9} (\frac{32}{\tau} + \frac{272}{T}) + \frac{A^2}{T^6} (\frac{24}{\tau^2} + \frac{336}{\tau T} + \frac{1356}{T^2}) \right. \\ & \left. - \frac{A}{T^3} (\frac{8}{\tau^3} + \frac{132}{\tau^2 T} + \frac{864}{\tau T^2} + \frac{2184}{T^3}) + (\frac{1}{\tau^4} + \frac{16}{\tau^3 T} + \frac{120}{\tau^2 T^2} + \frac{480}{\tau T^3} + \frac{840}{T^4})\right].\end{aligned} \tag{23}$$

To simplify Eq. (23) and to apply it to both detectors, let

$$T = 2K\Delta$$
$$\Delta = \lambda$$
$$A_1 = (1024)\Delta^2$$
$$A_2 = (12544)\Delta^2 \tag{24}$$

where

$$2\Delta = 80\ \mu\text{sec.}$$

Also, because τ is so large compared to Δ, every term in which it appears can be neglected. Thus

$$\eta_1(K) = \frac{1.667}{K^2} - \frac{468}{K^4} + \frac{2.06\cdot 10^4}{K^6} + \frac{2.008\cdot 10^5}{K^8} - \frac{1.03\cdot 10^7}{K^{10}} + \frac{1.55\cdot 10^8}{K^{12}}$$

and

$$\eta_2(K) = \frac{1.667}{K^2} - \frac{5232}{K^4} + \frac{3.265\cdot 10^6}{K^6} + \frac{3.0\cdot 10^7}{K^8} - \frac{1.885\cdot 10^{10}}{K^{10}} + \frac{3.48\cdot 10^{12}}{K^{12}} . \tag{25}$$

These parameters have been computed for a few values of K and are listed in Table 10. Note that these corrections are quite small beyond $K_1 = 12$ ($K_2 = 42$).

Since the goal of this appendix is to compare Eq. (17) with the ratio $F(T_2)/F(T_1)$, using Eq. (22) and Eq. (18), this ratio becomes

$$\frac{F(T_2)}{F(T_1)} = \left[\frac{g'_{d_2}(0,T_2)}{g'_{d_1}(0,T_1)} \cdot \frac{1 + \eta_2(T_2)}{1 + \eta_1(T_1)}\right]_{\frac{T_1}{d_1} = \frac{T_2}{d_2}} . \tag{26}$$

Table 10. Convolution corrections.

K_1	$\eta_1(K)$	K_2	$\eta_2(K)$	$\Lambda(K)$
5	0.73			
6	0.15	21	0.0151	0.883
7	0.026			
8	-0.0046	28	0.0004	1.005
9	-0.034			
10	-0.0084	35	-0.00035	1.008
11	-0.0052			
12	-0.0038	42	-0.00014	1.004
13	-0.0021			
14	-0.0009	49	0.00002	1.001

Comparing with Eq. (17)

$$\frac{F(T_2)}{F(T_1)} = \frac{d_1}{d_2} \cdot R(T_2 - T_1) \cdot \Lambda(T_1,T_2)$$

where

$$\Lambda(T_1,T_2) = \frac{1 + \eta_2(T_2)}{1 + \eta_1(T_1)} \tag{27}$$

and

$$T_2 = \frac{d_2}{d_1} \cdot T_1 \ , \quad T_1 = 2K\Delta \ .$$

The parameter Λ is also computed and listed in Table 10 for a few values of K.

There is one other convolution which could be included with gun pulse width and collection channel width; that is, position of excitation in the electron gun. The distribution g now has three parameters x, s, and t, where x is the position measured positively from the center of the gun for increasing d_1 and d_2. The total convolved count for a given detector at a time T is now

$$F(T) = \int_{-\lambda}^{\lambda} ds \int_{T-\Delta}^{T+\Delta} dt \int_{d-\delta}^{d+\delta} dx \ g(x,s,t) \ , \tag{28}$$

where 2δ is the height of the electron gun. As before, the convolution requires that

$$g(x,s,t) = g(0,0,t - s + \frac{x}{d} t) \ . \tag{29}$$

But x/d has a maximum value for detector 1 of $2.6 \cdot 10^{-3}$ when $x = \delta = 0.5$ cm, and a correspondingly smaller maximum value for detector 2. Since this extra term is too small to have very much effect, it can be ignored; that is, if $t = 20\Delta = 800$ μsec (Channel 10), then s_{max} is 5% of t and $\left(\frac{x}{d}\right)_{max}$ is 0.26% of t for detector 1.

G. Analysis Program

[See the following 7 pages]

```
      PROGRAM ANALZ3(INPUT,OUTPUT,PUNCH,TAPE5=INPUT,TAPE6=OUTPUT)
C     ***********************************************************************
C     *
C     *   ANALYSES DATA FROM NUMEROUS RUNS WITH MODULATION ON OR OFF.
C     *   OUTPUTS THE INPUT DATA, THE RATIO OF N2 TO N1, THE LOG OF THE RATIO. *
C     *   PLOTS OUT THE VARIOUS INTERESTING QUANTITIES                         *
C     *                                                                        *
C     ***********************************************************************
      DIMENSION N1(300), N2(300), T1(300), T2(300), R(300), ALR(300),
     2 T(300), TALR(300), TT(300),    SIGON1(300), SIGON2(300), INFO(12),
     3 SIGOF1(300), SIGOF2(300), Y(300), SIGMAR(300), SIGMAL(300),
     4TITLE3(12),TITLE4(12),TITLEP(12),TITLE(12),SIGMAN(300),SIGMAD(300)
      LOGICAL LAMP,LCOUNT,PUNOUT
      REAL N1, N2, INFO
C     ***********************************************************************
C     *                                                                        *
C     *   CONSTANTS                                                            *
C     *                                                                        *
C     ***********************************************************************
      DATA D1/1.9345/,D2/6.7145/
      DATA ISTART/12/,NUMCHN/200/
      DATA TITLE3/6H   RUN,6H        ,6HRATIO ,6H= UPPE,6HR/LOWE,
     1            6HR WITH,6H  LAMP,5*6H       /
      DATA TITLE4/6H   RUN,6H        ,6H LOGAR,6HITHM O,6HF RATI,
     1            6HO WITH,6H  LAMP,5*6H       /
      DATA TITLE /6H   RUN,6H        ,6H  LAMP,6H  OFF ,6H  ON  ,6H----IR,
     1            6HIPLETS,6H----SI,6HNGLETS,6H  NORM,6HALIZED,6H       /
C     ***********************************************************************
C     *                                                                        *
C     *   RECYCLE BEGINNING. START BY ZEROING ARRAYS                           *
C     *                                                                        *
C     ***********************************************************************
  100 CONTINUE
      DO 5 K=8,12
      KSKIP = K-4
      TITLE3(K) = 10H
      TITLE4(K) = 10H
      TITLEP(KSKIP) = 10H
    5 CONTINUE
      DO 10 K = 1,300
      N1(K) = 0.0
      N2(K) = 0.0
      T1(K) = 0.0
      T2(K) = 0.0
      R(K) = 0.0
      ALR(K) = 0.0
      TALR(K) = 0.0
      T(K) = 0.0
      TT(K) = 0.0
      SIGMAN(K) = 0.0
      SIGMAD(K) = 0.0
      SIGMAR(K) = 0.0
      SIGMAL(K) = 0.0
      SIGOF1(K) = 0.0
      SIGOF2(K) = 0.0
      SIGON1(K) = 0.0
      SIGON2(K) = 0.0
      X(K) = 0.0
   10 CONTINUE
C     ***********************************************************************
C     *                                                                        *
C     *   READ AND WRITE NON-EXECUTABLE STATEMENTS                             *
C     *                                                                        *
C     ***********************************************************************
      TEST = 1H*
      READ 5000, INFO
      TITLE(2) = INFO(2)
      INFO(1) = TITLE(1)
      PRINT 1000,(INFO(K), K = 1,12)
   20 READ 5001, (INFO(K), K = 1,9)
      IF (INFO(1) - TEST) 21, 22, 21
   21 PRINT 1001,(INFO(K), K = 2,9)
      GO TO 20
   22 CONTINUE
C     ***********************************************************************
C     *                                                                        *
C     *   READ AND WRITE EXECUTABLE STATEMENT CONTROLS                         *
C     *                                                                        *
C     ***********************************************************************
      READ 5003, DELTA
      READ 5005, LAMP,PUNOUT
      PRINT 1004, DELTA
C     ***********************************************************************
C     *                                                                        *
C     *   CALCULATE AND WRITE CALCULABLE PARAMETERS                            *
C     *                                                                        *
C     ***********************************************************************
```

```
      LAST = NUMCHN-1
      D = D2 - D1
      DELTAC = D*DELTA/D1
      ICELL = LAST*(D1/D2)-0.5
      PRINT 1009, D1
      PRINT 1010, D2
      PRINT 1013, DELTAC
      PRINT 1014, LAST
      PRINT 1015, ICELL
C     ***********************************************************************
C     *                                                                     *
C     *  CALCULATE VARIOUS TIME SCALES                                      *
C     *                                                                     *
C     ***********************************************************************
      DO 50 K = 1,LAST
      T1(K) = K*DELTA
      T2(K) = K*DELTA
   50 CONTINUE
      DO 70 K = 1,ICELL
      T(K) = K*DELTAC
   70 CONTINUE
C     ***********************************************************************
C     *                                                                     *
C     *  READ DATA AND WRITE CALCULATED CONSTANTS                           *
C     *                                                                     *
C     ***********************************************************************
      LCOUNT = .FALSE.
      CALL REDATA(NUMCHN,LCOUNT,TITLE(2),SIGOF1,SIGOF2)
      CALL SUMMAT(SIGOF2,T2,LAST,5,ICELL,D2,DELTA,D1,N2)
      DO 75 K = 1,ICELL
      N1(K) = SIGOF1(K)
      SIGOF2(K) = N2(K)
      SIGMAN(K) = SQRT(N2(K))
      SIGMAD(K) = SQRT(N1(K))
   75 CONTINUE
      DO 80 K = 1,4
      TITLEP(K) = TITLE(K)
   80 CONTINUE
      DO 85 K = 2,8,6
      KSKIP = 2 + (K - 2)/3
      TITLE3(K) = TITLE(KSKIP)
      TITLE4(K) = TITLE(KSKIP)
   85 CONTINUE
      IF (.NOT.LAMP) GO TO 120
      LCOUNT = .TRUE.
      CALL REDATA(NUMCHN,LCOUNT,TITLE(2),SIGON1,SIGON2)
      CALL SUMMAT(SIGON2,T2,LAST,5,ICELL,D2,DELTA,D1,N2)
      DO 90 K = 1,ICELL
      N1(K) = SIGON1(K)
      SIGON2(K) = N2(K)
      SIGMAN(K) = SQRT(N2(K))
      SIGMAD(K) = SQRT(N1(K))
   90 CONTINUE
      TITLEP(4) = TITLE(5)
      TITLE3(8) = TITLE(5)
      TITLE4(8) = TITLE(5)
      DO 95 K = 9,10
      KSKIP = K - 4
      TITLE3(K) = TITLE(K-3)
      TITLE4(K) = TITLE(K-3)
      TITLEP(KSKIP) = TITLE(K-3)
   95 CONTINUE
      GO TO 120
  110 LAMP = .FALSE.
C     ***********************************************************************
C     *                                                                     *
C     *  CALCULATE AND PRINT RATIOS, LOGS, SIGMARATIOS, AND SIGMALOGS       *
C     *                                                                     *
C     ***********************************************************************
  120 CONTINUE
      DO 140 K = 1,ICELL
      IF (N1(K) -0.001) 141, 141, 142
  142 IF (N2(K) -0.001) 141, 141, 143
  141 R(K) = 1.0
      SIGMAL(K) = 10.0
      GO TO 144
  143 R(K) = N2(K)/N1(K)
      SIGMAL(K) = SQRT(SIGMAN(K)*SIGMAN(K)/(N2(K)*N2(K)) +
     1  SIGMAD(K)*SIGMAD(K)/(N1(K)*N1(K)))
  144 ALR(K) = ALOG(R(K))
      SIGMAR(K) = R(K)*SIGMAL(K)
  140 CONTINUE
      IF(PUNOUT) PUNCH 5000, (TITLEP(K),K=1,8)
      IF(PUNOUT) PUNCH 1026, ICELL
      PRINT 1025, (TITLEP(K), K = 1,8)
      PRINT 1022
      DO 190 K = 1,ICELL
      PRINT 1023, K, N1(K), N2(K), R(K),ALR(K),SIGMAR(K),SIGMAL(K),T(K)
      IF(PUNOUT) PUNCH 1027, K,T(K),R(K),SIGMAR(K),TITLE(2)
  190 CONTINUE
```

```
C     ***********************************************************************
C     *                                                                     *
C     *  FIT LOG OF RATIO TO STRAIGHT LINE AND PLOT  RESULTS                *
C     *                                                                     *
C     ***********************************************************************
      SIGMIN = SIGMAL(1)
      DO 490 K = 1,ICELL
      IF (SIGMAL(K) - SIGMIN) 495, 495, 499
  495 SIGMIN = SIGMAL(K)
  499 CONTINUE
  490 CONTINUE
      SIGMIN = SIGMIN*10.0
      K = 25
  500 K = K + 1
      IF(K-ICELL) 510,520,520
  510 IF (SIGMAL(K+1) - SIGMIN) 500, 500, 520
  520 ILAST = K
      NII = ILAST - ISTART
      DO 530 K = 1,NII
      TT(K) = T(K + ISTART)
      SIGMAL(K) = SIGMAL(K + ISTART)
      Y(K) = ALR(K + ISTART)
  530 CONTINUE
      CALL LINFIT(TT,Y,SIGMAL,TALR,TAU,SIGTAU,NII)
      DO 540 K = 1,NII
      Y(K) = TALR(K)
  540 CONTINUE
      DO 550 K = 1,ICELL
      TALR(K) = ALR(K)
  550 CONTINUE
      DO 560 K = 1,NII
      KI = K + ISTART
      TALR(KI) = Y(K)
  560 CONTINUE
      CALL PLOT(T,R,R,ICELL,1H+,1HF,1,TITLE3,12,6)
      CALL PLOT(T,ALR,TALR,ICELL,1H+,1HF,2,TITLE4,12,6)
      PRINT 1024, TAU, SIGTAU
C     ***********************************************************************
C     *                                                                     *
C     *  REDEFINE FOR LAMP ON                                               *
C     *                                                                     *
C     ***********************************************************************
      IF (.NOT.LAMP) GO TO 100
      DO 260 K = 1,ICELL
      G1 = SIGOF1(K) - SIGON1(K)                                        ANA10212
      G2 = SIGOF2(K) - SIGON2(K)                                        ANA10213
      IF (G1) 261, 261, 262                                             ANA10214
  261 N1(K) = 0.0                                                       ANA10215
      GO TO 263                                                         ANA10216
  262 N1(K) = G1                                                        ANA10217
  263 IF (G2) 264, 264, 265                                             ANA10218
  264 N2(K) = 0.0                                                       ANA10219
      GO TO 266                                                         ANA10220
  265 N2(K) = G2                                                        ANA10221
  266 SIGMAD(K) = SQRT(SIGOF1(K) + SIGON1(K))                           ANA10222
      SIGMAN(K) = SQRT(SIGOF2(K) + SIGON2(K))                           ANA10223
  260 CONTINUE                                                          ANA10224
      DO 270 K = 9,10                                                   ANA10225
      KSKIP = K - 4                                                     ANA10226
      TITLE3(K) = TITLE(K-1)                                            ANA10227
      TITLE4(K) = TITLE(K-1)                                            ANA10228
      TITLEP(KSKIP) = TITLE(K-1)                                        ANA10229
  270 CONTINUE                                                          ANA10230
       GO TO 110
C     ***********************************************************************
C     *                                                                     *
C     *  FORMAT LIST                                                        *
C     *                                                                     *
C     ***********************************************************************
 1000 FORMAT (1H1,12A6//)
 1001 FORMAT (1H ,7A10,A9//)
 1004 FORMAT (17H CHANNEL WIDTH = ,F8.5,13H MILLISECONDS//)
 1009 FORMAT (27H LOWER DETECTOR DISTANCE = ,F6.4,7H METERS//)
 1010 FORMAT (27H UPPER DETECTOR DISTANCE = ,F6.4,7H METERS//)
 1013 FORMAT (19H PARTITION WIDTH = ,F9.5,13H MILLISECONDS//)
 1014 FORMAT (47H NUMBER OF CELLS IN LOWER DETECTOR PARTITION = ,I3//)
 1015 FORMAT (47H NUMBER OF CELLS IN UPPER DETECTOR PARTITION = ,I3//)
 1022 FORMAT(/5X,2H K,9X,5HN1(K),9X,5HN2(K),4X,11HN2(K)/N1(K),5X,
     2 10HLOG(N2/N1),3X,12HSIGMA(N2/N1),2X,13HSIGMA(LOG(R)),7X,4HTIME)
 1023 FORMAT(4X,I3,2(3X,F11.3),2(4X,F11.6),3(8X,F7.3))
 1024 FORMAT (40X,11HMEANLIFE = ,F9.2,8H  + OR -,F8.3,14H  MILLISECONDS)
 1025 FORMAT (1H1,8A6)
 1026 FORMAT (1X,8HNPTS  = ,I3)
 1027 FORMAT (2HK=,I3,4H T= ,F10.7,10H  RATIO = ,F10.7,
     1                              10H  SIGMA = ,F10.7,14X,A6)
 5000 FORMAT (12A6)
 5001 FORMAT (A1,7A10,A9)
 5003 FORMAT (16X,F8.5,20X,F8.5)
 5005 FORMAT (9X,L1,19X,L1,19X,L1)
      END
```

```
      SUBROUTINE REDATA(NUMCHN,LCOUNT,RUN,SIG1,SIG2)
C     ***********************************************************************
C     *                                                                     *
C     *  THIS SUBROUTINE READS DATA FOR A RUN AND GIVES BACK                *
C     *  A SIGNAL MINUS BACKGROUND. IT ALSO PRINTS OUT THE INPUT SIGNAL.    *
C     *                                                                     *
C     ***********************************************************************
      DIMENSION SIG1(300), SIG2(300),  T(300), TITLE(8)
      LOGICAL LCOUNT
      TITLE(1) = 6H   RUN
      TITLE(2) = RUN
      TITLE(3) = 6H LOWER
      TITLE(4) = 6H DETEC
      TITLE(5) = 6HTOR DA
      TITLE(6) = 6HTA WIT
      TITLE(7) = 6HH LAMP
      TITLE(8) = 6H OFF
      READ 5000, BAKGD1, BAKGD2
      READ 5001, (SIG1(K), K = 1,NUMCHN)
      READ 5001, (SIG2(K), K = 1,NUMCHN)
      DO 5 K=1,300
      T(K) = K-1
    5 CONTINUE
      LAST = NUMCHN-1
      SUM1 = 0.0
      SUM2 = 0.0
      DO 50 K=3,NUMCHN
      SUM1 = SUM1+SIG1(K)
      SUM2 = SUM2+SIG2(K)
   50 CONTINUE
      IF (LCOUNT) GO TO 100
      PRINT 1001, RUN
      TITLE(8) = 6H OFF
      GO TO 110
  100 PRINT 1002, RUN
      TITLE(8) = 6H ON
  110 PRINT 1003, BAKGD1, SUM1
      PRINT 1004, BAKGD2, SUM2
      PRINT 1005
      III = NUMCHN/5
      DO 180 K = 1,III
      K1 = K + III
      K2 = K1 + III
      K3 = K2 + III
      K4 = K3 + III
      J=K-1
      J1=K1-1
      J2=K2-1
      J3=K3-1
      J4=K4-1
      PRINT 1006, J, SIG1(K), SIG2(K), J1, SIG1(K1), SIG2(K1),
     2 J2, SIG1(K2), SIG2(K2), J3, SIG1(K3), SIG2(K3),
     3 J4, SIG1(K4), SIG2(K4)
  180 CONTINUE
      SIG1(1) = 0.0
      SIG2(1) = 0.0
      J = NUMCHN/2
      CALL PLOT  (T,SIG1,SIG1,J,1H+,1HF,1,TITLE,8,6)
      TITLE(3) = 6H UPPER
      J = NUMCHN
      CALL PLOT  (T,SIG2,SIG2,J,1H+,1HF,1,TITLE,8,6)
      DO 30 K=2,LAST
      SIG1(K) = SIG1(K+1)-BAKGD1
      IF(SIG1(K).LT.0.0) SIG1(K)=0.0
      SIG2(K) = SIG2(K+1)-BAKGD2
      IF(SIG2(K).LT.0.0) SIG2(K)=0.0
   30 CONTINUE
 5000 FORMAT(2(19X,F11.5))
 5001 FORMAT ((2X,10F7.0,8X))
 1001 FORMAT (1H1,6H   RUN,A6,10H  LAMP OFF,10X,26HBACKGROUND     TOTAL C
     1OUNTS//)
 1002 FORMAT (1H1,6H   RUN,A6,10H  LAMP ON ,10X,26HBACKGROUND     TOTAL C
     1OUNTS//)
 1003 FORMAT (19X,14HLOWER DETECTOR,3X,F7.2,6X,F10.0//)
 1004 FORMAT (19X,14HUPPER DETECTOR,3X,F7.2,6X,F10.0//)
 1005 FORMAT (1H ,125H    CHN     LOWER     UPPER    CHN     LOWER     UPPER
     2    CHN     LOWER     UPPER    CHN     LOWER     UPPER    CHN     LOWER
     3    UPPER)
 1006 FORMAT (1H ,5(1X,1H/,1X,I3,3X,F7.0,2X,F7.0))
      RETURN
      END

      SUBROUTINE BOB(I,J,P,IZ)
      DIMENSION P(18,53)
      DATA IS/00000000000000000077/
      IY=RIGHT(IZ,54)
      M=MOD(I,6)
      IF(M.EQ.0) M=6
      NS=6*(10-M)
      II=1+(I-1)/6
      IY=LEFT(IY,NS)
      IA=LEFT(IS,NS)
      P(II,J)=(P(II,J).AND..NOT.IA).OR.IY
      RETURN
      END
```

```
      SUBROUTINE SUMMAT (N,T,LAST,NUMLAG,ICELLS,D,DELTA,D1,SUM)          SUM10001
C     ******************************************************************
C     *                                                                *
C     *  INPUT ..........                                              *
C     *                                                                *
C     *  DATA POINTS = N                                               *
C     *  DATA TIME SCALE = T                                           *
C     *  NUMBER OF DATA POINTS = LAST                                  *
C     *  LAGRANGIAN TYPE USED = NUMLAG                                 *
C     *  NUMBER OF CELLS IN PARTITION OF PARTICULAR DETECTOR = ICELLS  *
C     *  DISTANCE TO PARTICULAR DETECTOR = D                           *
C     *                                                                *
C     *  CONSTANTS ..........                                          *
C     *                                                                *
C     *  CHANNEL WIDTH = DELTA                                         *
C     *  DISTANCE TO FIRST DETECTOR = D1                               *
C     *                                                                *
C     *  OUTPUT ..........                                             *
C     *                                                                *
C     *  COUNTS IN CELL OF PARTICULAR DETECTOR = SUM                   *
C     *                                                                *
C     *  COMMENTS ..........                                           *
C     *                                                                *
C     *  LOWER DETECTOR DETERMINES THE TIME SCALES                     *
C     *                                                                *
C     *  THIS SUBROUTINE FINDS THE NUMBER OF COUNTS IN                 *
C     *  EACH PARTITION CELL FOR THIS DISTRIBUTION OF DATA POINTS      *
C     *  VERSUS TIME AND ENTERS THOSE NUMBERS INTO THE ARRAY SUM       *
C     *  WITH DIMENSION  = ICELLS                                      *
C     *                                                                *
C     ******************************************************************
      DIMENSION T(300), N(300), SUM(300), TDELTA(301)                   SUM10002
      REAL N                                                            SUM10003
      JJ = 1 + ICELLS                                                   SUM10004
      DO 20 K = 1,JJ                                                    SUM10005
      TDELTA(K) = D*(T(1) + (2*K - 3)*DELTA/2.0)/D1                     SUM10006
   20 CONTINUE                                                          SUM10007
      DO 30 J = 1,300                                                   SUM10008
      SUM(J) = 0.0                                                      SUM10009
   30 CONTINUE                                                          SUM10010
      KK = 0                                                            SUM10011
  301 KK = KK + 1                                                       SUM10012
      IF (TDELTA(1) - T(KK)) 302, 301, 301                              SUM10013
  302 DO 40 K = KK,LAST                                                 SUM10017
      IF (TDELTA(ICELLS + 1) - T(K)) 40, 400, 400                       SUM10018
  400 J = 0                                                             SUM10019
C     ******************************************************************
C     *                                                                *
C     *  J = 1 WILL NEVER SATISFY THE SEARCH CRITERIA                  *
C     *                                                                *
C     ******************************************************************
  401 J = J + 1                                                         SUM10020
      IF (TDELTA(J) - T(K)) 401, 110, 110                               SUM10021
  110 IF (T(K) + DELTA/2.0 - TDELTA(J)) 410, 410, 420                   SUM10023
  410 SUM(J - 1) = SUM(J - 1) + ENTGRL (N,LAST,K,0.0,0.5,NUMLAG,1.0)    SUM10024
      GO TO 460                                                         SUM10025
  420 TT = (TDELTA(J) - T(K))/DELTA                                     SUM10026
                                                                        SUM10027
      SUM(J - 1) = SUM(J - 1) + ENTGRL(N,LAST,K,0.0,TT,NUMLAG,1.0)      SUM10028
      IF (J - 1 - ICELLS) 450, 460, 460                                 SUM10029
  450 SUM(J) = SUM(J) + ENTGRL(N,LAST,K,TT,0.5,NUMLAG,1.0)              SUM10030
                                                                        SUM10031
  460 IF (TDELTA(J - 1) - T(K) + DELTA/2.0) 480, 480, 490               SUM10032
  480 SUM(J - 1) = SUM(J - 1) + ENTGRL(N,LAST,K,-0.5,0.0,NUMLAG,1.0)    SUM10033
      GO TO 40                                                          SUM10034
  490 TT = (T(K) - TDELTA(J - 1))/DELTA                                 SUM10035
      SUM(J - 1) = SUM(J - 1) + ENTGRL(N,LAST,K,-TT,0.0,NUMLAG,1.0)     SUM10036
      IF (J - 2) 40, 40, 500                                            SUM10037
  500 SUM(J - 2) = SUM(J - 2) + ENTGRL(N,LAST,K,-0.5,-TT,NUMLAG,1.0)    SUM10038
   40 CONTINUE                                                          SUM10039
      RETURN                                                            SUM10040
      END                                                               SUM10041
1G1
      SUBROUTINE LINFIT(X,Y,SIGMAY,TY,TAU,SIGTAU,NPTS)
C     ******************************************************************
C     *                                                                *
C     *                          ***  LINFIT  ***                      *
C     *                                                                *
C     *  SUBROUTINE TO FIT LEAST SQUARES STRAIGHT LINE                 *
C     *                                                                *
C     ******************************************************************
      DIMENSION X(300),Y(300),TY(300),SIGMAY(300), WT(300), W(300)
      DO 5 I=1,NPTS
      WT(I)=1.0/(SIGMAY(I)*SIGMAY(I))
    5 CONTINUE
```

```
      WMIN=WT(1)
      DO 10 I=2,NPTS
      WMIN=AMIN1(WMIN,WT(I))
   10 CONTINUE
      SX=0.0
      SY=0.0
      SX2=0.0
      SXY=0.0
      SW=0.0
      DO 20 I=1,NPTS
      W(I)=WT(I)/WMIN
      SW=SW+W(I)
      SX=SX+W(I)*X(I)
      SY=SY+W(I)*Y(I)
      SX2=SX2+W(I)*X(I)*X(I)
      SXY=SXY+W(I)*X(I)*Y(I)
   20 CONTINUE
      DEM=(SW*SX2)-(SX*SX)
      A=((SX2*SY)-(SX*SXY))/DEM
      B=((SW*SXY)-(SX*SY))/DEM
      TAU = -1.0/B
      SDEL2=0.0
      DO 30 J=1,NPTS
      TY(J)=A+B*X(J)
      SDEL2=SDEL2+W(J)*(Y(J)-TY(J))*(Y(J)-TY(J))
   30 CONTINUE
      TNPTS=NPTS
      SIGY=SQRT(SDEL2/TNPTS)
      SIGA=SIGY*SQRT(SX2/DEM)
      SIGB=SIGY*SQRT(SW/DEM)
      SIGTAU = SIGB/(B*B)
      RETURN
      END
      REAL FUNCTION ENTGRL (F,LAST,K,AA,BB,NUMLAG,DELTA)                NTL10000
C     ***********************************************************************
C     *                                                                     *
C     *  INPUT DATA POINTS = F                                              *
C     *  DIMENSION OF F = LAST                                              *
C     *  FUNCTION POINT = K                                                 *
C     *  LOWER LIMIT OF INTEGRATION = AA                                    *
C     *  UPPER LIMIT OF INTEGRATION = BB                                    *
C     *  LAGRANGIAN TYPE USED = NUMLAG                                      *
C     *                                                                     *
C     *  THE INTEGRAL USES 5 OR 7 POINT LAGRANGE INTERPOLATION              *
C     *  TO DO THE INTEGRATION BETWEEN A AND B                              *
C     *                                                                     *
C     ***********************************************************************
      DIMENSION F(300),  AF(306),   A(7), AB(7)                         NTL10001
      DO 10 M = 1,3                                                     NTL10002
      AF(M) = 0.0                                                       NTL10003
      I = M + 3 + LAST                                                  NTL10004
      AF(I) = 0.0                                                       NTL10005
   10 CONTINUE                                                          NTL10006
      DO 20 M = 1,LAST                                                  NTL10007
      I = M + 3                                                         NTL20008
      AF(I) = F(M)                                                      NTL10008
   20 CONTINUE                                                          NTL10009
      DO 30 M = 1,7                                                     NTL10010
      AB(M) = BB**M - AA**M                                             NTL10011
   30 CONTINUE                                                          NTL10012
      ENTGRL = 0.0                                                      NTL10013
      N5 = (NUMLAG - 5)/2                                               NTL10014
      N7 = (7 - NUMLAG)/2                                               NTL10015
      A(1) = N5*(AB(7)/7.0 - AB(6)/2.0 - AB(5) + 15.0*AB(4)/4.0 +       NTL10016
     1  4.0*AB(3)/3.0 - 6.0*AB(2))/720.0                                NTL10017
      A(2) = N7*(AB(5)/5.0 - AB(4)/2.0- AB(3)/3.0 + AB(2))/24.0         NTL10018
     1  - N5*(AB(7)/7.0 -AB(6)/3.0 - 2.0*AB(5) + 5.0*AB(4)              NTL10019
     2  + 3.0*AB(3) - 9.0*AB(2))/120.0                                  NTL10020
      A(3) = -N7*(AB(5)/5.0 - AB(4)/4.0 - 4.0*AB(3)/3.0 + 2.0*AB(2))/6.0NTL10021
     1  + N5*(AB(7)/7.0 - AB(6)/6.0 - 13.0*AB(5)/5.0 + 13.0*AB(4)/4.0   NTL10022
     2  + 12.0*AB(3) - 18.0*AB(2))/48.0                                 NTL10023
      A(4) = N7*(AB(5)/5.0 - 5.0*AB(3)/3.0 + 4.0*AB(1))/4.0             NTL10024
     1  - N5*(AB(7)/7.0 - 14.0*AB(5)/5.0 + 49.0*AB(3)/3.0               NTL10025
     2  - 36.0*AB(1))/36.0                                              NTL10026
      A(5) = -N7*(AB(5)/5.0 + AB(4)/4.0 - 4.0*AB(3)/3.0 -2.0*AB(2))/6.0 NTL10027
     1  + N5*(AB(7)/7.0 + AB(6)/6.0 - 13.0*AB(5)/5.0 - 13.0*AB(4)/4.0   NTL10028
     2 + 12.0*AB(3) + 18.0*AB(2))/48.0                                  NTL10029
      A(6) = N7*(AB(5)/5.0 + AB(4)/2.0 - AB(3)/3.0 - AB(2))/24.0        NTL10030
     1  - N5*(AB(7)/7.0 + AB(6)/3.0 - 2.0*AB(5) - 5.0*AB(4)             NTL10031
     2  + 3.0*AB(3) + 9.0*AB(2))/120.0                                  NTL10032
      A(7) = N5*(AB(7)/7.0 + AB(6)/2.0 - AB(5) - 15.0*AB(4)/4.0         NTL10033
     1  + 4.0*AB(3)/3.0 + 6.0*AB(2))/720.0                              NTL10034
      DO 40 M = 1,7                                                     NTL10035
      ENTGRL = ENTGRL + AF(K + M - 1)*A(M)                              NTL10036
   40 CONTINUE                                                          NTL10037
      ENTGRL = ENTGRL*DELTA                                             NTL20038
      RETURN                                                            NTL10038
      END                                                               NTL10039
```

```
      SUBROUTINE PLOT (X,Y,PY,NOX,YOBSER,PYDICT,NOFUNC,TITLE,NTITLE,
     1 KOUTTP)
      INTEGER TITLE (12)
      REAL X(100),Y(100),PY(100),P(18,53),XLABEL(11),YLABEL(11)
      DATA Q000HL,Q001HL,Q002HL/10H          ,10H......    ,10H.....
     1  /
      INC = (NOX +99)/100
      IF(NTITLE.GT.12) NTITLE = 12
      XMAX=X(1)
      DO 10 I=1,NOX,INC
   10 XMAX=AMAX1(XMAX,X(I))
      XMIN=X(1)
      DO 20 I=1,NOX,INC
   20 XMIN=AMIN1(XMIN,X(I))
      YMAX=Y(1)
      DO 30 I=1,NOX,INC
   30 YMAX=AMAX1(YMAX,Y(I))
      YMIN=Y(1)
      DO 40 I=1,NOX,INC
   40 YMIN=AMIN1(YMIN,Y(I))
      IF(NOFUNC.EQ.1) GO TO 60
      DO 50 I=1,NOX,INC
      YMAX=AMAX1(YMAX,PY(I))
   50 YMIN=AMIN1(YMIN,PY(I))
   60 XSCALE=(XMAX-XMIN)/100.0
      XTERVL=XSCALE*10.0
      XLABEL(1)=XMIN
      DO 70  I = 1, 10
   70 XLABEL(I+1)=XLABEL(I)+XTERVL
      YSCALE=(YMAX-YMIN)/50.0
      YTERVL=YSCALE*5.0
      YLABEL(1)=YMIN
      DO 80  I = 1, 10
   80 YLABEL(I+1)=YLABEL(I)+YTERVL
      P(18,1) = Q000HL
      DO 90 I=1,18
      DO 90 J=2,53
   90 P(I,J) = Q000HL
      IF(YMIN*YMAX) 100,110,110
  100 J=IFIX(-YMIN/YSCALE+.5)+1
      IF(J.GT.50) GO TO 110
      CALL BOB(103,J,P,1HZ)
      GO TO 120
  110 J=1
  120 DO 130 I=1,16
  130 P(I,J) = Q001HL
      P(17,J)=Q002HL
      CALL BOB(104,J,P,1HX)
      IF (J-1) 110,140,110
  140 IF(XMIN*XMAX)150,170,170
  150 I=IFIX(-XMIN/XSCALE+.5)+1
      IF (I-100) 160,160,170
  160 CONTINUE
      CALL BOB (I,52,P,1HZ)
      GO TO 180
  170 I=1
  180 DO 190 J=1,51
  190 CALL BOB (I,J,P,1H.)
      CALL BOB (I,53,P,1HY)
      IF (I-1) 170,200,170
  200 IF(NOFUNC.GE.2) GO TO 230
  210 DO 220 I=1,NOX,INC
      IX=IFIX((X(I)-XMIN)/XSCALE+.5)+1
      JY=IFIX((Y(I)-YMIN)/YSCALE+.5)+1
      CALL BOB (IX,JY,P,YOBSER)
  220 CONTINUE
      GO TO 270
  230 DO 260 I=1,NOX,INC
      IX=IFIX((X(I)-XMIN)/XSCALE+.5)+1
      JY=IFIX((Y(I)-YMIN)/YSCALE+.5)+1
      JPY=IFIX((PY(I)-YMIN)/YSCALE+.5)+1
      IF(JY-JPY)240,250,240
  240 CALL BOB (IX,JY,P,YOBSER)
      CALL BOB (IX,JPY,P,PYDICT)
      GO TO 260
  250 CALL BOB (IX,JY,P,1HC).
  260 CONTINUE
  270 WRITE (KOUTTP,320)(TITLE(I),I=1,NTITLE)
      M=11
      DO 310 J=1,53
      K=54-J
      L=K-1
      IF(MOD(L,5)) 300,280,300
  280 WRITE (KOUTTP,290)YLABEL(M),(P(I,K),I=1,18)
  290 FORMAT(1H F16.4,1X,1H-,18A6)
      M=M-1
      GO TO 310
  300 WRITE (KOUTTP,330)(P(I,K),I=1,18)
  310 CONTINUE
      WRITE(KOUTTP,340) (XLABEL(I),I=1,11),XSCALE,YSCALE
      RETURN
  320 FORMAT(1H1,12A6)
  330 FORMAT(1H 18X,18A6)
  340 FORMAT (1H 18X,101H1          1          1          1          1          1
     1 1          1          1          1          1          1/
     1 1H 14X,11(F9.4,1X)/ 9H0XSCALE=  E16.8/9H YSCALE=  F16.8)
      END
```

H. LINFIT Theory

Suppose $y_1, y_2, \cdots, y_n$ are the values of a measured quantity y with experimental errors σ_{y_i}, corresponding to the values $x_1, x_2, \cdots, x_n$ of another quantity x with no experimental errors. Assume also that a linear relation exists between x and y, namely

$$y = A + Bx \ . \tag{1}$$

According to the standard method of least squares, the quantity Q, defined as (YOU 62, p. 124)

$$Q = \sum_s \frac{1}{\sigma_s^2} (y_s - A - Bx_s)^2 \ , \tag{2}$$

is minimized. The normal equations, obtained by differentiating Q with respect to A and B and setting these derivatives equal to zero, are

$$\begin{aligned} \sum_s w_s(y_s - A - Bx_s) &= 0 \\ \sum_s w_s x_s(y_s - A - Bx_s) &= 0 \end{aligned} \tag{3}$$

where $w_s = \sigma_s^{-2}$. To make these equations manageable, define the quantities

$$\begin{aligned} S_1 &= \sum_s w_s \\ S_x &= \sum_s w_s x_s \\ S_y &= \sum_s w_s y_s \end{aligned} \tag{4}$$

$$S_{xy} = \sum_s w_s x_s y_s$$

$$S_{xx} = \sum_s w_s x_s^2 \ . \tag{4}$$

Then Eq. (3) becomes

$$S_y - AS_1 - BS_x = 0$$

$$S_{xy} - AS_x - BS_{xx} = 0 \ . \tag{5}$$

Solving for the coefficients A and B,

$$A = \frac{1}{\Delta}(S_y S_{xx} - S_x S_{xy})$$

$$B = \frac{1}{\Delta}(S_1 S_{xy} - S_x S_y) \tag{6}$$

where

$$\Delta = S_1 S_{xx} - S_x^2 \ .$$

The errors in the quantities A and B are found using (YOU 62, p. 123)

$$\sigma_A^2 = \frac{\sigma^2 S_{xx}}{\Delta}$$

$$\sigma_B^2 = \frac{\sigma^2 S_1}{\Delta} \ , \tag{7}$$

where

$$\sigma^2 = \frac{1}{N}\sum_s w_s [y_s - y_s(\text{fitted})]^2 \ ,$$

all modified for the case of unequal weights. Because $\tau = -1/B$, it

follows that

$$\sigma_\tau = \tau^2 \, \sigma_B$$

$$= \tau^2 \left[\frac{(\sum_s w_s)(\sum_s w_s[y_s - y_s(\text{fitted})]^2)}{N(\sum_s w_s)(\sum_s w_s x_s^2) - N(\sum_s w_s x_s)^2} \right]^{\frac{1}{2}} . \qquad (8)$$

This is the quantity computed by subroutine LINFIT for program ANALZ.

ACKNOWLEDGMENTS

I would like to express my gratitude to Professor Howard A. Shugart for introducing me to this interesting problem, and for his valuable aid in designing and building the experimental apparatus and the data-taking system in particular. I wish to extend my gratitude to Dr. Charles E. Johnson for his advice, guidance and support in carrying out his experiment to a quick and successful conclusion.

I would also like to thank our engineer Douglas MacDonald for his valuable technical assistance, Warren Harnden for his expert graphic work, Patrick Yarnold for general assistance, and Jean Atteridge for typing this thesis.

I am grateful to the National Science Foundation for a 4-year Traineeship and to the Lawrence Radiation Laboratory for a Research Assistantship and for financial support of this research.

Finally, I give thanks to my wife Penny, for her patience and encouragement during my graduate career.

REFERENCES

ABR 64 Milton Abramowitz and Irene A. Stegun, ed., Handbook of Mathematical Functions (NBS - U.S. Government Printing Office, Washington, D.C., 1964), p. 879.

ALL 54 Lawrence H. Aller, Astrophysics: Nuclear Transformations, Stellar Interiors, and Nebulae (Ronald Press Co., New York, 1954), pp. 144-148.

BAT 62 D. R. Bates, Atomic and Molecular Processes (Academic Press, New York, 1962), p. 3.

BLE 57 B. C. Blevis, J. M. Anderson, R. W. McKay, Can. J. Research 35, 941 (1957).

BOW 28 I. S. Bowen, Astrophys. J. 67, 1 (1928).

BOW 36 I. S. Bowen, Rev. Mod. Phys. 8, 55 (1936).

BRE 40 G. Breit and E. Teller, Astrophys. J. 91, 215 (1940).

DAL 63 A. Dalgarno, Rev. Mod. Phys. 35, 522 (1963).

DAL 66 A. Dalgarno, Mon. Nat. R. Astr. Soc. 131, 311 (1966).

DAL 66a A. Dalgarno and G. A. Victor, Proc. Phys. Soc. 87, 371 (1966).

DRA 69 G. W. F. Drake, G. A. Victor, and A. Dalgarno, Phys. Rev. 180, 25 (1969).

DUG 67 J. L. G. Dugen, H. L. Richards, and E. E. Muschlitz, Jr., J. Chem. Phys. 46, 346 (1967).

EVA 55 Robley D. Evans, The Atomic Nucleus (McGraw-Hill Book Co, Inc., New York, 1955), p. 786.

FAL 67 L. M. Falicov, Group Theory and Its Physical Application (Univ. of Chicago Press, Chicago, 1967), pp. 46-48.

FRY 69 E. S. Fry and W. L. Williams, Rev. Sci. Instr. 40, 1141 (1969).

FRY 69a E. S. Fry and W. L. Williams, Phys. Rev. 183, 81 (1969).

GIB 63 Hyatt M. Gibbs, The Lifetimes of the $^3P_2$ Metastable States of Neon and Argon, Atomic Structure Group Seminar Report (Univ. of California, unpublished work), April 1963.

GOT 66 Kurt Gottfried, Fundamentals, in Quantum Mechanics (W. A. Benjamin, Inc., New York, 1966), Vol. I.

HAE 39 A. V. Haeff, Proc. Inst. Radio Engrs. 27, 586 (1939).

HAG 53 Homer D. Hagstrum, Phys. Rev. 89, 244 (1953).

HAG 54 Homer D. Hagstrum, Phys. Rev. 96, 336 (1954).

HAM 40 D. R. Hamilton, Phys. Rev. 58, 122 (1940).

HER 44 Gerhard Herzberg, Atomic Spectra and Atomic Structure (Dover Publications, New York, 1944), p. 154.

HER 58 Gerhard Herzberg, Proc. Roy. Soc. (London) 248 (1958).

HOD 55 Charles D. Hodgman, Ed.-in-Chief, Handbook of Chemistry and Physics (Chemical Rubber Publ. Co., Cleveland, Ohio, 1955), 37th Edition.

HOL 65 Helen K. Holt, Excitation of the 2^1S, 2^3S and 2^3P States of Helium by Electron Bombardment (Ph.D. Thesis), Yale University, 1965, p. 99.

JAC 70 Verne Jacobs (Weizmann Institute of Science, Rehovoth, Israel), private communication. The lifetimes 19.6 and 20.2 msec are calculated using velocity and length matrix elements, respectively.

KUH 62 H. G. Kuhn, Atomic Spectra (Academic Press, New York, 1962), pp. 82-83.

LAM 51 W. E. Lamb and R. C. Retherford, Phys. Rev. 81, 222 (1951).

LAN 23 Irving Langmuir, Phys. Rev. 22, 357 (1923).

LIP 65 M. Lipeles, R. Novick, and N. Tolk, Phys. Rev. Letters 15, 690 and 815 (1965).

MAY 31 Maria Goeppert-Mayer, Ann. Physik 9, 273 (1931).

MRO 44 S. Mrozowski, Rev. Mod. Phys. 16, 153 (1944).

MUS 66 E. E. Muschlitz, Jr., Molecular Beams, in Advances in Chemical Physics, John Ross, ed. (Interscience Publishers, New York, 1966), Vol. X, pp. 171-193.

OLI 29 M. L. Oliphant, Proc. Roy. Soc. A124, 228 (1929).

PEA 68 A. S. Pearl, Ph.D. Thesis, University of New South Wales, 1968.

PEA 70 A. S. Pearl, Phys. Rev. Letters 24, 703 (1970).

PHE 59 A. J. Phelps, Phys. Rev. 114, 1011 (1959).

REI 65 F. Reif, Fundamentals of Statistical and Thermal Physics (McGraw-Hill Book Co., San Francisco, 1965).

RUB 32 A. Rubinowicz and J. Blaton, Ergeb exakt Naturwiss XI, 176 (1932).

SCH 69 C. L. Schwartz (Department of Physics, University of California, Berkeley), private communication, 1969.

SEA 65 M. J. Seaton, Ann. Astrophys. 17, 296 (1954).

SEG 65 Emilio Segrè, Nuclei and Particles (W. A. Benjamin, Inc., New York, 1965).

SHA 59 J. Shapiro and G. Breit, Phys. Rev. 113, 179 (1959).

SLA 60 John C. Slater, Quantum Theory of Atomic Structure (McGraw-Hill Book Co., Inc., New York, 1960), Vol. I.

SPI 51 L. Spitzer, Jr. and J. L. Greenstein, Astrophys. J. 114, 407 (1951).

STE 68 Murray Steinberg, Experimental Studies on the Metastable Lifetimes in Helium and Neon (Ph.D. Thesis), Lawrence Radiation Laboratory Report UCRL-18387, August 1968.

STE 69 M. Steinberg and H. A. Shugart, Bull. Am. Phys. Soc. 14, 32 (1969).

TOP 65 J. Topping, Errors of Observation and Their Treatment (Reinhold Publ. Corp., New York, 1965), 3rd edition, p. 88.

VAR 65 Varian Vacuum Division Instruction Manual for Ionization Gauge Control Unit Model Nos. 971-0003 and 971-0023 (Varian Associates, Palo Alto, California, February 1965), Manual #87-400-074.

VIC 67 G. A. Victor, Proc. Phys. Soc. 91, 825 (1967).

WEB 24 H. W. Webb, Phys. Rev. 24, 113 (1924).

YOU 62 Hugh D. Young, Statistical Treatment of Experimental Data (McGraw-Hill Book Co., Inc., New York, 1962).

LEGAL NOTICE

This report was prepared as an account of Government sponsored work. Neither the United States, nor the Commission, nor any person acting on behalf of the Commission:

A. Makes any warranty or representation, expressed or implied, with respect to the accuracy, completeness, or usefulness of the information contained in this report, or that the use of any information, apparatus, method, or process disclosed in this report may not infringe privately owned rights; or

B. Assumes any liabilities with respect to the use of, or for damages resulting from the use of any information, apparatus, method, or process disclosed in this report.

As used in the above, "person acting on behalf of the Commission" includes any employee or contractor of the Commission, or employee of such contractor, to the extent that such employee or contractor of the Commission, or employee of such contractor prepares, disseminates, or provides access to, any information pursuant to his employment or contract with the Commission, or his employment with such contractor.

TECHNICAL INFORMATION DIVISION
LAWRENCE RADIATION LABORATORY
UNIVERSITY OF CALIFORNIA
BERKELEY, CALIFORNIA 94720